~~CONFIDENTIAL~~
~~RESTRICTED DATA~~
~~Atomic Energy Act - 1954~~

Inpc-8
63-?2

Astronuclear
WANL-TNR-052

178

NOTICE
This report was prepared as an account of work sponsored by the United States Government. Neither the United States nor the United States Energy Research and Development Administration, nor any of their employees, nor any of their contractors, subcontractors, or their employees, makes any warranty, express or implied, or assumes any legal liability or responsibility for the accuracy, completeness or usefulness of any information, apparatus, product or process disclosed, or represents that its use would not infringe privately owned rights.

WESTINGHOUSE ELECTRIC CORPORATION
ASTRONUCLEAR LABORATORY
P. O. Box 10864
Pittsburgh 36, Pa.
March, 1962

MASTER

Classification cancelled ~~or changed to~~
by authority of DOC
by (illegible initials) TIC, date SEP 0 1973

FLIGHT SAFETY STUDIES
PHASE 1
(Title Unclassified)
NERVA NUCLEAR SUBSYSTEM

~~CONFIDENTIAL~~
~~RESTRICTED DATA~~
~~Atomic Energy Act - 1954~~

FLIGHT SAFETY STUDIES PHASE I

1.0 INTRODUCTION

Considerations of the safety aspects of conducting orbital missions with a nuclear rocket are presented in WANL-TNR-052. These considerations include various aspects of reactor destruct, problems of determining required data on fission product release from NERVA fuel material, and the burnup of the reactor upon re-entry. This report comprises three (3) topical reports. A brief abstract of each of these topical reports is given in the following paragraphs.

2.0 WANL-TNR-038, TRANSIENT REACTOR EXPERIMENTS ON NERVA FUEL MATERIAL

Considerations of the safety aspects of orbital missions with a nuclear rocket indicates that an effective way to minimize hazards related to the possibility of an intact reactor falling on land is to destroy the reactor while in flight. This report is concerned with an experimental program to determine the feasibility of using a reactor transient to destroy the core of a nuclear rocket. In addition to this primary objective, the transient experiments provide information on the nature of the shutdown mechanism, a determination of fission product release during controlled reactor transients, and a study of reactions between NERVA fuel and water during a reactor transient.

3.0 WANL-TNR-039, RE-ENTRY AND BURNUP OF REACTOR FRAGMENTS

If the reactor in orbit is broken into fragments prior to re-entry, it might be expected that aerodynamic heating would result in burnup of the resulting fragments thereby reducing the hazard to the general population. This report presents both a theoretical approach and experimental approach designed to establish the amount of particle burnup which can be expected during re-entry This information will be obtained for various size particles and will be combined with data being obtained on allowable particle sizes reaching the earth and reactor destruct capabilities to establish a criteria for orbital or near orbital core disposal

4 0 WANL-TNR-040, SURVEY OF FISSION PRODUCT RELEASE FROM NERVA FUEL MATERIAL

One of the major sources of concern in regard to the eventual use of nuclear rockets is related to the fission product activity of the reactor core after operation of the reactor. The primary purpose of this report is to consider the problem of fission product release from an intact core during a decay heat cycle In particular, it describes the results of a literature review of fission product release from fueled graphite and considers the problem of an experimental program which would provide fission product release data required in several phases of the NERVA program

CONFIDENTIAL
RE~~STRICTED DATA~~
Atomic Energy Act - 1954

Astronuclear
WANL-TNR-038

WESTINGHOUSE ELECTRIC CORPORATION
ASTRONUCLEAR LABORATORY
P. O. Box 10864
Pittsburgh 36, Pa.
March, 1962

Author: A. Boltax

TRANSIENT REACTOR EXPERIMENTS ON NERVA FUEL MATERIAL

(Title Unclassified)

NERVA NUCLEAR SUBSYSTEM

CONFIDENTIAL
RE T[redacted]TA
Ato ... Act - 1954

TABLE OF CONTENTS

		Page
1.0	Introduction	1
2.0	Experimental Technique	2
3.0	Results of the First Series of Transient Experiments	8
4.0	Discussion of Results	34
5.0	Future Work	42
6.0	Conclusions	45
7.0	Acknowledgments	46

TABLES

No.	Title	Page
I	Summary of Results of First Series of TREAT Experiments	6
II	Maximum Heating and Cooling Rates for Calibration Experiment	14
III	Results of Radiochemical Analyses of Gas Phase in Irradiation Capsule	16
IV	Observations on Irradiated Fuel Material	26
V	Results of Particle Size Measurements on Fragmented Fuel	28
VI	Results of Radiochemical Analysis of Fragmented Fuel and Uranium Flux Monitors	31
VII	Results of LASL Electrical Heating Experiments	41

BLANK PAGE

TABLE OF CONTENTS

(continued)

REFERENCES

	Page
Nos. 1 through 7	47

LIST OF FIGURES

No.	Title	Page
1	Detailed Drawing of Stainless Steel Autoclave and Internal Graphite Components	4
2	View of Stainless Steel Autoclave and Internal Graphite Components	5
3	Schematic Diagram of Thermocouple Circuitry for Calibration Run (CEN-73) of First Series of TREAT Experiments	7
4	Comparison of Predicted and Experimental Results for First Series of TREAT Experiments	9
5	Oscillographic Record of Fuel Temperature, Autoclave Pressure, Reactor Power, and Integrated Power as a Function of Time for Calibration Run CEN-73, Transient 359	11
6	Oscillographic Record of Fuel Temperature, Autoclave Pressure, Reactor Power, and Integrated Power as a Function of Time for Calibration Run CEN-73, Transient 363	12
7	Fuel Temperature Histories for Each of the Calibration Transients (CEN-73)	13
8	Graphite Fuel Specimen after Transient CEN-73	17

TABLE OF CONTENTS

(continued)

LIST OF FIGURES

No.	Title	Page
9	Macrographs of Some Particles from Transient CEN-73	18
10	Graphite Fuel Specimen after Transient CEN-74	19
11	Macrographs of Some Particles from Transient CEN-74	20
12	Graphite Fuel Specimen after Transient CEN-75	21
13	Macrographs of Some Particles from Transient CEN-75	22
14	Graphite Fuel Specimen after Transient CEN-76	23
15	Macrographs of Some Particles from Transient CEN-76	24
16	Graphite Crucibles and Plug after Transient CEN-76	25
17	Particle Size Distribution of Fragmented NERVA Fuel	27
18	Average Particle Size of Fragmented Fuel as a Function of Reactor Energy Level	30
19	Integrated Neutron Flux as a Function of Reactor Energy Level	32
20	Comparison of Calculated and Experimental Results for First Series of TREAT Experiments	33
21	Distribution of Activity in Particles of a Given Size Range	35
22	"AR" Value as a Function of Particle Size	36

ACKNOWLEDGMENTS

The experimental work described in this report is the result of the efforts of a considerable number of people located at various sites throughout the country. The most active participants in this work included L. D. P. King, P. Wagner, W. Stratton, and E. Bryant of the Los Alamos Scientific Laboratory; L. Baker, R. C. Liimatainen, R. O. Ivins and F. Testa of the Chemical Engineering Division, Argonne National Laboratory, J. Boland and S. Lawroski of TREAT Reactor (Argonne National Laboratory); and W. H. Esselman, A. B. Rothman, M. A. Vogel, E. V. Anderson, and C. Boehmer of the Westinghouse Astronuclear Laboratory. The authors are grateful to S. Lawroski and R. C. Vogel of the Chemical Engineering Division, Argonne National Laboratory for permission to use their facilities for this program. The photographs given in the report are presented with the permission of Argonne National Laboratory.

TRANSIENT REACTOR EXPERIMENTS ON NERVA FUEL MATERIAL

1.0 INTRODUCTION

Consideration of the safety aspects of conducting orbital missions with a nuclear rocket indicates that one effective way to minimize hazards related to the possibility of an intact reactor falling on land is to physically destroy the reactor while still in flight. Various methods of reactor destruct have been considered. These involve the use of high explosives, thermochemical techniques, aerodynamic heating, oxidation, ablation, chemical additives, and reactor transients. Each of the reactor destruct methods has been examined theoretically and several experimental programs are underway to determine their feasibility. This report is concerned with an experimental program to determine the feasibility of using a reactor transient to destroy the core of a nuclear rocket. In addition to this primary objective, the transient experiments will also provide:

a. Information on the nature of the shutdown mechanism which will form the basis for estimating the maximum credible incident in the NERVA core.

b. A determination of fission product release during controlled reactor transients.

c. A study of reactions between the NERVA fuel and water during a reactor transient occurring as a result of an intact reactor falling into water.

The experimental approach involved irradiation of encapsulated sections of NERVA fuel in the TREAT (Transient Reactor Test Facility) reactor. A brief description of the TREAT Reactor Facility is given in a later section of this report. The samples of NERVA fuel material can be contained in instrumented capsules in various environments including helium, vacuum and water. The experiments in vacuum will mock up the conditions to be encountered in outer space; those in helium will mock up the environmental conditions associated with transients occurring on the launch pad.* Finally, as mentioned previously, the water will mock up a transient occurring as a result of an intact reactor falling into water.

Studies of the behavior of the fuel material are planned as a function of the integrated power of the transient. That level of integrated power which initiates fragmentation of the fuel will be of particular interest. In the case of the transient experiments in water, consideration must also be given to fuel-water reactions which may give rise to partial destruction of the fuel material prior to complete fragmentation.

2.0 EXPERIMENTAL TECHNIQUE

The transient experiments were carried out in the TREAT reactor which is a homogeneous graphite-moderated reactor located at the National Reactor Testing Station in Idaho. This facility is designed to produce large transient thermal fluxes of short duration. At an integrated power of 1000 megawatt-seconds (MWS), the maximum integrated neutron flux of approximately 2×10^{15} can be produced in the order of 40 milliseconds. The carbon-to-uranium ratio of the TREAT fuel is approximately 10,000 to 1. In a 1000 MWS transient, the change in fuel temperature is of the order of 200°C. The carbon-to-uranium ratio for the NERVA fuel (KIWI B-4 containing 400 milligrams of

*It is assumed here that the reactor system will be flushed with an inert atmosphere while on the launch pad.

fully enriched uranium per cubic centimeter) is approximately 100 to 1, and the maximum temperature attainable is above the sublimation temperature of graphite ($\sim$3350°C).

The irradiation capsules and dummy fuel element assemblies used in this program were provided by the Chemical Engineering Division of the Argonne National Laboratory (ANL) and are described elsewhere.[1] Figure 1 shows a drawing of the capsule and the graphite assembly containing a section of the KIWI B-4 element. The fuel sample was a half-inch diameter by three-quarter inch long, 7-hole section of the KIWI B-4 element. This fuel section was used in place of the full 19-hole hexagonal element (3/4-inch across the flats) because of space limitations. Figure 2 is a photograph of the autoclave capsule and several of the components. Table I presents a summary of the instrumentation used, the reactor conditions, and results obtained for the first series of TREAT experiments.

The first experiment CEN-73 was designed to permit calibration of the temperature of the fuel specimen and stainless steel capsule as a function of the integrated power of the transient. The fuel temperature was measured by a sixteenth-inch diameter thermocouple made up with 10-mil tungsten-7% rhenium versus tungsten-26% rhenium with beryllia insulation and a 4-mil tantalum sheath. The thermocouple was positioned in a peripheral hole of the 7-hole fuel specimen with a graphite plug which centered the thermocouple axially and partially covered the ends of the sheath. The capsule wall temperature was measured by a bare chromel-alumel (20 mil) thermocouple contained in an alundum tube. The chromel-alumel thermocouple was positioned in a groove in the outer graphite crucible which can be seen in Figure 2. Figure 3 shows a schematic diagram of the thermocouple circuit.

The calibration experiment involved successive temperature-limited transients of approximately 50, 100, 200, 250, 375 and 550 megawatt-seconds. It was

~~CONFIDENTIAL~~
~~RESTRICTED DATA~~
[redacted]

Astronuclear

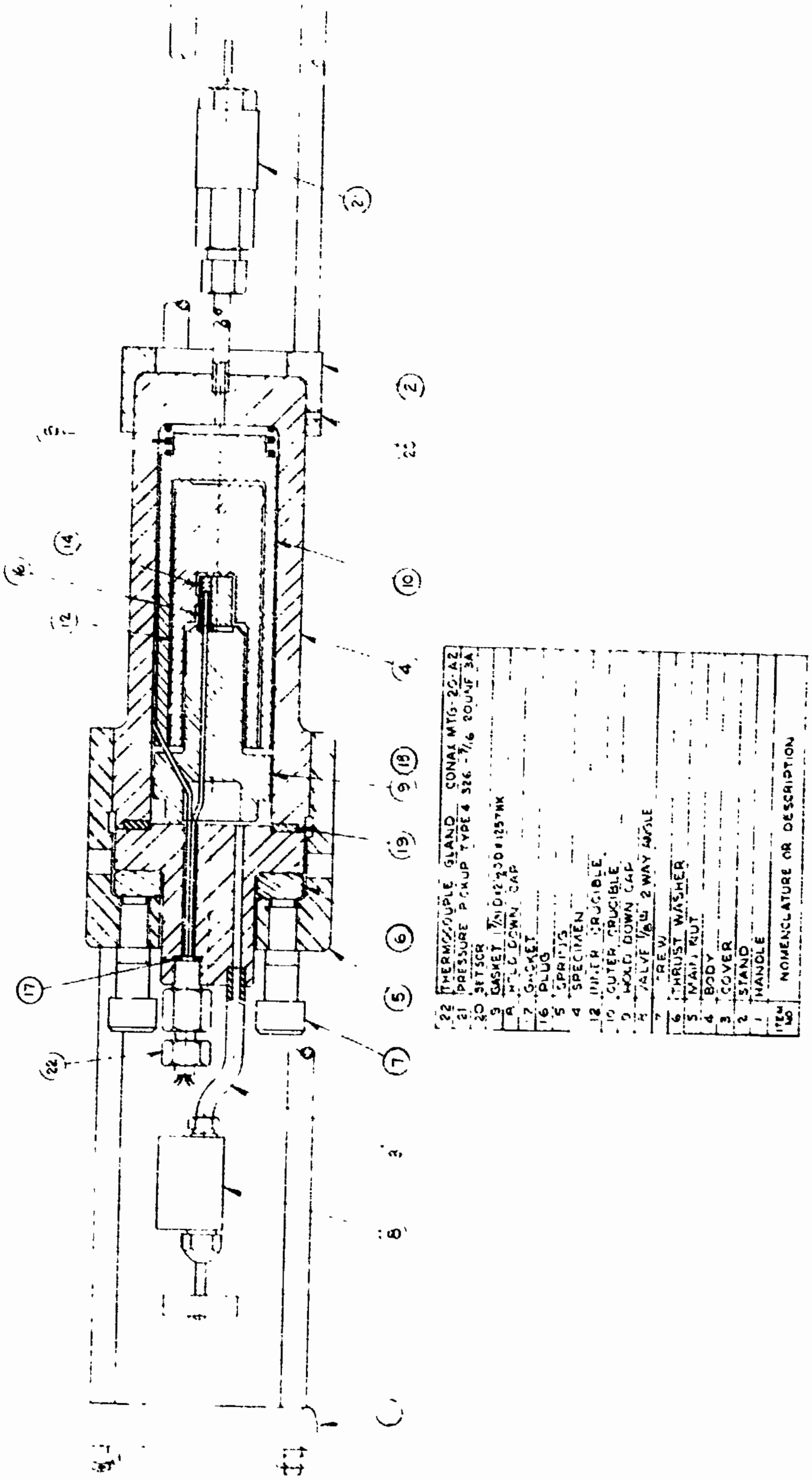

~~CONFIDENTIAL~~
~~RESTRICTED DATA~~
Atomic Energy Act 1954

Figure 1

Detailed Drawing of Stainless Steel Autoclave and Internal Graphite Components

~~CONFIDENTIAL~~
~~RESTRICTED DATA~~
~~Atomic Energy Act 1954~~

Astronuclear

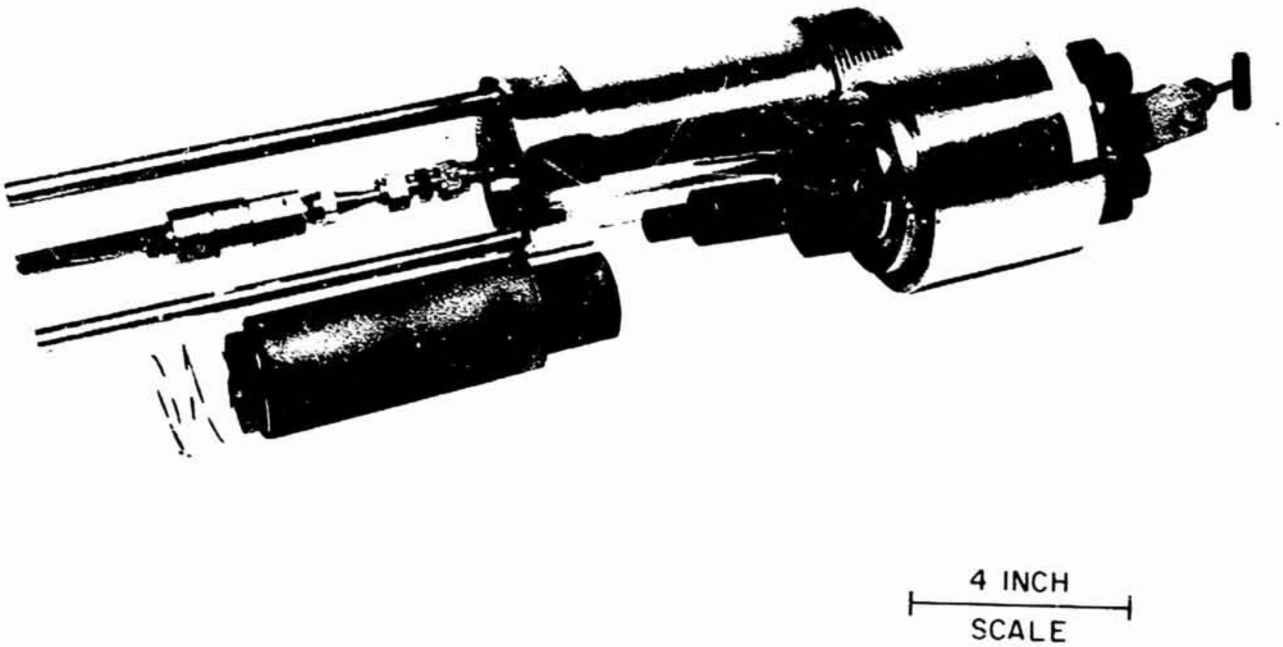

Figure 2

View of Stainless Steel Autoclave and Internal Graphite Components

~~CONFIDENTIAL~~
~~RESTRICTED DATA~~
~~Atomic Energy Act 1954~~

TABLE I

SUMMARY OF RESULTS OF FIRST SERIES OF TREAT EXPERIMENTS[a]

		Reactor Conditions				Capsule Conditions			Instrumentation[d]
Experiment Number	Transient Number	Integrated Power MWS	Reactor Period Milliseconds	Reactor Peak Power Megawatts	Change in Temperature of Reactor[b] °C	Maximum Fuel Temperature °C	Maximum Pressure Rise in Capsule psi[c]	Wall Temperature Rise °C	Thermocouples
CEN-73	358	53	152	174	27	510	40	4	W-7Rh vs. W-26Rh in Ta sheath with BeO ceramic Chromel-Alumel (bare) in alundum tubing
	359	108	152	265	51	940	35	5	
	360	195	152	264	80	1470	35	17	
	361	236	76	1065	101	1600	90	20	
	362	373	77	1097	148	2040	112	23	
	363	546	54	2390	208	2750	222	48	
CEN-74	364	386	54	2440	153	e	f	65	Chromel-Alumel in stainless steel sheath Chromel-Alumel (bare) in alundum tubing
CEN-75	365	645	40	3820	240	e	110	90	Same as CEN-74
CEN-76	366	885	40	3850	308	e	120	100	2 Chromel-Alumel (bare) in alundum tubing

---

[a] Fuel sample size 0.5 inch diameter, 0.75 inch long, 7 holes each 0.095 inch diameter, weight 3.75 grams.

[b] Initial reactor temperature ~ 30° C

[c] A major portion of the indicated pressure increase is probably due to a spurious irradiation effect on unbonded strain gauge transducers.

[d] Transducers were obtained from Consolidated Electrodynamics Corp., with pressure range 0-1000 psi.

[e] Not measured.

[f] No reliable pressure data.

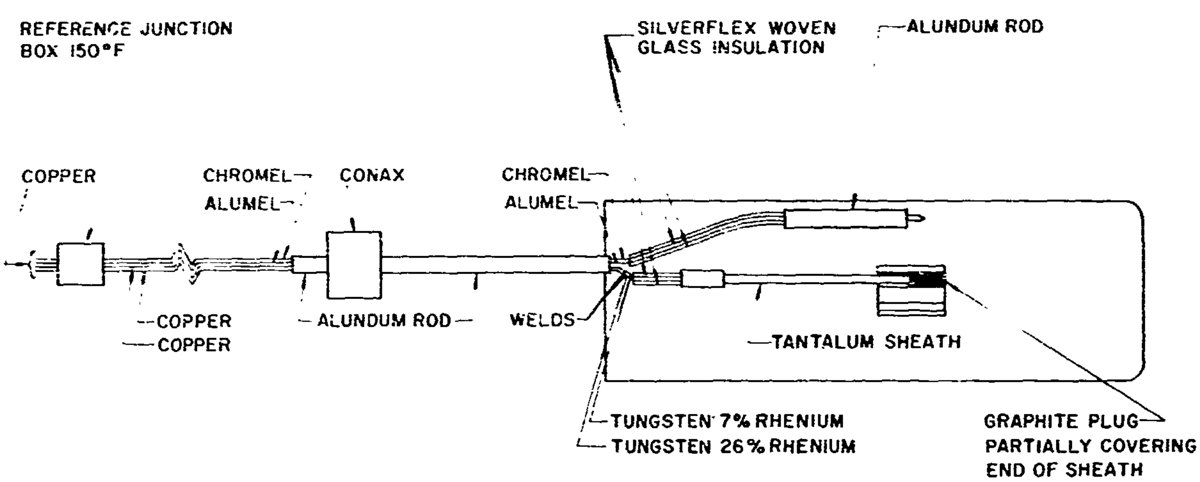

Figure 3 570A630
Schematic Diagram of Thermocouple Circuitry for Calibration Run (CEN-73) of First Series of TREAT Experiments

anticipated that the data obtained in these experiments would permit an estimate of the fuel temperature attained during the higher level transients above 2500°C when temperature measurement techniques are limited. The tungsten-rhenium thermocouple is not reliable much above 2500°C. In addition, the gradual approach to the high temperatures planned for the subsequent transient experiments permitted verification of a safety analysis of the experiment which predicted that no damaging pressure or temperature buildups would occur in the irradiation capsule.

In the three experiments which followed CEN-73 relatively high level integrated power levels were used. The purpose of this series of experiments was to determine if physical disintegration of the graphite fuel occurred as a consequence of the reactor transient. Observations made following the transient experiments included radiochemical studies to determine fission product release and particle size analysis of the irradiated fuel.

3.0 RESULTS OF THE FIRST SERIES OF TRANSIENT EXPERIMENTS

Table I, mentioned previously, presents a summary of the measured integrated power levels, temperatures, and pressures recorded during the individual transient experiments. Results obtained in the calibration experiments are shown in Figure 4 where the calculated adiabatic temperatures and the actual measured temperatures of the fuel are plotted as a function of integrated power level. The adiabatic fuel temperature was calculated using integrated neutron flux data obtained in previous ANL transient experiments.* The data in Figure 4 indicates that the fuel specimen is heated in an

*The actual values of integrated neutron flux for the present experiment were approximately [illegible]0 per cent higher than used in the original calculation of adiabatic fuel temperature. Further discussion of this point will be presented later in this section.

~~CONFIDENTIAL~~
~~RESTRICTED DATA~~
~~Atomic Energy Act - 1954~~

Astronuclear

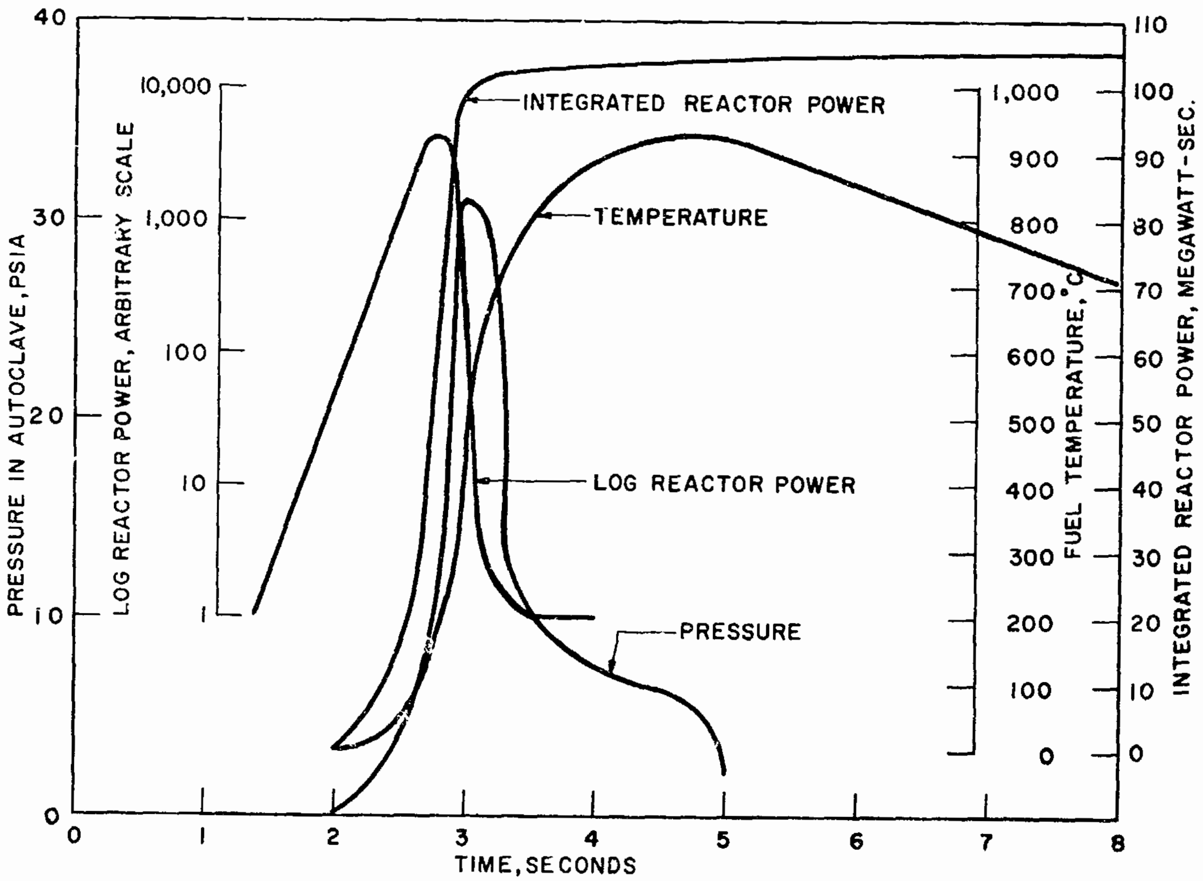

Figure 5 537343

Oscillographic Record of Fuel Temperature, Autoclave Pressure, Reactor Power, and Integrated Power as a Function of Time for Calibration Run CEN-73, Transient 359

CONFIDENTIAL
RESTRICTED DATA
Atomic Energy Act - 1954

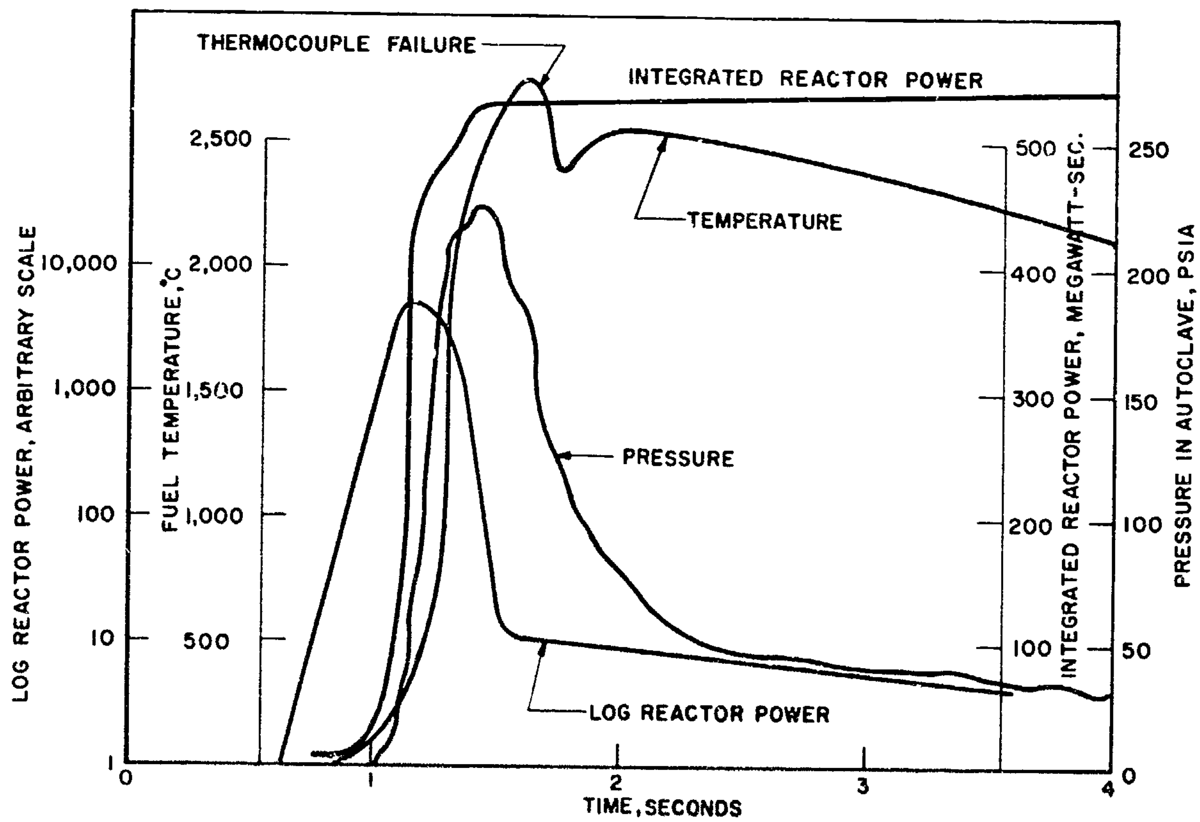

Figure 6 537342

Oscillographic Record of Fuel Temperature, Autoclave Pressure, Reactor Power, and Integrated Power as a Function of Time for Calibration Run CEN-73, Transient 363

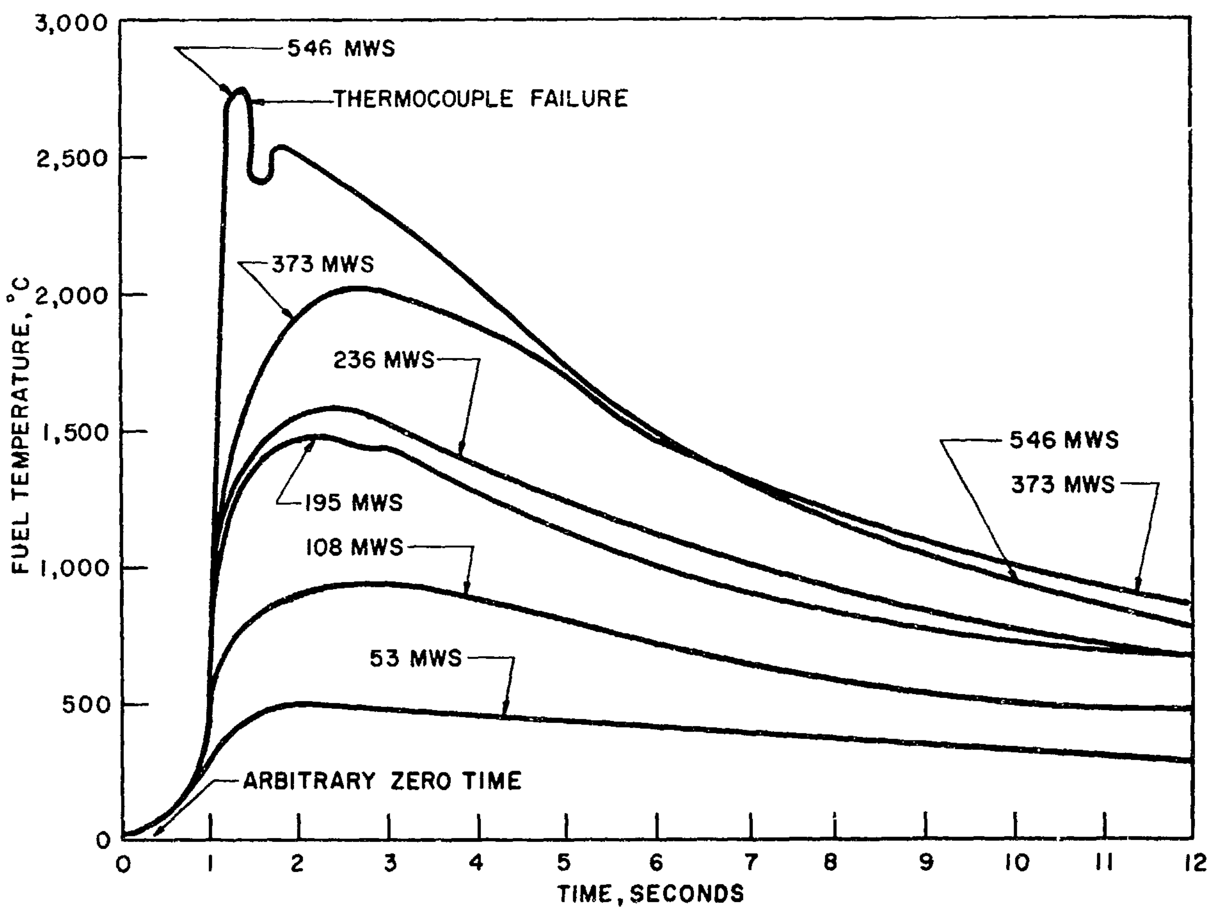

Figure 7 547061

Fuel Temperature Histories for Each of the Calibration Transients (CEN-73)

TABLE II MAXIMUM HEATING AND COOLING RATES FOR CALIBRATION EXPERIMENT

Transient	Integrated Power MWS	Period Milliseconds	Maximum Fuel Temperature	Time To Attain Maximum Temperature Seconds*	Maximum Heating Rate °C/sec	Maximum Cooling Rate °C/sec
358	53	152	510	4.8	550	30
359	108	152	940	4.5	1150	80
360	195	152	1470	4.2	1800	140
361	236	76	1600	3.1	2200	150
362	373	77	2040	3.4	2500	280
363	546	54	2750	1.6	8500	290

*Measured from initiation of transient.

bulbs. Absolute gamma counting of the gas samples with a sodium iodide crystal detector showed the presence of xenon 133 as the main isotope; with about 1 per cent of the total activity coming from iodine 131. By integrating under the 80 kilovolt gamma peak of xenon 133 the results shown in Table III were obtained. The amount of xenon 133 was corrected back to the time of the irradiation on the basis of a 5.27 day half-life.

The autoclaves were then dismantled and photographs were made of the fuel and of the graphite crucibles. These are shown in Figures 8 through 16. It is evident that the transients were energetic enough to cause destruction of the original cylindrical fuel element. Additional observations on the fragmented fuel are described in Table IV.

Sieve-screen analysis was made of the fragments and particles formed in the transient experiments. The mean diameter of the particles produced by the destructive transients were computed from the relationship:

$$d_{sv} = \frac{1}{\sum_{i=1}^{N} \frac{W_i}{d_i}}$$

where d_{sv} = mean surface to volume diameter

d_i = average diameter of the ith size group

W_i = fraction by weight of particles in the ith group

$\sum_{i=1}^{N}$ = summation over N size groups

Numerical values for W_i and d_i are shown as the ordinate and abscissa respectively of the histograms for the particle size distribution shown in Figure 17. Results of these measurements and calculations are shown in Table V.

TABLE III RESULTS OF RADIOCHEMICAL ANALYSES OF GAS PHASE IN IRRADIATION CAPSULE

Transient Run No.	Integrated Power MWS	Microcuries of Xe-133 in Gas Phase of Autoclave*
CEN-73	Calibration Run	4700
CEN-74	386	1400
CEN-75	645	2100
CEN-76	885	2300

---

*Uncertainty of ± 40 per cent.

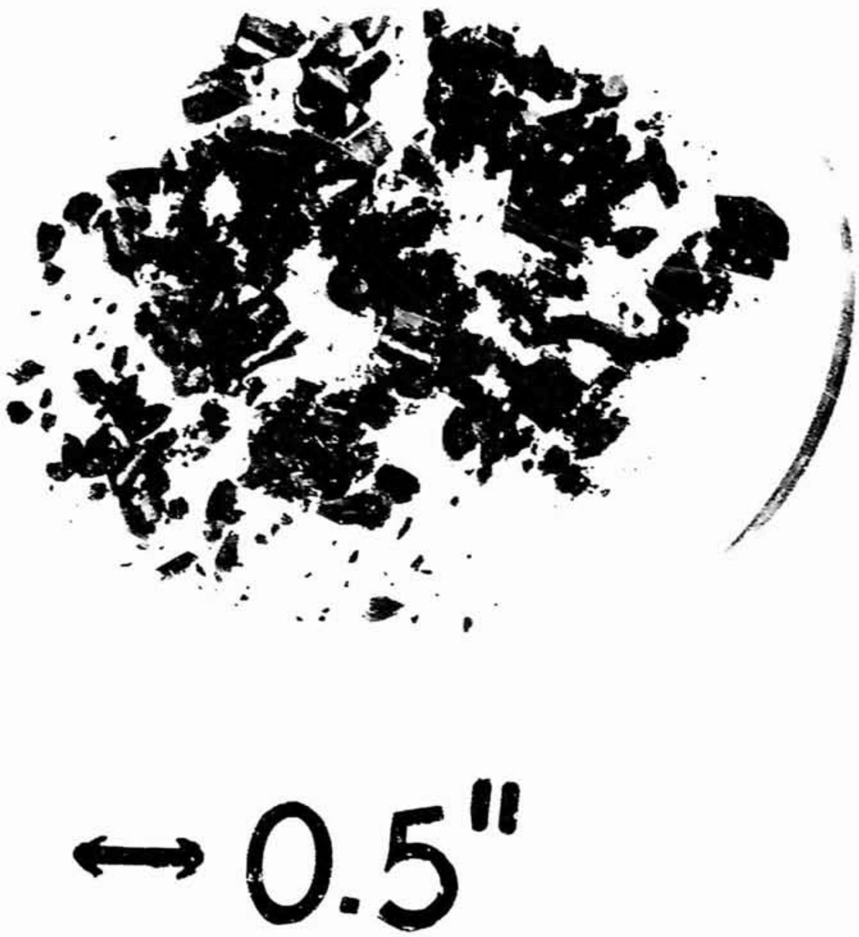

~~CONFIDENTIAL~~
~~RESTRICTED DATA~~
~~Atomic Energy Act - 1954~~

Figure 8

Graphite Fuel Specimen after Transient CEN-73

Figure 9

Macrographs of Some Particles from Transient CEN-73

~~CONFIDENTIAL~~
~~RESTRICTED DATA~~
~~Atomic Energy Act 1954~~

~~CONFIDENTIAL~~
~~RESTRICTED DATA~~
~~Atomic Energy Act - 1954~~

Astronuclear

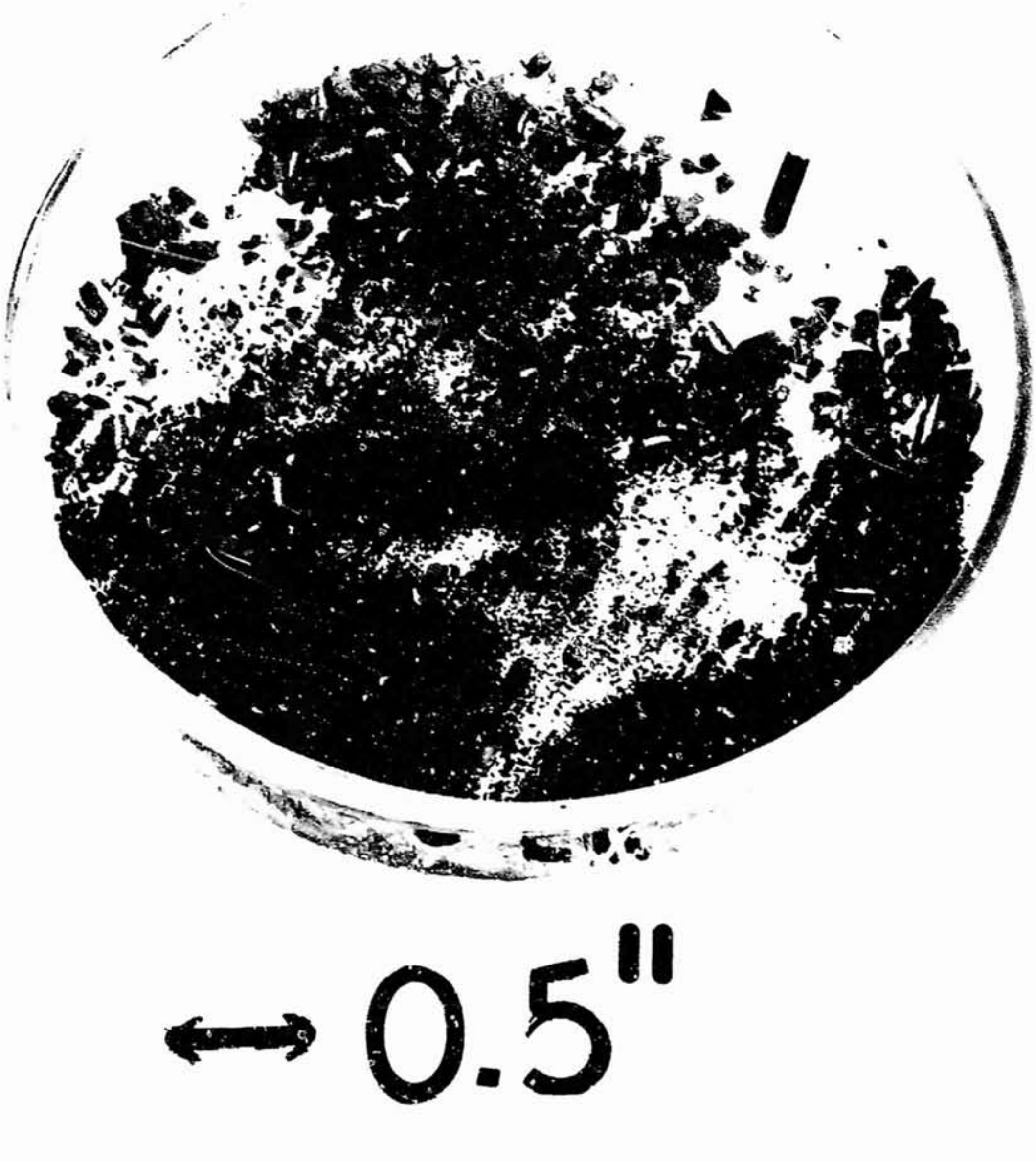

~~CONFIDENTIAL~~
~~RESTRICTED DATA~~
[redacted] 1954

Figure 10

Graphite Fuel Specimen after Transient CEN-74

~~CONFIDENTIAL~~
~~RESTRICTED DATA~~
~~Atomic Energy Act - 1954~~

Figure 11

Macrographs of Some Particles from Transient CEN-74

~~CONFIDENTIAL~~
~~RESTRICTED DATA~~
~~Atomic Energy Act - 1954~~

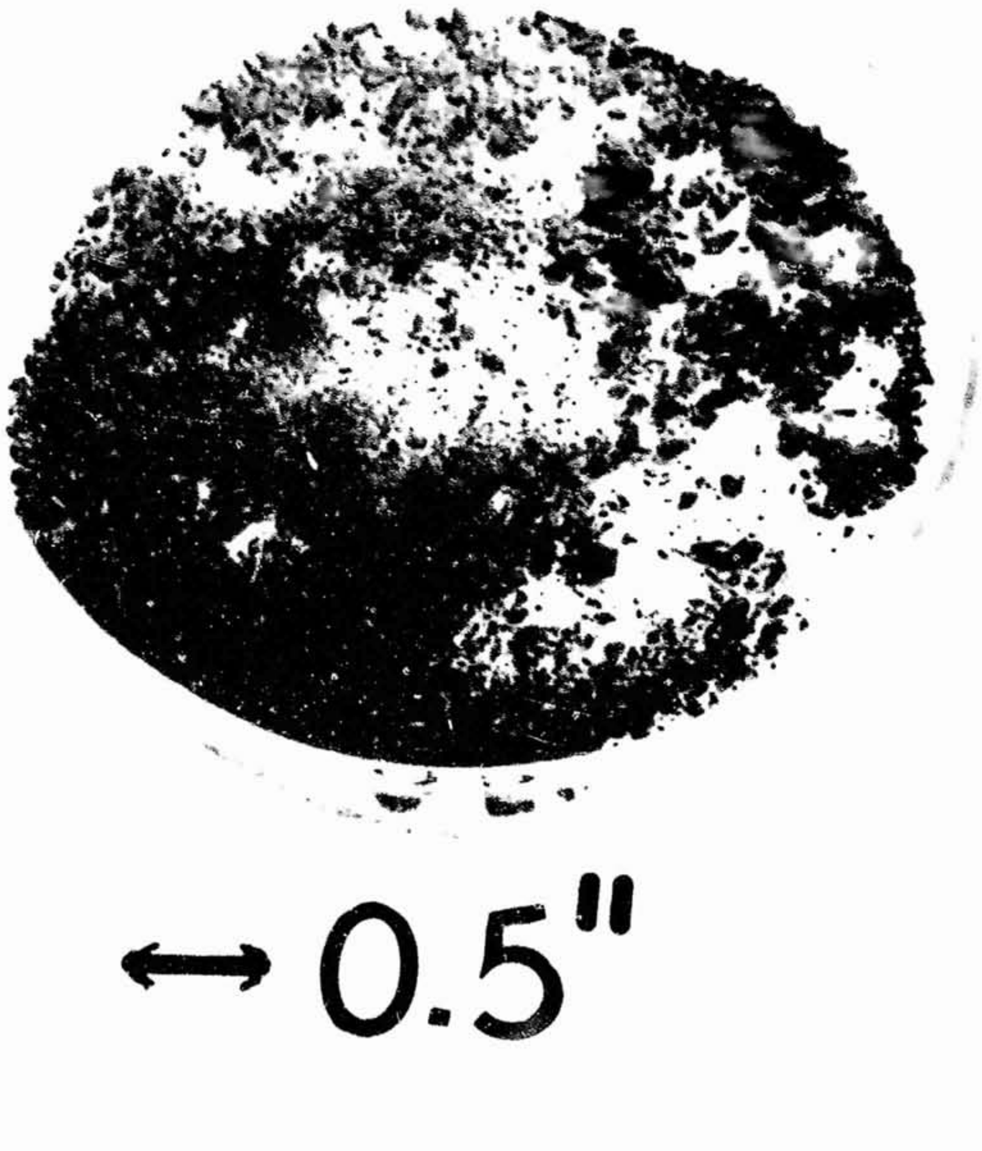

Figure 12

Graphite Fuel Specimen after Transient CEN-75

Figure 13

Macrographs of Some Particles from Transient CEN-75

Figure 14

Graphite Fuel Specimen after Transient CEN-76

Figure 15

Macrographs of Some Particles from Transient CEN-76

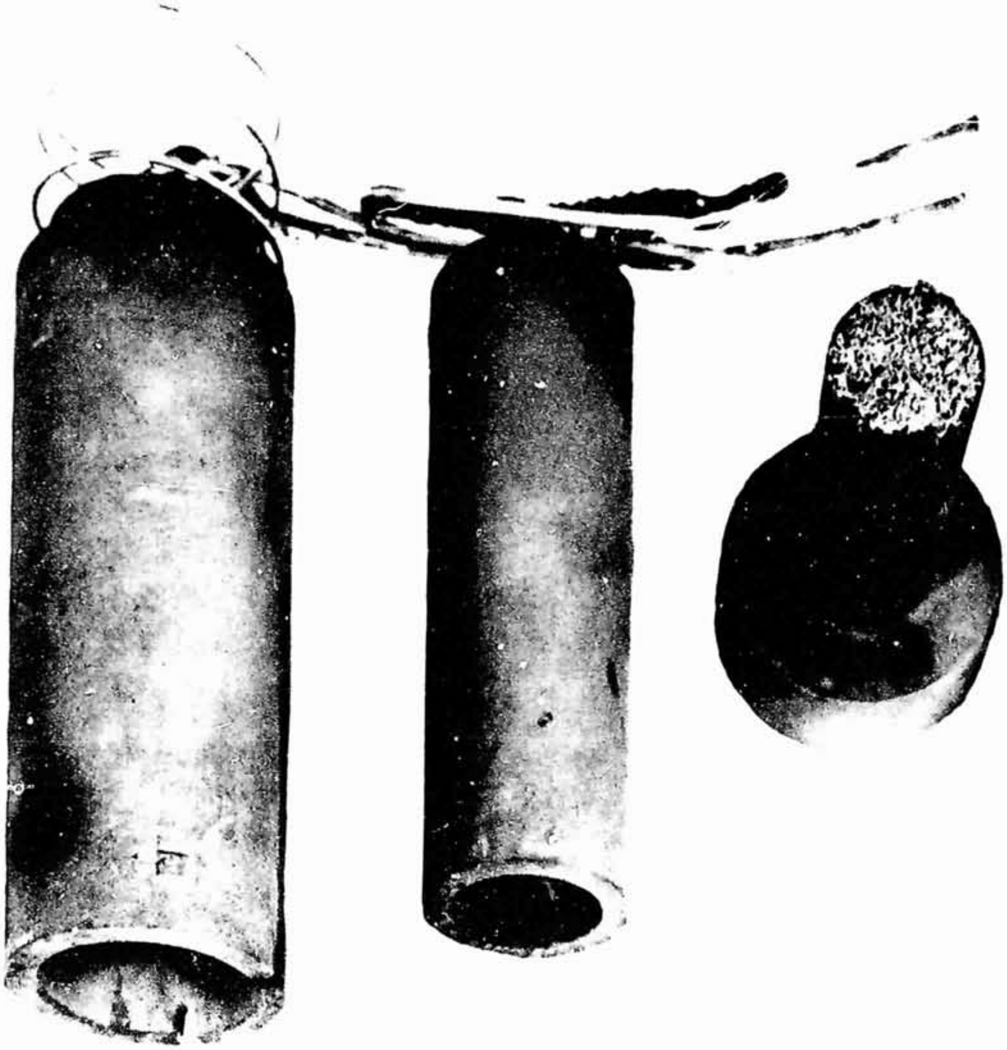

Figure 16

Graphite Crucibles and Plug after Transient
CEN-76

TABLE IV OBSERVATIONS ON IRRADIATED FUEL MATERIAL

Transient Run No.	Integrated Power MWS	Observations of Fuel Material
CEN-73	Calibration Run	The graphite fuel material was completely fragmented. Most segments were under an eighth inch maximum dimension with some fragments coarser than this size. The tungsten-tungsten/rhenium thermocouple reacted with the beryllia sheath as expected from the anomalous thermocouple readings taken during the last calibration run.
CEN-74	386	The graphite fuel was fragmented as in the previous experiment. Preliminary examination indicated that the approximate size range was similar to that in CEN-73. In addition, some graphite powder was found at the bottom of the autoclave. The source of this graphite powder is not known at the present time.
CEN-75	645	The graphite fuel was completely fragmented and appeared to be finer in size than either CEN-73 or 74. There were some indications that the fuel might be somewhat spongy. It was noted that the fuel coated on the graphite plug which held the fuel sample in place. Graphite powder was also found on the bottom of this autoclave.
CEN-76	885	As in previous experiments, the fuel was completely fragment[illegible] with the particle size finer than CEN-75. The fuel coated the plug to a greater extent than in CEN-75. Low power microscopic examination revealed some evidence for fused material. It is possible that this may be agglomerated UC_2.

~~CONFIDENTIAL~~
~~RESTRICTED DATA~~
~~Atomic Energy Act - 1954~~

Astronuclear

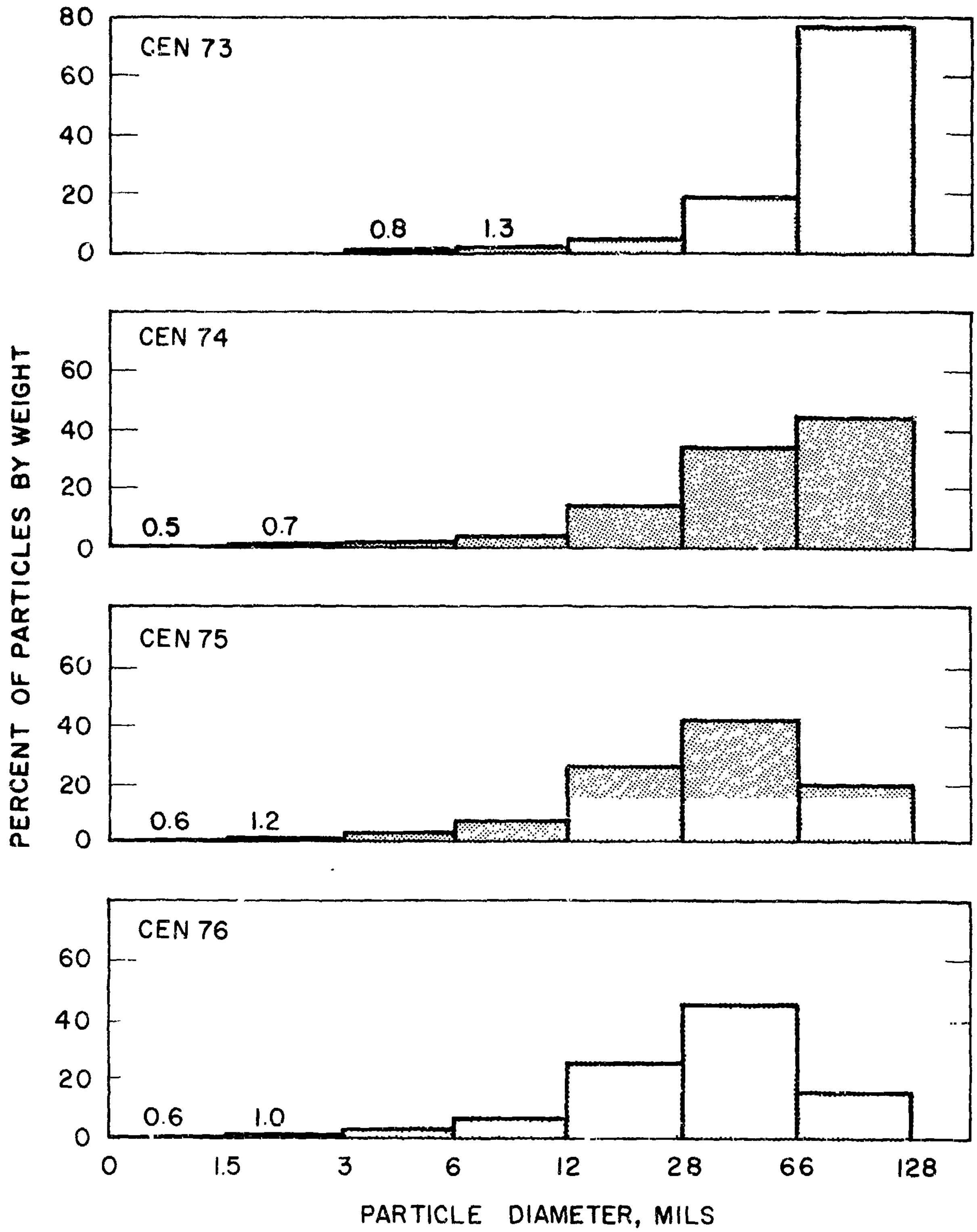

Figure 17 547064

Particle Size Distribution of Fragmented NERVA Fuel

~~CONFIDENTIAL~~
~~RESTRICTED DATA~~
~~Atomic Energy Act - 1954~~

TABLE V RESULTS OF PARTICLE SIZE MEASUREMENTS ON FRAGMENTED FUEL

Transient Run No.	Integrated Power MWS	Average Particle Size
CEN-73	Several Transients	62.4
CEN-74	386	31.7
CEN-75	645	23.3
CEN-76	885	22.0

By comparing the data on mean diameters with the integrated power of the reactor pulse, it is evident that there is a trend towards smaller particles as the burst becomes more energetic. It is postulated that the relatively large value of the average particle size (62.4 mils) for CEN-73 is caused by fragmentation of the fuel at one of the lower energy bursts and that the additional more energetic transients cause only negligible changes in geometry. Figure 18 shows a plot of the average particle size versus integrated power of the transients. The particle size data is consistent with the interpretation that the fragmentation occurred in the vicinity of 200 MWS, at which energy the experimental curve shown in Figure 4 departed from the calculated curve for adiabatic heating. Since the original fuel cylinder had a diameter of 0.5 inch, it is apparent that the specific surface area of the fuel has increased by a factor of about 25 as a result of the fragmentation during transients CEN-75 and 76.

Results of radiochemical analysis of the fragmented fuel and flux monitor foils are presented in Table VI. The differences in the results obtained from the fuel and flux monitor foils can be accounted for in the following manner; the results obtained on the foils must be corrected for the flux depression through the stainless steel capsule and through the fuel sample. The flux depression through the capsule is approximately 20 per cent whereas in the fuel it is between 15 and 20 per cent. A total correction of about 35 per cent brings the results in close agreement. The experimental data were then used to calculate the total heat input and the integrated neutron flux. The present results indicate that the integrated flux is approximately 50 per cent higher than obtained in similar ANL experiments on metal fuel samples. The difference in integrated flux is related to the presence of graphite in and around the capsule in the present experiments and to the use of zircalloy-2 rather than stainless steel dummy fuel elements. Figures 19 and 20 show the flux and calculated adiabatic fuel temperature for the ANL data and for the present data.

~~CONFIDENTIAL~~
~~RESTRICTED DATA~~
~~Atomic Energy Act - 1954~~

Astronuclear

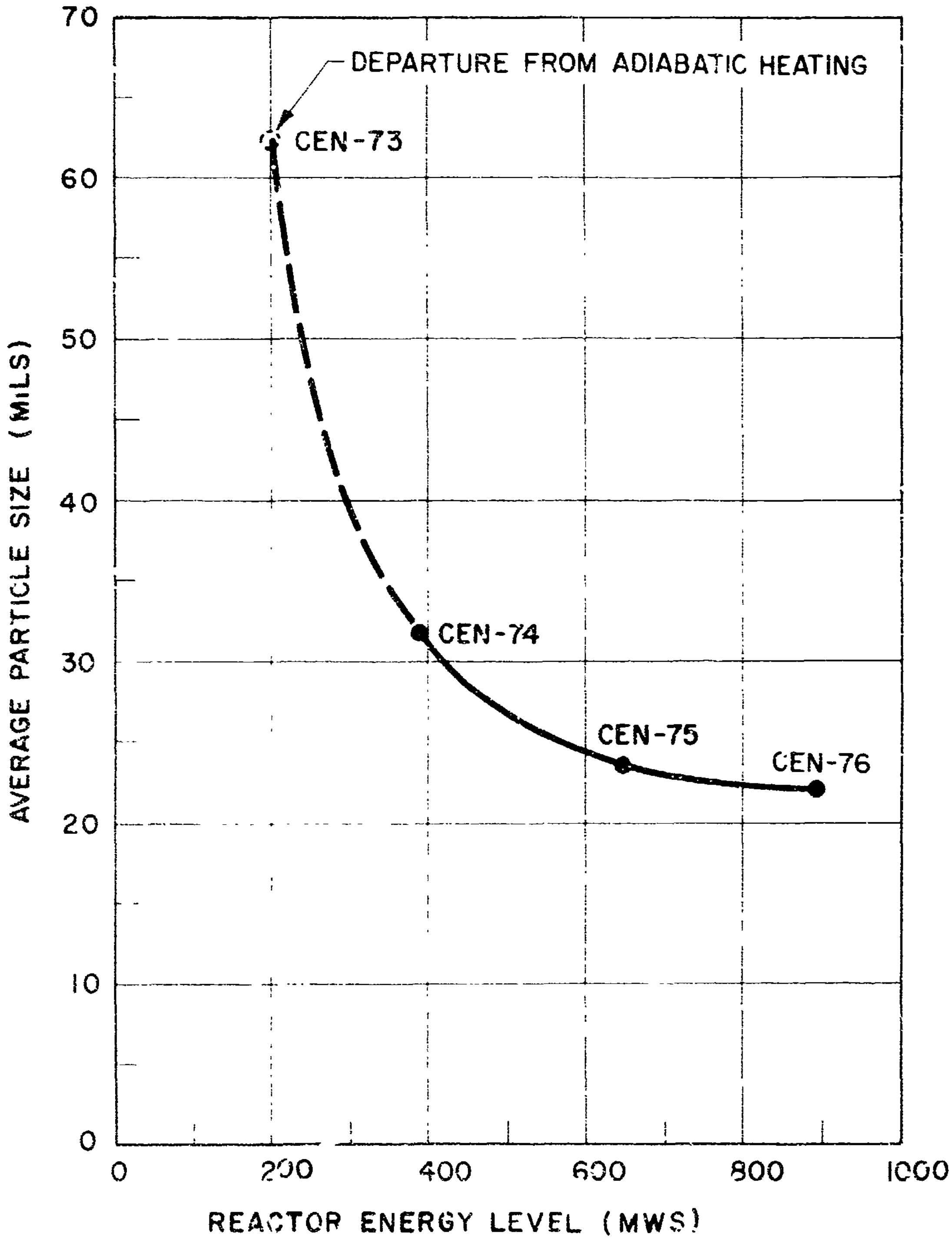

Figure 18 547013

Average Particle Size of Fragmented Fuel as a Function of Reactor Energy Level

~~CONFIDENTIAL~~
~~RESTRICTED DATA~~
~~Atomic Energy Act - 1954~~

TABLE VI RESULTS OF RADIOCHEMICAL ANALYSIS OF FRAGMENTED FUEL AND URANIUM FLUX MONITORS

Sample Number	Integrated Dose MWS	Fissions per Milligram of $U^{235} \times 10^{-12}$ Fuel*	Flux Monitor**	Ratio of Flux Monitor Data to Fuel Data	Fraction of Activity Lost from Sample
74	386	0.98	1.27	1.30	0.33
75	645	1.74	2.38	1.37	0.58
76	887	2.35	3.33	1.42	0.51***

* Radiochemical analysis of Mo^{99} in fragmented fuel material. Results reported by LASL with probable error of $\pm$ 5%.

** Radiochemical analysis of Zr^{95} in uranium flux monitor fuels located on outside surface of stainless steel irradiation capsule. Results obtained by ANL with probable error of $\pm$ 5%.

*** Value probably too low because portion of sample which collected on centering plug was not included in analysis.

CONFIDENTIAL
RESTRICTED DATA
Atomic Energy Act 1954

Astronuclear

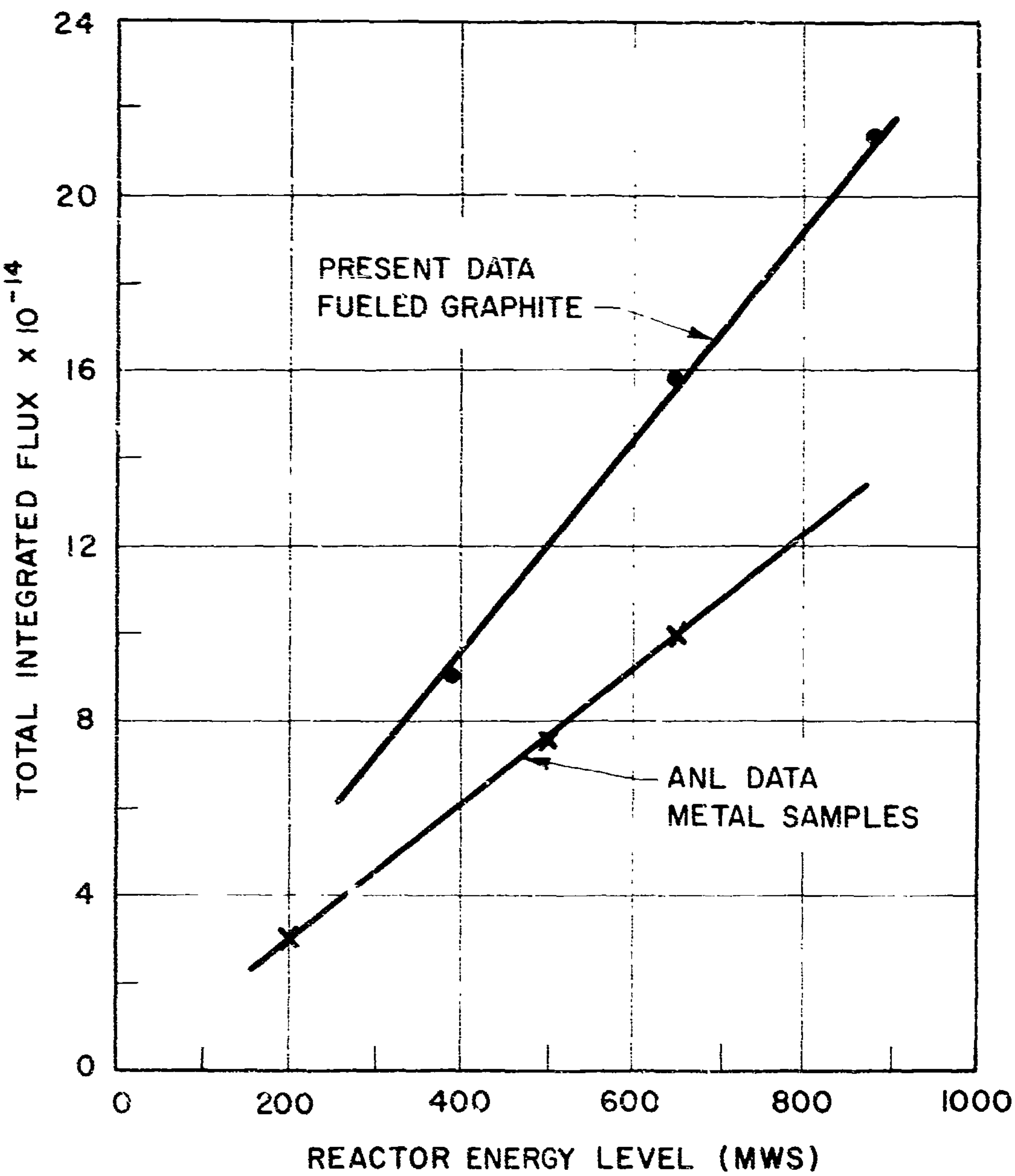

Figure 19 547012

Integrated Neutron Flux as a Function of Reactor Energy Level

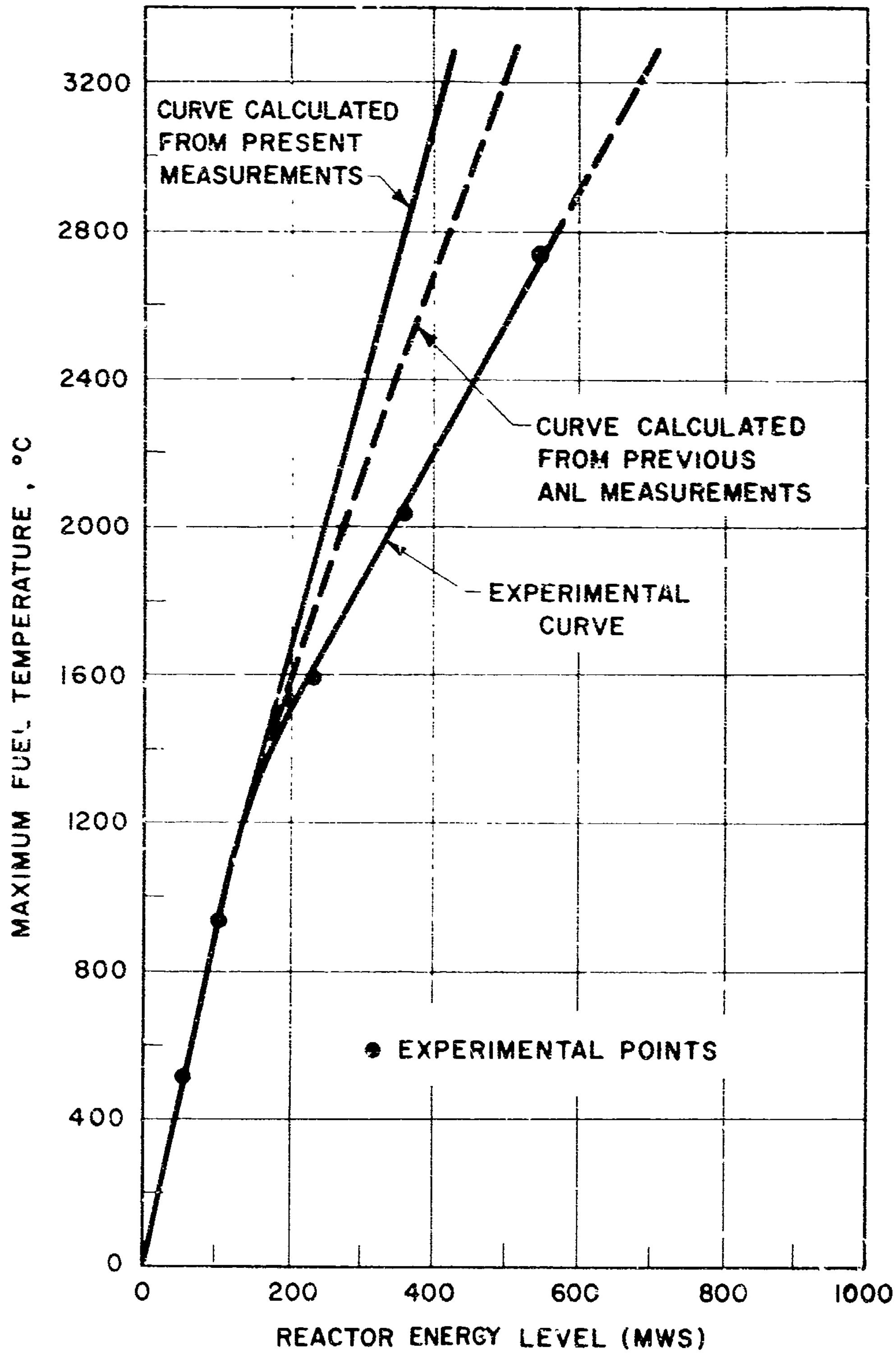

Figure 20 547011

Comparison of Calculated and Experimental Results for First Series of TREAT Experiments

Figure 21 shows the fraction of total activity produced in particles of a given size range. A comparison of this data with the particle size histograms presented previously in Figure 17 shows that there is a greater loss of activity in the larger size particles than in the smaller size particles. This is shown in Figure 22 where the activity remaining, "AR" value, for particles of a given size is plotted as a function of the average particle size of a particle size group. The "AR" value for a particular size group is given by:

$$\text{"AR"} = \frac{\text{Activity in Particles/Total Activity Produced}}{\text{Weight of Particles/Total Weight of Particles}}$$

This result is somewhat unexpected since, at first thought, it would be anticipated that the fission product release would be greater for the small size particles than the large size particles. However, the observation may be explained when one considers that the larger particles cool at a slower rate than the smaller particles. The slower cooling rate of the large particles may account for the greater fission product release.

4.0 DISCUSSION OF RESULTS

The most significant results of the first series of transient experiments on uncoated (off-the-shelf) KIWI B-4 fuel material was the fragmentation of the fuel samples in all cases. Of particular interest is the determination of the integrated power which caused the initiation of fracture. Examination of the available data indicates that fragmentation occurs at an integrated power level of about 200 MWS or a maximum fuel temperature of about 1500°C. The indirect evidence which supports this view is as follows:

a. Examination of Figure 20, the maximum fuel temperature versus integrated power, shows that the deviation of the actual

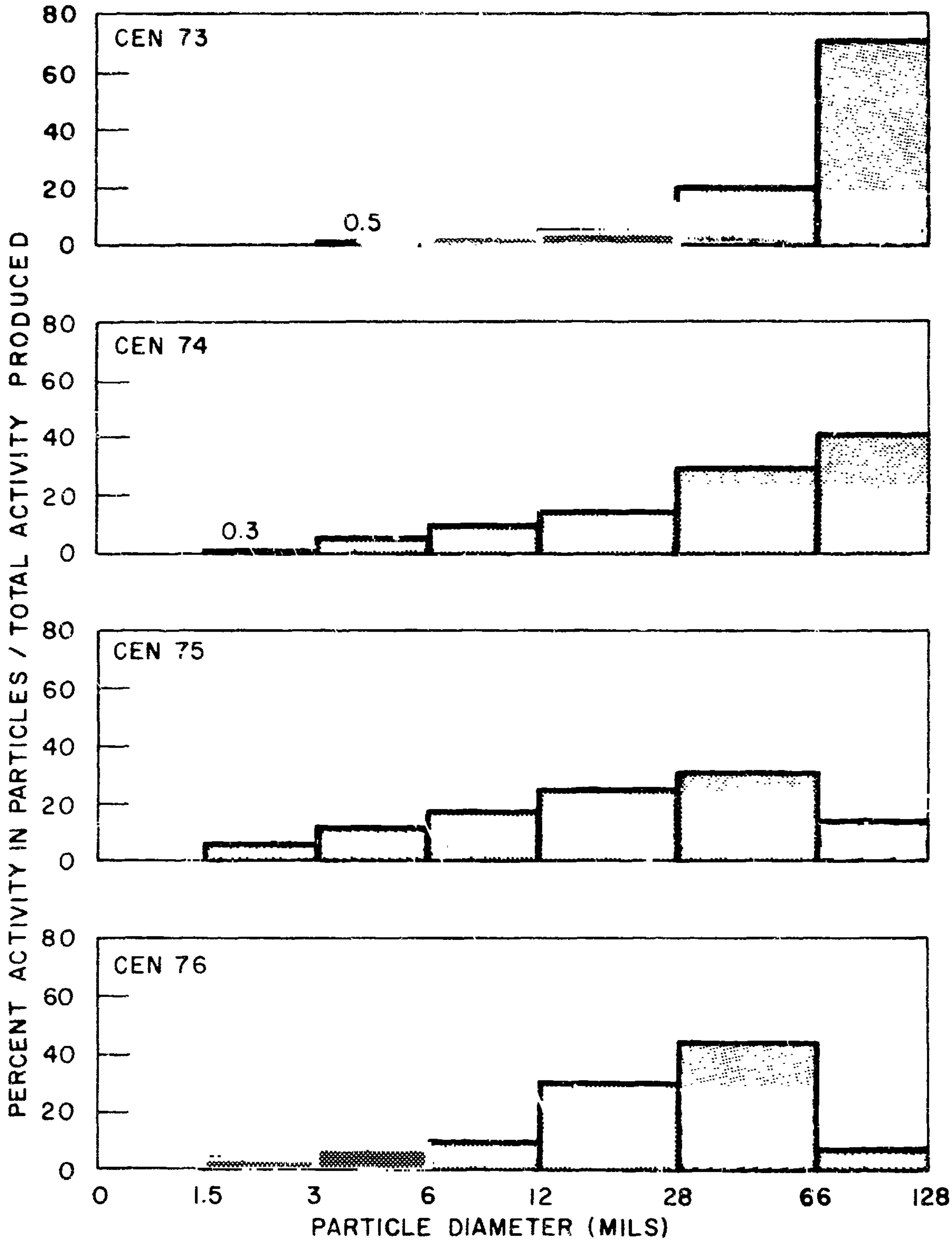

Figure 21

547039

Distribution of Activity in Particles of a Given Size Range

~~CONFIDENTIAL~~
~~RESTRICTED DATA~~
~~Atomic Energy Act 1954~~

Astronuclear

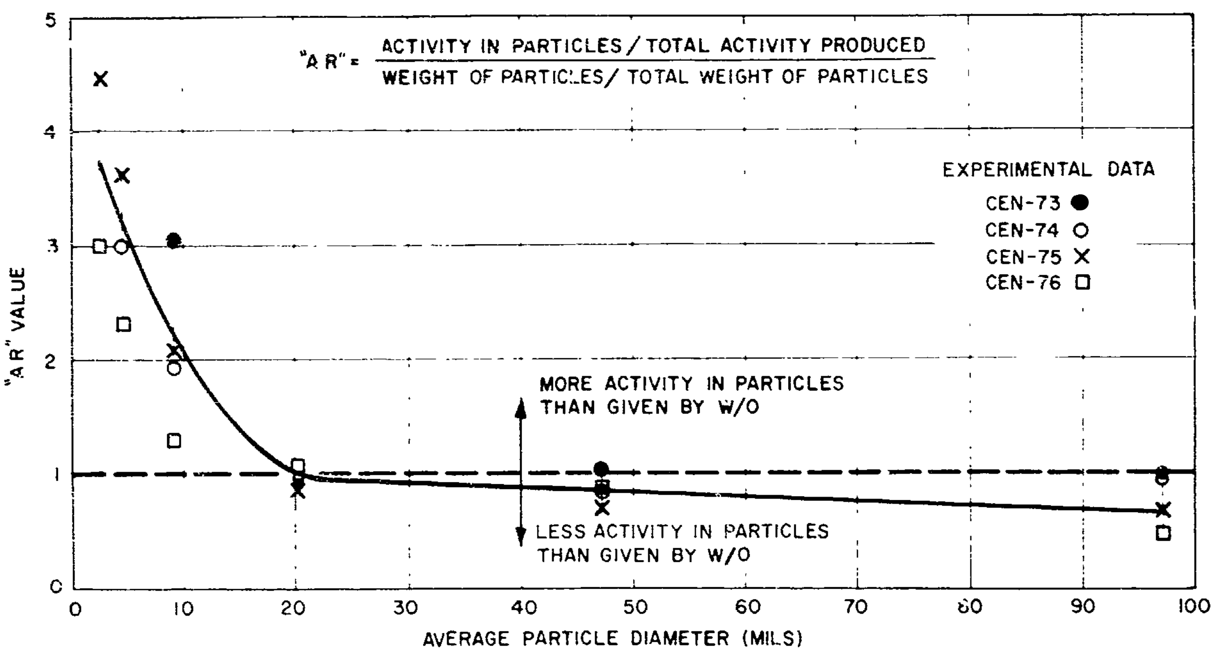

~~CONFIDENTIAL~~
~~RESTRICTED DATA~~
~~Atomic Energy Act 1954~~

Figure 22 547014

"AR" Values as a Function of Particle Size experimental data from the calculated curves for adiabatic heating occurs in the vicinity of 200 MWS. This result is consistent with fragmentation occurring at this integrated power level since departure from adiabatic heating would be enhanced by an increase in the surface area of the fuel as a result of fragmentation.

b. Examination of the time-temperature histories (Figure 7) obtained in the calibration series reveals some irregularity in temperature in the transient at 195 MWS. The tentative assumption is that the irregularity may be related to the fragmentation of the fuel during this portion of the transient. The data on heating and cooling rates given in Table II, however, do not reveal any clear-cut evidence for fragmentation of the fuel in the vicinity of 200 MWS.

c. Consideration of Figure 18, plot of the average particle size of the fragmented fuel versus integrated power, shows that the data obtained in the calibration experiment are consistent with similar data obtained in the other transient experiments when the fragmentation is considered to occur at approximately 200 MWS.

Prior to an examination of the possible mechanisms for fragmentation of fueled graphite by a nuclear transient, it is important to consider the characteristics of the fuel material itself. The experiments described were performed on uncoated off-the-shelf sections of KIWI B-4 fuel elements. The fabricated fuel consists of a dispersion of UC_2 particles (~5 microns in diameter) in graphite. The uranium loading was 400 milligrams per cubic centimeter. During subsequent exposure of this fuel to air, there is partial hydrolysis which gives rise to a considerable amount of UO_2 (estimated at 20 per cent of total UC_2) and associated hydrolysis products. Other forms of KIWI B-4 fuel which are of interest include:

a. Completely carbided fuel: This is identical to off-the-shelf fuel described above except that precautions have been taken to prevent the hydrolysis reaction.

b. Coated fuel: This may be either off-the-shelf or completely carbided fuel which is completely coated with pyrolytic graphite or coated with pyrolytic graphite on all surfaces except along the holes where a niobium carbide cladding is used.

Future experiments already in progress will evaluate the stability of these latter two kinds of fuel under transient reactor irradiation.

Theoretical consideration of the possible mechanisms of fragmentation of fueled graphite indicate that the following phenomena must be considered:

a. Thermal shock: A sudden rise in temperature of the fuel will give rise to anisotropic expansion and temperature gradients in the graphite crystals which make up the bulk of the fuel. The resulting local stresses may give rise to internal cracking which can lead to fuel fragmentation.

b. In off-the-shelf fuel material, an internal pressure buildup can occur due to a reaction between UO_2 and carbon to form either carbon monoxide or carbon dioxide gas. The free energy for this reaction becomes negative at about 1500°C. If the reaction proceeds rapidly as compared to the ability of the generated gas to diffuse away from the reaction interface then local pressures as high as 10,000 atmospheres could be generated. This internal pressure could cause destruction of the fuel.

c. Another mechanism for internal pressure buildup in off-the-shelf fuel is due to the decomposition of the hydrolysis products. This reaction cannot be specified in detail since the nature of the products formed in the hydrolysis reaction given by:

$$UC_2 + H_2O \rightarrow UO_2 + C_xH_yO_z \text{ combinations}$$

are unknown. However, decomposition of the various possible organic materials ($C_xH_yO_z$) can give rise to locally high pressures.

d. In completely carbided fuel material fragmentation may occur in the following manner. Vaporization of carbon and expansion of entrapped gas in the porous fuel material may give rise to internal pressures of the order of 10-20 atmospheres which could result in fragmentation of the graphite at temperatures in the vicinity of the sublimation temperature. Work reported by Malmstrom, Keen, and Green,[2] indicate that the tensile strength of graphite decreases to about 100 psi at temperatures in the vicinity of 3200°C. It is thus apparent that the pressures of the order of 10-20 atmospheres may initiate fragmentation of fueled graphite at temperatures of the order of the sublimation temperature, i.e., 3350°C. The value of 3350°C for the sublimation temperature of graphite was obtained in recent work at National Carbon Company.[3]

e. Destruction of completely carbided fuel might also occur by melting which can occur at the triple point at approximately $3570^{\circ}C$ and 100 atmospheres.[3] Destruction of the fuel could occur as a result of the rapid release of the entrapped gases within the fuel resulting in dispersion of the liquid phase.

The explanation for the behavior of the off-the-shelf fuel material used in the present series of experiments may be related to one or more of the first three mechanisms described above. Further experimental evidence obtained by Los Alamos Scientific Laboratory (LASL) on electrical heating of fueled and unfueled graphite indicated that the thermal shock mechanism is probably not responsible for the observed fragmentation.[4] The LASL experiments were performed by electrically heating a 15-inch length of 7-hole KIWI B-4 off-the-shelf fuel material by means of a 3.5 megawatt power supply while the fuel was exposed to air. The results obtained are described in Table VII. The results indicate that hydrolyzed fuel material fragments under transient electrical heating whereas completely carbided material or non-fueled graphite will not fragment. Thus, it is apparent that either the presence of UO_2 or the hydrolysis products are responsible for fragmentation of the fuel in the electrical heating experiments. Their results indicate that thermal shock alone is not the cause of fragmentation in the nuclear transient experiments and that the hydrolysis products may be intimately connected with the fragmentation. Additional transient nuclear experiments on off-the-shelf fuel at integrated power levels near 100-200 MWS are expecred to shed further light on this question.

TABLE VII RESULTS OF LASL ELECTRICAL HEATING EXPERIMENTS

	Sample	Energy Given to Sample	Sample Appearance
1.	Lined and loaded off-the-shelf fuel elements	750 kilo-calories in 1.5-2 seconds	All elements burst into small pieces. At the higher voltages some arcing was observed.
2.	Freshly carbided elements	200 kilo-calories	Elements did not burst but burned in two.
3.	Loaded and lined fuel elements that had been reacted to oxide by being stored in a humidity cabinet	130 kilo-calories	All elements burst.
4.	Unloaded fuel elements		Did not burst.

It should be noted that the fragmentation of fuel material at integrated power levels of the order of 200 MWS places an upper limit on the startup transients which can be used for the NERVA engine. For example, a 200 MWS transient in the TREAT reactor corresponds to a 4600 MWS transient in the NERVA engine. This indicates that the startup transients less than about 4500 MWS are necessary to prevent possible accidents with fuel material which may have become hydrolyzed during storage prior to reactor startup.

TREAT EXPERIMENTS

5.0 FUTURE WORK

The second and third series of transient experiments are in progress at this time. The second series involves the irradiation of uncoated off-the-shelf sections of KIWI B-4 fuel material in transients of the order of 100-200 MWS to determine the reactor energy required to initiate fragmentation.* The third series of experiments, involving five capsules, consists of the following:

a. A temperature calibration will be made on an uncoated fully carbided KIWI B-4 fuel specimen in a helium atmosphere. The instrumentation in the capsule is designed to detect fragmentation of the fuel during the transient.

---

*Preliminary results indicate that the two samples making up the second series of experiments were pulsed at energies of 115 and 250 MWS. Cursory inspection of the fuel material indicates that the specimen irradiated at 115 MWS was perfectly intact, whereas the sample irradiated at 250 MWS showed some cracking at the upper edges of the sample. Thus, it appears that fragmentation is initiated at about 250 MWS.

b. An uncoated, fully carbided specimen will be subjected to a high energy pulse that should give rise to disintegration of the sample as indicated from the results of the previous test. As in the first test in this third series, the sample will be a helium atmosphere.

c. This experiment is similar to the previous one except that the sample will be in vacuum.

d. This experiment is designed to permit determination of the extent of chemical reaction between water and off-the-shelf KIWI B-4 fuel material coated with pyrolytic graphite. As in the case of the first experiment in this third series, the instrumentation in the container is designed to detect fragmentation of the sample.

e. Similar to experiment 4, except that a higher energy transient will be delivered to the sample.

Regarding the expected behavior of the fully carbided material, the theoretical analysis of possible mechanisms of fragmentation described in the previous section should be noted. The analysis indicated that fragmentation might be expected in the vicinity of the sublimation temperature (3350°C) or as a result of melting (3570°C, 100 atmospheres). From Figure 20 it can be seen that the integrated power required to achieve these temperatures is greater than 400 MWS in the TREAT reactor. This corresponds to approximately 10,000 MWS in the NERVA engine. Thus, the theoretical analysis indicates that fragmentation of completely carbided fuel material may not be a possible means of core destruction. * However, chemical treatment of the carbided

*Preliminary evidence from the third series of TREAT tests indicates that the carbided fuel material was intact after a 540 MWS transient.

fuel, prior to or during a nuclear transient may offer a means for destroying the core. Various methods of chemically treating the carbided fuel are being considered.

Finally, a recent re-evaluation of the primary objectives of the transient reactor experiments has led to the decision to design experiments to provide basic information on:

a. The disintegration mechanism of off-the-shelf type and fully carbided fuel samples when subjected to high energy neutron induced transients when the samples are placed in vacuum, inert gas or water.

b. The existence or non-existence of an explosive water reaction with KIWI B-4 fuel.

c. The effect of initial sample temperature on the break up threshold and particle size distribution of various forms of KIWI B-4 fuel.

d. The safe KIWI startup conditions for fully carbided versus partially carbided fuel material.

e. Determination of the equation of state for KIWI B-4 fueled graphite under reactor transient conditions.

Long-range planning of experiments to accomplish these goals is presently underway. It is apparent that transient reactor experiments will be extremely useful in providing a better understanding of the behavior of the NERVA fuel material under a variety of environmental conditions.

6.0 CONCLUSIONS:

a. The principal conclusion reached, based on the work completed, is that uncoated sections of off-the-shelf KIWI B-4 fuel material will fragment when pulsed with a nuclear transient of the order of 200 MWS, in the TREAT reactor. An equivalent pulse can be delivered in the nuclear rocket by a transient of the order of 5000 MWS. Fragmentation initiated by the transient gives rise to the formation of particles less than approximately 1/8 inch in diameter.

b. Theoretical consideration of the mechanisms of fragmentation of KIWI B-4 fuel material indicates that the most probable mechanism of fragmentation of the off-the-shelf fuel (partially hydrolyzed) is due to internal pressure buildup from either reaction between UO_2 and carbon or the decomposition of the products of the hydrolysis reaction. Both the results of electric heating experiments performed at LASL and the present results obtained in the transient experiments are consistent with the proposed mechanism.

c. Fission product release accompanying the fragmentation of the fuel gives rise to loss in activity of from 30 to 60 per cent. The fission product release is greater for the larger particles than the smaller particles, presumably because of the slower cooling rate of the large particles.

d. Transient reactor experiments offer a means of obtaining basic information on behavior of NERVA fuel material relative to: a) the use of a nuclear transient as a destruct device; b) reactions between KIWI B-4 fuel and water; c) safe startup conditions for the reactor; d) and the equation of state of fueled graphite. These items form the basis for further work in this program.

7.0 ACKNOWLEDGMENTS

The experimental work described in this report is the result of the efforts of a considerable number of people located at various sites throughout the country. The most active participants in this work included L. D. P. King, P. Wagner, W. Stratton, and E. Bryant of the Los Alamos Scientific Laboratory; L. Baker, R. C. Liimatainen, R. O. Ivins and F. Testa of the Chemical Engineering Division, Argonne National Laboratory; J. Boland and S. Lawroski of TREAT Reactor (Argonne National Laboratory); and W. H. Esselman, A. B. Rothman, M. A. Vogel, E. V. Anderson, and C. Boehmer of the Westinghouse Astronuclear Laboratory. The authors are grateful to S. Lawroski and R. C. Vogel of the Chemical Engineering Division, Argonne National Laboratory for permission to use their facilities for this program. The photographs given in the report are presented with the permission of Argonne National Laboratory.

REFERENCES

1. Monthly Progress Reports, Chemical Engineering Division, Argonne National Laboratory, 1960, 1961 and 1962. A summary report will be issued early in 1962.

2. C. Malmstrom, R. Keen, and L. Green, Jr., "Some Mechanical Properties of Graphite at Elevated Temperatures," Jnl. Appl. Phys. 22, 5, 1951.

3. M. T. Jones, "The Phase Diagram of Carbon," National Carbon Research Laboratories, Parma, Ohio, PRC-3, 1958.

4. Monthly Status Report for LASL NERVA Activities for Period Ending November 20, 1961, LAMS-2645, (Confidential).

~~CONFIDENTIAL~~
~~RESTRICTED DATA~~
~~Atomic Energy Act - 1954~~

Astronuclear
WANL-TNR-039

WESTINGHOUSE ELECTRIC CORPORATION
ASTRONUCLEAR LABORATORY
P. O. Box 10864
Pittsburgh 36, Pa.
March, 1962

RE-ENTRY AND BURNUP OF REACTOR FRAGMENTS

(Title Unclassified)

NERVA NUCLEAR SUBSYSTEM

~~CONFIDENTIAL~~
~~RESTRICTED DATA~~
~~Atomic Energy Act - 1954~~

TABLE OF CONTENTS

			Page
1.0	Introduction		1
2.0	Analytical Program		3
	2.1	Computer Program	6
	2.1.1	Environmental Conditions During Re-Entry	6
	2.1.2	Analytical Model	7
	2.1.3	Trajectory Calculations	9
	2.1.4	Convective Aerodynamic Heating	13
	2.1.5	Average Convective Heating	14
	2.1.6	Radiation Heating	15
	2.1.7	Oxidation	15
	2.1.8	Sublimation	
	2.1.9	Fission Product Decay Heat	18
	2.1.10	Calculation of Particle Surface Temperatures	19
	2.1.11	Summary of Program Formulation	20
	2.2	Presentation of Analytical Results	21
3.0	Experimental Program		25
	3.1	Experimental Procedure	27
	3.2	Test Results	29
	3.3	Discussion of Results	34
	3.4	Comparison of Experimental Data with Scala's Theory	35

TABLE OF CONTENTS
(continued)

		Page
4.0	Future Work Program	37
	4.1 Analytical Program	37
	4.2 Experimental Program	38
5.0	Summary and Conclusions	39

TABLES

No.	Title	Page
3.1	Summary of Test Point Data	30
3.2	Model Weight Loss Rates	31
3.3	Comparison of Experimental Data with Scala's Theory on Graphite Burnup During Re-Entry	36

REFERENCES

1 through 13 ... 43

LIST OF FIGURES

No.	Title	Page
2.1	Graphite Particle Re-Entry Analytical Model	44
2.2	Analytical Cases for Grahpite Particle Re-Entry	45
2.3	Particle Velocity as a Function of Altitude	46

LIST OF FIGURES
(continued)

No.	Figure	Page
2.4	Particle Velocity as a Function of Altitude	47
2.5	Particle Velocity as a Function of Altitude	48
2.6	Particle Velocity as a Function of Altitude	49
2.7	Particle Velocity as a Function of Altitude	50
2.8	Particle Velocity as a Function of Altitude	51
2.9	Particle Velocity as a Function of Altitude	52
2.10	Particle Radius as a Function of Altitude	53
2.11	Percent Mass Consumed as a Function of Altitude	54
2.12	Stagnation Point Heat Flux as a Function of Altitude	55
2.13	Stagnation Point Heat Flux as a Function of Altitude	56
2.14	Particle Surface Temperature as a Function of Altitude	57
3.1	Representative Surface Temperature for Half-inch Model	58
3.2	Representative Surface Temperature for Quarter-inch Model	59
3.3	Representative Surface Temperature for Eighth-inch Model	60

LIST OF FIGURES
(continued)

No.	Title	Page
3.4	Weight Loss Rate-Point B	61
3.5	Weight Loss Rate- Point C	62
3.6	Weight Loss Rate-Point D	63
3.7	Specimen Surface Temperature as a Function of Exposure Time	64
3.8	Specimen Surface Temperature as a Function of Exposure Time	65
3.9	Specimen Surface Temperature as a Function of Exposure Time	66
3.10	Specimen Surface Temperature as a Function of Exposure Time	67
3.11	Specimen Surface Temperature as a Function of Exposure Time	68
3.12	Specimen Surface Temperature as a Function of Exposure Time	69
3.13	Specimen Surface Temperature as a Function of Exposure Time	70
3.14	Specimen Surface Temperature as a Function of Exposure Time	71
3.15	Specimen Surface Temperature as a Function of Exposure Time	72
3.16	Specimen Surface Temperature as a Function of Exposure Time	73

Astronuclear

WANL-TNR-039

RE-ENTRY HEATING AND BURN-UP OF REACTOR FRAGMENTS

1.0 INTRODUCTION

A major objective of the NERVA flight safety program is to establish that re-entry of the rocket engine does not introduce a hazard to the general population. One method of controlling this problem is to break the core into small fragments and to rely on the aerodynamic heating at re-entry to reduce the particles to an acceptable size and level of radioactivity. One criterion for particle size which has been presented in the literature (1) (2) is that the particles sizes should be 25 microns or less when they reach an altitude of 100,000 feet. Particles of this size would be widely dispersed in the atmosphere. This criteria is based on conservative assumptions, and it is desirable to determine the largest size particles which can be tolerated. Larger allowable particle sizes will reduce the requirements on the explosive destruct system.

Calculations have been made which show that flight safety requirements cannot be met if the integral core enters the atmosphere and is allowed to undergo a "passive" re-entry, subject only to aerodynamic heating. Preliminary considerations show that initial particle sizes of 1/32 to 1/64 inch at re-entry will result in particles which meet the 25 micron criterion at 100,000 feet. A modified criterion may allow diameters of particles which can be met by a conventional destruct system. Such a system could conceivably utilize the thermochemical methods, nuclear excursions, explosives or integral additives to reduce the reactor to small particles.

It is the purpose of this study to establish the amount of particle burn-up which can be expected during re-entry. This information will be obtained for various size particles and will be combined with data being obtained on allowable particle sizes reaching the earth and reactor destruct capabilities to establish a criteria for orbital or near-orbital core disposal.

Both a theoretical and experimental approach have been initiated to study this problem.

The theoretical approach reported in Section 2 involves the incorporation of one of the existing oxidation theories[3] into a digital computer program. This program calculates the fate of a re-entry particle based upon various initial velocities and angles of re-entry. The analyses include the effects of aerodynamic heating, radiation from the particle and decay heat from fission products. Previous investigations had not taken all of these features into account. The initial conditions which are used in analyses are those believed to be realistic with respect to re-entry of the NERVA engine particles.

The experimental approach described in Section 3 is based upon using an arc plasma wind tunnel in which specimens of graphite and fuel graphite are exposed to simulated re-entry conditions. The re-entry conditions for the particle at a particular altitude and velocity are simulated by proper adjustment of gas enthalpy and mass flow rate in the experimental equipment. Mass losses due to oxidation are measured for various particle sizes at various exposure times.

The results from the theoretical analysis and the experimental data are then compared to determine the degree of validity of the theory. If verified, the theory can be applied under a variety of re-entry conditions to preduct the particle burn-up at various altitudes.

The first phase of the work has dealt primarily with unfueled material (pure graphite). This was chosen because the available theory only applied to this material. Once theory and experiment can be reconciled for pure graphite, modification of the theory to account for the behavior of fueled graphite would be undertaken.

The subsequent phases of work will be primarily concerned with extension of present techniques to the study of fueled materials, with some work being done to complete the data on pure graphite. The final goal as noted previously is specification of the maximum particle size for the core destruct system.

2.0 ANALYTICAL PROGRAM

Analysis has shown that there will be insufficient heat generated by convective aerodynamic heating during re-entry of a NERVA reactor to accomplish complete burn-up before ground or water impact. Consequently, an active or passive type of destruct system is contemplated whereby the integral reactor will be reduced to a large number of small particles at the time of re-entry. These particles will be sufficiently small to achieve complete combustion or dispersion of the material as an aerosol. This can be done by reducing the size, since the aerodynamic stagnation point heating rate is inversely proportional to the square root of the body radius.

The reason that an analytical technique for prediction of burn-up is required is because complete combustion cannot be achieved in any known experimental equipment for the materials and particle sizes considered in this study. Therefore, a verified model must be constructed to predict when this event will occur under any re-entry condition.

There are no analytical or experimental data available on the oxidation characteristics of fueled graphite at the present time. There are several published theories on the oxidation of pure graphite in high velocity gas streams [(3)(4)(5)(6)]. In order to develop a reasonable analytical model for the behavior of fuel material, it is first necessary to develop a verified model based on unfueled material. As noted before, such a theory can be modified to take the fuel characteristics into account. The oxidation rates of fueled and unfueled graphite can be compared experimentally in an arc wind tunnel, thus furnishing a base for theory modification.

There are several factors to be considered in the fueled graphite analysis which make it different from pure graphite. One involves the effective surface distribution of fuel in the matrix (UC_2 in C). Since oxidation is primarily a surface phenomenon, the actual coverage of available area by UC_2 is important. If there is sufficient space between fuel particles and graphite particles to permit elemental graphite to oxidize, its behavior will be akin to that of pure graphite, provided sufficient oxygen is available for the reaction to proceed unimpeded. Another factor is that the oxidation rates of fueled graphite material are believed to be somewhat greater than for pure graphite because of greater porosity and the presence of UC_2 in the fueled material. However, no information has yet been obtained to verify this.

The initial analytical study on unfueled graphite is based on developing an IBM 7090 digital computer program. This program was formulated incorporating the following parameters:

a. An initial circular orbit at an altitude of 300 nautical miles is assumed. This is consistent with early flight mission plans for the NERVA engine.

b. Re-entry angles from 1° to 90° are assumed, thus covering the complete range of possible re-entry flight paths.

c. Re-entry velocity of 25, 000 ft/sec is selected as being a reasonable value for re-entry from the assumed orbit.

d. A sphere is selected as the particle shape because of the simplicity of the mathematical treatment. This is conservative since the surface area-to-volume ratio is smaller for a sphere than for any other shape. Actual particles would probably burn more rapidly upon re-entry because of presence of greater surface areas.

e. The analytical theory of S.M.Scala for graphite oxidation during re-entry is employed. The heat balance employed considers convective aerodynamic heating, sublimation, radiation from the particle surface and fission product heating. Also considered, by virtue of the analytical theory used, are the effects of exothermic heats of combustion of carbon in the boundary layer and the heat blocking effect of combustion products in the boundary layer. The effects of radiation from ionized air in the stagnation region are not included, but the error introduced is considered to be negligible at the altitudes and velocities of interest.

f. Calculation of particle trajectory is based on a polar co-ordinate or modified rectilinear system.

g. A continuum flow regime in the atmosphere is assumed for calculation purposes. This means that the mean free path of air molecules is very small compared to the diameter of the body.

h. Laminar heat transfer conditions are specified. No turbulence is expected on the assumed spherical shape.

i. The shape of the particle is assumed to remain the same during re-entry (a sphere) but the particle mass and diameter are changed as combustion proceeds.

j. The particle is assumed to spin because of residual angular momentum and the heat transfer is calculated to be uniform over the entire surface.

2.1 Computer Program

The following sections discuss in some detail the approaches used to formulate the computer program, from which the analytical results were derived.

2.1.1 Environmental Conditions During Re-Entry

A spinning sphere, re-entering the earth's atmosphere from altitudes above 400,000 feet, will pass through three flow regimes during its descent. These regimes are defined as "free molecule", "slip", and "continuum", and deal with the effects of air density on kinetic energy transmitted to the body in the form of aerodynamic heating. It is convenient to define the Knudsen Number (N_{kn}) which relates a characteristic body dimension (diameter in the case of a sphere) to the mean free path of air molecules at any stated altitude. This relationship is $N_{kn} = \frac{Mo}{D_b}$ (Mo = mean free path of molecules; D_b = characteristic body dimension). The three flow regimes are defined in terms of this number as follows:

$N_{kn} \geq 2$	Free Molecule Flow
$2 > N_{kn} > 0.1$	Slip Flow
$N_{kn} \leq 0.1$	Continuum Flow

Free molecule flow exists at high altitudes. The "slip" regime is a narrow transition region between free-molecule and continuum flow. Continuum flow exists at the lower altitudes where maximum heating rates occur. It may be noted that the free molecule regime will persist to progressively lower altitudes with decreasing size of the re-entering particle. In the range of particle sizes to be considered (1/64 inch to 1 inch diameter), it can be shown by calculation of the Knudsen Number that the smaller particles will be in the free molecule flow regime for a significant portion of their flight. The analysis of heating in this regime, particularly assignment of accommodation coefficients (fraction of energy transferred from gas to body) and calculation of heat input from chemical reactions, is difficult and subject to error without more detailed knowledge of oxidation mechanisms and kinetics. Since the assumption of a continuum flow regime throughout the flight trajecto tends to result in lower burn-up rates, such an analysis will give a conservative result, or a lower order of minimum particle size which could be consumed during re-entry. Such a treatment of continuum flow analysis during re-entry has been developed by S.M. Scala on a theoretical basis and appears to be generally accepted. Therefore, for the initial study conducted in this program, Scala's analysis of graphite oxidation on re-entry was used to calculate mass loss and predict burn-up characteristics. A free molecule flow analysis has not been made as yet, although it is realized that this must be done before a fully developed knowledge of re-entry behavior can be realized.

2.1.2 Analytical Model

To formulate a program for digital computer analysis of re-entry, it is necessary to develop a schematic model which includes all parameters of concern arranged in a logical functional sequence. One method of accomplishing this is to set up a block diagram in a flow analysis pattern which contains the inputs available and the outputs desired as a function of the variables involved. By processing these inputs and outputs through the functional blocks, it is possible by an iterative procedure to determine the behavior of the re-entering body throughout the flight path. If each of the descriptive equations involving behavior as a function of time, then a series of these equations can be solved to give instantaneous values of desired variables. By continuous solution with sufficiently short time intervals, the effect of iteration can be achieved by substituting the results of the previous solution into the next solution to give a continuously changing description of particle behavior during re-entry. Since the particle mass is constantly changing during re-entry due to combustion, the body diameter is also changing and its aerodynamic characteristics are changing. Therefore, this type of analysis is well suited to calculation of re-entry behavior where a continuous change of input variables is occurring.

In establishing the analytical model, the following factors which influence particle behavior are included:

a. Trajectory of the particle from initiation of re-entry to an altitude of approximately 100,000 feet as a function of particle size, mass and re-entry conditions.

b. Effective aerodynamic heat input over the forward region (stagnation point) of the particle and its resolution to effective heating over the entire particle surface.

c. Heat input due to radioactive fission product decay heat in the particle.

d. Heat radiated from the particle and its effect on particle surface temperature.

e. Particle mass loss due to oxidation at the surface.

f. Particle mass loss due to sublimation at the surface.

g. Particle radius change due to mass loss.

A diagram of this analytical model is shown in Figure II-1.

In the following sections the elements of the theoretical formulation are discussed.

2.1.3 Trajectory Calculations

The initial step in the analysis of re-entry burn-up is to determine the trajectories of the graphite particle sizes of interest. From this information, the aerodynamic heating equations of motion for a point mass may be expressed in either rectilinear or polar co-ordinate systems as follows.

Rectilinear

$$\frac{d^2x}{dt^2} = \frac{du}{dt} = \frac{-D}{M}\cos\theta - \frac{L}{M}\sin\theta - \frac{uv}{R} \quad \text{(Tangential)}$$

$$\frac{d^2y}{dt^2} = \frac{dv}{dt} = g - \frac{L}{M}\cos\theta - \frac{u^2}{R} \quad \text{(Radial)}$$

Polar

$$\frac{\ddot{}}{R}\left(2\dot{R}\dot{\theta} - R\ddot{\theta}\right) = -\frac{D}{M}\cos\theta - \frac{L}{M}\sin\theta \quad \text{(Tangential)}$$

$$\frac{}{R} = R\left(\ddot{R} - R\dot{\theta}^2\right) + g - \frac{L}{M}\cos\theta - \frac{D}{M}\sin\theta \quad \text{(Radial)}$$

	SYMBOLS	UNITS
x	distance along flight path (horiz.)	feet
y	altitude	feet
u	velocity along x-direction $\left(\frac{dx}{dt}\right)$	ft/sec.
v	velocity along y-direction $\left(\frac{dy}{dt}\right)$	ft/ sec.
t	time	sec.
M	mass of particle	lbs.
D	drag parameter	lbs. ft/sec.^{2}
L	lift parameter	lbs. ft/sec.^{2}
θ	re-entry angle	deg.
R	radius of earth + altitude	feet
g	gravitational effect	ft/sec.^{2}
$\hat{\tau}$	tangential unit vector	-
R	radial unit vector	-

SYMBOLS		UNITS
$\dot{R}$	velocity along R	ft/sec
$\dot{\theta}$	angular momentum	deg/sec
$\ddot{R}$	acceleration along R	ft/sec^2
$\ddot{\theta}$	angular acceleration	deg/sec^2

Other relationships necessary for application of the above equations are:

$$V^2 = u^2 + v^2 \qquad D = \frac{C_D \rho_A V^2 A_D}{2} \qquad L = \frac{C_L \; {}_A V^2 A_L}{2}$$

where,

V	=	resultant velocity
u	=	velocity along x-direction
D	=	drag parameter
L	=	lift parameter
C_D	=	drag coefficient
C_L	=	lift coefficient
A_D	=	reference area for drag
A_L	=	reference area for lift
ρ_A	=	atmosphere density

$$A_L = A_D = \pi r^2 \text{ for sphere}$$

The Newtonian vector notation is used to express the polar system. The most accurate solutions to the motion equations for the cases of interest are provided by the polar form, since the earth is considered to be a sphere of finite radius. Solutions have been derived from the rectilinear form by many investigators and introduce only a small error, even in the case of a shallow re-entry angle. Since $y \ll$ the distance to the earth's center for aerodynamic heating in most cases, and since the drag regime occupies a limited altitude range, such treatment is permissible.

Certain assumptions have been made to facilitate calculation of the basic trajectories. These are as follows:

a. The earth is a uniform non-rotating sphere of 2.1×10^7 feet radius.

b. The variation of atmosphere density with altitude was incorporated using the ARDC standard atmosphere of 1956[7]. Values were supplied as step input in tabular form.

c. The drag coefficient (C_D) is equal to 1 and remains constant throughout the flight. The drag coefficient varies with Mach and Reynolds numbers, but the approximation is valid at Mach numbers provided total drag is considered to be pressure drag. A planned study to be conducted soon will involve changing drag coefficients at lower velocities to evaluate the effects on trajectory of diminishing drag.

d. The lift coefficient (C_L) is equal to 0 and remains constant throughout the flight. This assumption is valid for a spinning sphere of constant shape where aerodynamic forces are equally distributed over upper and lower portions of the particle so as to provide zero pressure differential.

e. The acceleration of gravity varies with altitude. ARCD values for changing gravitational effects were supplied as step input in tabular form.

f. The re-entry angle changes constantly along the path, increasing gradually and approaching 90° in the extreme case.

g. The initial re-entry velocity has been specified as 25,000 ft/sec for all cases.

h. Particle dynamics are ignored. This is valid for a spinning, uniformly dense sphere of constant shape. This renders unnecessary the three-dimensional analysis which might be important if the particle suffered deflection on re-entry. Consequently, the analysis is treated as a two dimensional problem.

2.1.4 Convective Aerodynamic Heating

The effect of environmental conditions on particle heating during re-entry has been briefly discussed in a previous section. It is now of interest to determine what mathematical approximations can be employed to best determine actual heat flux incident on graphite particles of interest in this program.

When a particle first re-enters the atmosphere, and is in the region of free molecule flow, the stagnation point heat transfer as described by Kemp and Riddell[8] is as follows:

$$\dot{q}_s \cong 2.69 \times 10^7 \, n \left(\frac{\rho}{\rho_o}\right) \left(\frac{V}{V_E}\right)^3 \qquad \text{BTU/ft}^2\,\text{sec}$$

where:

$\dot{q}_s$ = stagnation heat flux

n = accommodation coefficient

ρ = density of air at altitude of particle

ρ_o = density of air at sea level

V = velocity of particle

V_E = initial re-entry velocity

where n is the accommodation coefficient based on energy transfer. The upper limit of this coefficient is 1 (all kinetic energy of the molecules transferred to the body). As the particle descends, the continuum flow regime is encountered where the approximate stagnation point heat flux is given by Kemp and Riddell as follows:

$$\dot{q}_s = \frac{17,600}{r_B} \left(\frac{\rho}{\rho} \right)^{1/2} \left(\frac{V}{V_E} \right)^{3.25} \left(1 - \frac{h_{wall}}{h_{gas}} \right) \text{BTU/ft}^2\text{sec}$$

where r_B is the radius of the particle and h refers to enthalpy.

The equili rium surface temperature of re-entry particles will change with altitude and the term $1 - \frac{h_{wall}}{h_{gas}}$ may have a great effect on heat transfer rate as the temperature differential between surface and gas becomes less. However, Lees and Cohn assume that realistic values can be obtained by cold wall approximations ($h_{wall} << h_{gas}$)[9] [10]. Calculations show the total hot wall heat input may average 20% lower than cold wall, but when conduction is considered it is believed this difference will be greatly decreased. Consequently, the above equation may be modified to:

$$\dot{q}_s = \frac{17,600}{r_B} \quad \frac{\rho}{\rho}^{\;1/2} \quad \frac{V}{V_E}^{\;3.25}$$

2.1.5 Average Convective Heating Rate as a Function of Body Shape

The above calculations determine the incident heat flux at the stagnation point of a body. To calculate the average heat flux over the entire surface of a spinning sphere requires a transformation involving the variation of the stream velocity gradient at every point on the surface. Oehrli[11] has developed these functions for local heat transfer for both a sphere and a cylinder, assuming laminar flow conditions. His values give a factor of 0.25 for a sphere and 0.333 for a cylinder. Therefore, the local surface heat flux for the spherical particles of interest as related to the stagnation heat flux is:

$$\dot{q}_s = 0.25\,\dot{q}_{stagnation} \qquad \text{where } \dot{q} = \text{heat flux}$$

2.1.6 Radiation Heating

A body re-entering the earth's atmosphere generates a bow shock wave of sufficient magnitude to cause extensive dissociation of air molecules passing through the shock region. The radiant heat emanating from this region constitutes a heat input to the body which varies with the altitude and velocity of the body. However, Lees(12) and Kivel(13) agreed that radiation heat transfer at the stagnation point is important only for bodies traveling at more than 30,000 ft/sec. at altitudes of 35 miles. Such conditions do not exist during orbital re-entry, so the effects of radiative heat transfer are ignored for the present cases.

2.1.7 Oxidation

The analysis of Scala, which is based on a continuum flow regime, is used to determine the mass loss rate due to oxidation during re-entry. In the interest of clarity, several other assumptions made in the development of this theory should be cited:

a. The oxidation reaction is diffusion controlled in the temperature range of interest. Products of combustion can be CO and CO_2, with CO_2 being predominant at the very low temperatures. Above 3000°R, the primary oxidation product is CO.

b. Nitrogen atoms do not enter into chemical reactions.

c. Equilibrium exists in the gaseous boundary layer and at the surface.

d. Radiation from the body is not included in the general expression, which accounts only for convective heat input.

e. Radiation into the body from the gas cap is assumed negligible.

f. Account is taken of the exothermic and endothermic chemical reactions occurring in the boundary layer, which effectively supplies an additional heat input.

g. The heat blocking effect of combustion products injected into the boundary layer is taken into account. This assumption effectively reduces total heat input by some degree.

As a result of these considerations, Scala developed a general formula for effective stagnation point heat flux as follows:

$$Q_{ST} = \dot{q}_s = (r^{-1/2})\ (C)\ (10)^a\ (V)^{2.5645} \quad \text{BTU/ft}^2\ \text{sec}$$

where

Q_{ST} = stagnation heat flux

$\dot{q}_s$ = $1.828 - 4.156 \times 10^{-4}\ T_w + 4.097 \times 10^{-8}\ T_w^{\ 2}$

T_w = Particle wall temperature in ^{o}R

a = $-(7.32 + 8.7763 \times 10^{-6}\ y)$

y = altitude of particle

r = radius of particle

V = velocity of particle

Heat fluxes calculated by the above formula will be generally higher than those computed from the method of Kemp and Riddell because of the various effects determined by Scala which tend to increase heat input (such as exothermic chemical reactions in the boundary layer).

Extending this reasoning to the prediction of stagnation point ablation rate of a graphite surface, Scala developed the following relationship for the mass loss rate M ($lbs/ft^2 sec$).

$$\dot{M}_{ox\ st} = (r^{-1/2})\ (C)\ (10)^a\ (V)^b\ \ lbs/ft^2\ sec$$

where:

$C = 0.508 + 1.4725 \times 10^{-4}\ T_w$ if $1000^\circ R < T_w < 3000^\circ R$

$C = 1.17 - 1.045 \times 10^{-6}\ y - (7.41 \times 10^{-5} - 2.85 \times 10^{-10} y)\ T_w$ if $T_w > 3000^\circ R$

$b = 0.875$

$a = -(4.6759 + 9.1600 \times 10^{-6} y)$

r = radius of particle

V = velocity of particle

T_w = particle wall temperature

To transform this localized mass loss rate to that existing uniformly over the surface of a rotating sphere, Scala used a modifying factor which results in over-all surface mass loss rate:

$$\dot{M}_{ox\ surf} = 0.130\ \dot{M}_{ox\ stag}$$

2.1 8 Sublimation

In addition to oxidation, there will be sublimation of elemental graphite if the surface temperature reaches the sublimation temperature during re-entry. The sublimation temperature is a function of the pressure existing at the body surface, and it decreases with a decrease in pressure. Tables have been compiled for this relationship and programmed for use on the digital computer.

To calculate the mass loss due to sublimation, it is necessary to write a heat balance between effective surface heat input and surface radiation. The net heat available can then be divided by the heat of sublimation of graphite to predict a mass loss rate from the surface. This relationship appears as follows:

$$\dot{M}_{sub} = \frac{f Q - \epsilon \sigma T_w^4}{25,600} \quad \text{if } T_w = T_{sub}$$

where :

Q = net convective stagnation heat flux

f = 0.25 (conversion factor for surface heat flux on sphere)

T_w = particle wall temperature

T_{sub} = sublimation temperature of graphite

σ = Stefan-Boltzmann Constant (4.8×10^{-13} BTU/ft^2 sec^{o}R)

ϵ = emissivity (normally assumed 0.8 for graphite)

H_{sub} = 25,600 BTU/lb. for graphite

2.1.9 Fission Product Decay Heat

The internal generation of heat within re-entering particles due to radioactive decay processes should be included in the general analysis. A table has been compiled which shows the percentage of original power remaining as a function of time. By incorporating volume factors for the particle sizes involved, it is possible to determine the amount of decay heat generated during re-entry. This term was included as a heat input in the following form:

$$\dot{q}_F = \frac{P_{eff}}{V_b}$$

P_{eff}	=	power remainint at time t (BTU/sec)
V_b	=	volume of particle (ft^3)
$\dot{q}_F$	=	decay heat ($BUT/ft^3 sec$)

2.1.10 Calculation of Particle Surface Temperature

The calculation of surface temperature and its change with time necessitates determination of a heat balance among the different kinds of heat inputs and heat losses. For the purposes of this investigation, the major heat inputs were assumed to be convective aerodynamic heating and fission product decay heat, and the heat loss was considered to be entirely through radiation from the particle surface. This leads to the following equation.

$$\dot{T}_w = \frac{1}{MC_p} \left(f\, Q\, A_s - \quad T_w^4\, A_s + \dot{q}_F\, V_b \right) \quad \text{if } T_w < 7000^\circ R$$

where:

$\dot{T}_w$	=	rate of change of temperature at particle wall
$\dot{q}_F$	=	decay heat ($BTU/ft^3 sec$)
Q	=	aerodynamic heat flux which includes heat of reaction ($BTU/ft^2 sec$)
f	=	0.25 for sphere
A_s	=	$4 \pi r^2$ for sphere
σ	=	Stefan-Boltzmann Constant
ϵ	=	emissivity (0.8 for graphite)
C_p	=	specific heat (constant pressure) of graphite
V_b	=	volume of particle
M	=	mass of particle

2.1.11 Summary of Program Formulation

The various parameters which have been described as parts of the analytical model were assembled by means of a FORTRAN code into the over-all program. This technique produced a set of equations which were solved simultaneously and continuously by the IBM 7090 digital computer throughout the re-entry flight of the graphite particle. Outputs of interest were printed as a function of time to furnish data for reduction to chart and graphical form. The complete grouping of equations appeared as follows:

a. Trajectory

$$\ddot{R} = (2\dot{R}\dot{\theta} + R\ddot{\theta}) - \frac{D}{M}\cos\theta - \frac{L}{M}\sin\theta \quad \text{(Tangential)}$$

$$\ddot{R} = R(\ddot{R} - R\dot{\theta}^2) + g - \frac{L}{M}\cos\theta - \frac{D}{M}\sin\theta \quad \text{(Radial)}$$

b. Aerodynamic Heat Input (including heat of combustion)

$$\dot{q}_{ST} = Q = (r^{-1/2})\,(C)\,(10)^a\,(V)^{2.5645} \quad \text{BTU/ft}^2\text{sec}$$

c. Oxidation Mass Loss

$$\dot{M}_{ox\ surf} = 0.130\,(r^{-1/2})\,(C)\,(10)^a\,(V)^b \quad \text{lbs/ft}^2\text{ sec}$$

d. Decay Heat

$$\dot{q}_F = \frac{P_{eff}}{V_b} \quad \text{BTU/ft}^3\text{sec}$$

e. Radiation Heat Loss

$$\dot{T}_w = \frac{1}{MC_p}\left(QA_s - T_w^4 A_s + q_F V_b\right) \quad {}^{o}\text{R/sec}$$

f. Sublimation Mass Loss

$$\dot{M}_{sub} = \frac{f\,Q - \epsilon T_w^4}{25,600} \quad \text{lbs/ft}^2\text{ sec}$$

g. Particle Radius Change

$$\dot{r} = \frac{1}{\rho} \left(\dot{M}_{ox.\,surf} + \dot{M}_{sub} \right)$$

2.2 PRESENTATION OF ANALYTICAL RESULTS

The various ranges of input parameters used for solution in the digital program are shown in Figure 2-2. These covered the complete range of conditions desired for evaluation in the program and permitted bracketing of particle size for which complete burn-up could be predicted.

The complete output from the computer consisted of the following terms as functions of time:

a. Altitude

b. Particle surface temperature

c. Particle radius

d. Particle velocity

e. Particle mass

f. Oxidation mass loss

g. Sublimation mass loss

h. Stagnation heat flux

i. Flight path angle

j. Horizontal flight distance

k. Tangential velocity component

l. Radial velocity component

It was not possible, in the available time, to conduct a complete study of all data and to present results in detailed form. However, the parameters of greatest interest have been investigated and assembled in graphical form to show effects of re-entry variables on aerodynamic heating rates and particle burn-up for a representative range of particle sizes.

Figures 2-3 to 2-9 show the variation of velocity with altitude for a number of particle sizes as a function of re-entry angle, initial altitude, initial temperature and initial velocity. The following conclusions may be drawn:

a. Maximum deceleration occurs at a higher altitude for a smaller re-entry angle.

b. Maximum deceleration occurs at a higher altitude for a smaller particle size.

c. Maximum deceleration takes place between 300,000 - 150,000 feet.

d. At 100,000 feet, the velocities of all particles have fallen to low values (20 - 2000 ft/sec depending on particle size).

e. The initial particle temperature has no effect on the re-entry trajectory of any particle size up to 1" diameter, when re-entry is from an altitude of 1.8×10^6 feet or 4×10^5 feet.

f. The basic trajectories are similar for re-entry from 1.8×10^6 feet or 4×10^5 feet since initial deceleration occurs in the range 400,000 - 300,000 feet. Above 400,000 feet there is actually an acceleration of the particle due to gravitational attraction in the absence of drag.

Figure 2-10 illustrates the change in particle radius with altitude, due to mass loss through oxidation. It can be seen that:

a. The larger particle sizes (1" and 1/2" diameter) exhibit a negligible size change on re-entry, which is independent of re-entry angle.

b. Particles of less than 1/4" diameter show a larger relative change in size. Also, the total decrease in radius is greater for the smaller re-entry angles indicating a greater mass loss for the shallow re-entry path.

c. Particles of 1/32" diameter will be reduced to 25 micron size above 100,000 feet if continued oxidation below 1000°R is assumed. There is serious doubt that this would be the case, due to low particle temperature. Scala's lower temperature limit is 1000°R and if it is assumed that oxidation ceases completely at 1000°R, then the 1/32" particle radius will be 150-250 microns at 100,000 feet, depending on re-entry angle.

d. On the basis of later analysis (not plotted here), it appears that 1/64" diameter particles will be reduced to 25 micron diameter above 100,000 feet, even if no mass loss from oxidation occurs below 1000°R.

e. Initial temperature of the particle has no effect on radius change during re-entry.

Figures II-II indicates the percentage of particle mass consumed as a function of altitude for 1/24" and 1/32" diameter bodies. From this information it can be concluded that:

a. More mass is lost from shallow angle re-entry. Although peak heat fluxes are higher at larger re-entry angles. The integrated heat flux is greater for small re-entry angles due to the much longer flight path.

b. The 1/24" diameter particles will be only 35 - 80% consumed if oxidation is presumed to cease below 1000°R. The total mass consumption increases with a decrease in re-entry angle.

c. If oxidation is assumed to continue below 1000°R, extending Scala's theory, then the 1/24" diameter particles will be reduced to 25 micron size (at 100,000 feet) for shallow re-entry angles.

d. The same theory is true of particles of 1/32" diameter, except that with continued oxidation, all particles will be completely consumed at any re-entry angle.

Figures 2-12 to 2-14 plot stagnation heat flux as a function of particle size, re-entry angle and altitude. This is done for 1/24" and 1/32" diameter particles. The following effects are noted:

a. The stagnation heat flux is greater for smaller particle sizes, at the same velocity and altitude. However, due to more rapid deceleration of the smaller particle at higher altitude, the peak heat flux is about the same for the larger particle size at the same re-entry angle.

b. The peak stagnation heat flux increases with an increase of re-entry angle, reaching a maximum at a 90° (vertical) angle.

c The altitude range of high heat flux input is limited, lying between 200,000-300,000 feet. The peak heating occurs at a velocity about 85% of the initial re-entry velocity.

d. There is no effective aerodynamic heating above 400,000 feet, nor below 150,000 feet. Above 400,000 feet air density is insufficient to cause heating. Below 100,000 feet, particle velocity is too low to cause heating.

e. The integrated heat flux is greater for a shallow re-entry angle although peak heat flux is greater for steep re-entry. This is because the total flight time is much longer with the smaller angle, thus leading to higher integrated heat fluxes.

One plot of particle surface temperature versus altitude was made for a 1/32" diameter re-entering body. It is seen in Figure II-16 that the temperature curve follows the form of the heat flux curve, which is to be expected. A peak temperature of 5000°R is calculated for a 90° re-entry at 250,000 feet, and a peak temperature of 3800°R is obtained at 320,000 feet for a 5° re-entry. The temperature calculations were based on a particle surface emissivity of 0.8.

There was no mass loss due to sublimation in any particle size, since surface temperatures did not reach the sublimation temperature upon re-entry.

3.0 EXPERIMENTAL PROGRAM

The purpose of the experimental program on graphite materials is to obtain empirical data under simulated re-entry conditions for comparison with theories of re-entry burn-up. Only in this manner can theory be validated and then extended to predict burn-up characteristics under a variety of conditions. Therefore, experimental work must be conducted under closely controlled conditions so that the data can be considered reliable for comparative purposes.

Facilities available for conducting simulated re-entry experiments are of four general types:

a. arc plasma wind tunnels,

b. hypersonic blowdown wind tunnels,

c. ballistic ranges and

d. shock tubes.

The arc plasma wind tunnel is able to duplicate stagnation enthalpy, stagnation pressure and gas density at a given altitude and velocity. It is not able to reproduce free stream velocity or exact chemical composition of air under re-entry conditions due to ionization of air by the arc. However, it is capable of being operated for extended run times, which is an important factor in materials studies. Hypersonic wind tunnels more closely reproduce free stream velocities and gas composition, but stagnation pressures are too high to simulate altitude. Short run times, less than a minute in duration, are the general rule. Ballistic ranges actually accelerate small particles to hypersonic velocities, but flight times are extremely short. Recovery of particles after test also presents somewhat of a problem. The shock tube is extremely well suited to gas dynamic studies, but run durations are measured in milliseconds. This makes the device basically useless for any realistic materials study.

Out of many discussions, and visits to various laboratories (19 in all contacted) Plasmadyne Corporation was selected to perform the arc plasma tests. An experimental program was outlined to include burn-up tests on both fueled and unfueled graphite core materials. The tests on pure graphite were performed first because developed theories are based on the use of pure, dense graphite.

It is physically impossible to test a free body (such as a sphere) in a plasma tunnel. Shapes must be supported in some type of insulated holder which does not create turbulence in the laminar stream. A common method of specimen preparation involves machining or grinding of hemispherical shapes incorporating a projecting shank, whereby the specimen can be mounted at the tip of a cone-shaped holder. In this manner, only the hemispherical portion is exposed to stagnation heating in the plasma stream. To keep the heat from flowing out of the specimen, a suitable thermal insulator should be interposed between the specimen and the holder.

The objective of tests in the plasma arc tunnel was to measure the mass loss rate, due to oxidation, of various size graphite hemispheres exposed to a plasma stream. Several parameters are controllable to produce varying conditions of simulated velocity and altitude. By exposing equal size specimens for different time intervals at one test condition, it is possible to determine average weight loss as a function of time after equilibrium has been established. Several test conditions are employed to determine mass losses over a range of re-entry altitudes and velocities.

To compare experimental data obtained in this initial phase involving unfueled graphite with the predictions of Scala's theory, it is necessary to know the simulated altitude, velocity and surface temperature of a particle of stated size which is exposed in the plasma arc tunnel. These are the only three variables necessary to predict particle mass loss rate. Therefore, the experimental program was oriented around a representative range of particle sizes which would logically cover the anticipated burn-up range.

3.1 Experimental Procedure

Specimens of Graphitite "G", a dense grade of structural graphite, were lathe-turned to hemispheres of 1", 1/2", 1/4" and 1/8" diameter. Approximately 100 of these specimens were prepared in the different sizes. The shape of the specimen is shown below:

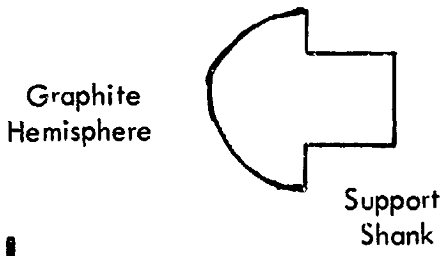

GRAPHITE
SPECIMEN

The surfaces of these specimens were machined to a fine finish, to keep surface porosity to a minimum, since surface condition will effect oxidation rates. Scala's theory assumes a non-porous reaction surface.

Initially, specimen holders were prepared from Lavite (a form of magnesium silicate) and from phenolic nylon. It was thought the insulating properties of Lavite would be attractive and its high temperature strength would be advantageous. Nylon was believed to be a good "ablation" material and would form surface char layers under high heat fluxes without degradation. An insulating length of Lavite was inserted in the nylon holders as a thermal barrier between the graphite specimen and holder. The holder specimen arrangements appeared as shown below:

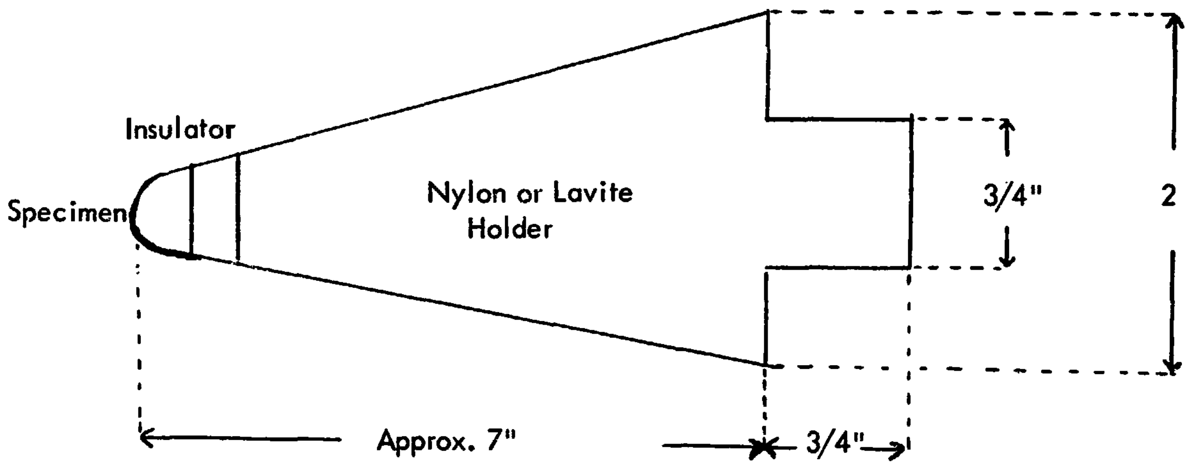

The initial experiments in Plasmdyne's arc tunnel were unsuccessful because the holders functioned poorly. The Lavite suffered badly from spalling due to thermal shock. The nylon warped, sagged and melted internally near the tip. The longest run time was approximately 15 seconds before failure occurred.

Following this experience, it was decided that graphite would probably be the only suitable holder material provided its high thermal conductivity could be blocked so as not to transfer too much heat out of the specimen. Holders of graphite were fabricated for the different specimen sizes and tests quickly showed the material was ideal for the application. At the present time, methods are being developed with the use of pyrolytic graphite to reduce heat transfer from specimen to holder to a minimum value. It is realized the initial test results reported here could give somewhat different values of mass loss than the realistic case, due to heat transfer out of the specimen into the holder. The improved holder assembly will be used as soon as the pyrolytic graphite insulators are available.

Table 3-1 shows a summary of test point data determined during equipment calibration for the experimental runs. Each test point simulates a specific altitude and velocity by duplicating the stagnation enthalpy and stagnation pressure at the specimen surface Test points B, C, and D are for air; point B_1 is for argon. The relationship between test points, altitude and velocity is as follows:

Test Point	Velocity	Altitude
B	17,500 ft/sec	190,000 ft.
B_1	17,500 ft/sec	190,000 ft.
C	24,000 ft/sec	250,000 ft.
D	25,500 ft/sec	350,000 ft.

3.2 Test Results

Table 3-2 lists the data on weight loss versus time for various size specimens at the different test points. Three exposure times were run at each test point for each size in order to provide curves which could be interpreted to furnish an accurate mass loss rate. The 1/2"

TABLE . 3-1

SUMMARY OF TEST POINT DATA

Test Point	Mean Stagnation Enthalpy-h BTU/lb	Nitrogen Flow Rate (lb/sec)	Oxygen Flow Rate (lb/sec)	Model Stagnation Pressure-p_T (atm)	Nozzle Stagnation Pressure-p (atm)	Nozzle Static Pressure-p (atm)	Stagnation Point *** Heat Flux-$\dot{q}_s$ BTU/ft^2 - sec) cal.
B	6,000	.00130	.0003456	.0419	.197	.00378	270
B_1	6,000	Argon - .00300		.0493	.197	.00438	240
C	10,500	.00106	.0002818	.0242	.126	.00225	270
D	12,800	.000810	.000215	.00358	.0197	.000345	180

*** Stagnation Point Heat Flux to Model may be computed from the following relationship:

$$\dot{q}_{s_{model}} = \dot{q}_{s_{calorimeter}} \cdot \left(\frac{\text{Model Radius}}{\text{Calorimeter Radius}} \right)^{-1/2} \cdot \frac{h_T - h_{W_{model}}}{h_T}$$

TABLE 3-2

MODEL WEIGHT LOSS RATES

Model Diameter	Model Number	Run Time (seconds)	Change in Weight (grams)	Weight Loss Rate (gms/sec)
Point D:				
Half-inch	23	180	.3548	.001971
	24	360	.6226	.001729
	22	[illegible]	.8797	.001629
Quarter-inch	21	85	.0514	.0006047
	20	190	.1184	.0006232
	19	245	.1346	.0005494
Eighth-inch	15	45	.0078	.0001733
	14	60	.0094	.0001567
	13	75	.0113	.0001507
Point C:				
Half-inch	9	105	.4355	.004147
	8	165	.6849	.004151
	7	240	.8225	.003427
Quarter-inch	12	45	.0723	.001607
	11	65	.0973	.001497
	10	84	.1141	.001358
Eighth-inch	38	15	.0066	.0004410
	37	30	.0121	.0004033
	36	40	.0151	.0003775
Point B:				
Half-inch	17	122	.5918	.004851
	31	180	.7948	.004416
	16	255	.9676	.003795
Quarter-inch	27	60	.0943	.001572
	26	105	.1273	.001212
	25	150	.1647	.001098
Eighth-inch	35	20	.00795	.0003975
	33	40	.01400	.0003500
	32	60	.01900	.0003170

TABLE .3-2

MODEL WEIGHT LOSS RATES
(continued)

Model Diameter	Model Number	Run Time (seconds)	Change in Weight (grams)	Weight Loss Rate (gms/sec)
Point B_1:				
Half-inch	30	120	.0227	.0001892
	29	270	.0483	.0001789
	28	540	.0892	.0001652

size was run in argon, to determine whether the samples lost weight by any process other than oxidation. The fact that there was some measurable weight loss in argon indicates that factors other than oxidation are operative in the burn-up behavior of these graphite specimens.

Figures 3-1 to 3-3 show the average temperatures measured on the surfaces of the 1/2", 1/4" and 1/8" diameter specimens as a function of (1) exposure time in the plasma stream and (2) test point location. An emissivity value of 0.9 (ϵ = 0.9) was assumed for both optical and radiation pyrometer readings. Optical pyrometer readings were obtained on the 1/2" and 1/4" sizes, but the 1/8" diameter specimens were too small to be read accurately with an optical pyrometer. Therefore, a radiation pyrometer was used. Results obtained by this method on the 1/8" specimen size are of questionable accuracy because the radiation pyrometer was removed some distance from the small specimen.

Figures 3-4 and 3-6 show mass loss rates as functions of specimen size, test point location and total exposure time. In all cases, a reasonable linear plot was obtained after a suitable induction time for attaining equilibrium surface temperatures. The average mass loss rate decreased with increasing exposure time in all cases.

Figures 3-7 to 3-16 illustrate the actual surface temperature-time histories of each model (specimen) exposed. This is done for each test point and each exposure within a test point. These curves are very useful in arriving at conclusions regarding (1) actual average surface temperature and (2) time to reach equilibrium surface temperature as a function of specimen size and test point location. The exposure times were sufficiently long in most cases to permit a reasonably accurate average surface temperature to be realized.

3.3 Discussion of Results

The exposure of graphite specimens in the arc plasma wind tunnel demonstrates that reasonable agreement was reached with the theory. This is considered to be significant and indicates that the basic assumptions used in the analysis are generally valid. The calculated average mass loss rates from the surfaces of the specimens tested showed a steady decrease with increasing exposure time. It is believed this is associated with the change in radius of the particles with extended exposure times and can be corrected in subsequent runs by limiting the exposure times to produce only small changes in radius. In addition to this interpretation, there are other effects which might exist at the surface which could possibly influence mass loss rates. These include:

a. Increase of surface emissivity, leading to greater radiation from the surface and lower oxidation rates.

b. Formation of a thickened boundary layer which slows down diffusion of reactants and products, effectively reducing oxidation.

c. Charge of porosity of the surface due to oxidation, thereby changing the rate of surface reactions.

For the purpose of assigning mass loss rates and surface temperatures for comparison with theory, either or both extremes of values may be considered, or an average may be taken. For initial comparison, average values are used.

Concerning temperature equilibrium at the surface, the following average times can be assigned for reaching equilibrium from start of exposure to the plasma stream:

1/2" size	1 min.
1/4" size	15 sec.
1/8" size	5 sec.

The data on the 1/8" size are somewhat erratic, as discussed previously. However, it appears reasonable to assume that the smallest particles will reach equilibrium very rapidly. The above times, based on conservative assumptions, are adequate for computing times to equilibrium. It must also be remembered that in a free particle, or in one which is thoroughly insulated, equilibrium will be attained more rapidly.

The surface temperatures are approximately the same for 1/2" and 1/4" specimens at a given test point. This would not be expected, unless the conductive heat loss is higher for the smaller particles. It is certain that convective stagnation point heat flux is higher for the smaller particles since the heat flux is inversely proportional to the square root of the radius. The reported temperatures on the 1/8" specimens are entirely too low to be realistic and probably reflect errors in radiation pyrometer readings. Another factor may be the proportionately larger amount of heat loss to the holder in the smaller specimens. Future tests will be conducted with the holders insulated as thoroughly as possible from the specimens.

3.4 Comparison of Experimental Data with Scala's Theory

Four cases were considered to provide a comparison between experimental data and Scala's theory. These were 1/2" and 1/4" particle diameters at test points B and D. The results are shown in Table 3-3.

The experimental data show greater mass loss rates than those predicted by Scala's theory. However, the maximum discrepancy is only one order of magnitude, which can be considered low in view of both the previously discussed limitations of the experiment and the assumptions of the theory. The agreement is better for the larger particle size and for the lower altitude position for both particle sizes. Scala's theory assumes continuum flow throughout the re-entry, which leads to lower burn-up rates than would be the case in free molecule

TABLE 3-3

COMPARISON OF EXPERIMENTAL DATA WITH SCALA'S THEORY ON GRAPHITE BURN-UP DURING RE-ENTRY

Particle Size	Exp. Test Point	Sim. Vel. (ft/sec)	Sim. Alt. (ft.)	Measured Surf. Temp. (°R)	Mass Loss Rate Experiment* ($lbs/ft^2 sec$)	Theory** ($lbs/ft^2 sec$)
1/2" dia.	B	17,500	190,000	4416°R	3.48×10^{-3}	1.68×10^{-3}
	D	25,500	350,000	3678°	1.46×10^{-3}	2.63×10^{-4}
1/4" dia.	B	17,500	190,000	4344°	9.46×10^{-3}	2.32×10^{-3}
	D	25,500	350,000	3732°	4.06×10^{-3}	3.82×10^{-4}

*Actual mass loss rate doubled to account for sphere rather than hemisphere.

**Stagnation mass loss rate multiplied by 0.130 to transform to sphere surface mass loss rate (See Section 2.1.7 for method of calculation).

flow. The actual flight regime of particles of this size will be a combination of continuum and free molecule flow, leading to burn-up rates greater than those predicted by Scala. The smaller particles will be in free molecule flow for a greater portion of their flight than the larger ones, therefore, experiencing a higher heating rate. Thus, the spread between theoretical and experimental values should be greater for the smaller particles, which is indeed the case. The fact that better agreement is found at the lower altitudes may be attributed to the samples being in continuum flow only.

4.0 FUTURE WORK PROGRAM

4.1 Analytical Program

Several detailed investigations are being conducted at the present time to extend the assumptions applicable to the basic analytical model. This is designed to permit the widest interpretation of possible re-entry parameters in the given model so as to cover the extremes of possible behavior. Two points being studied are:

a. Variation of surface emissivity (ϵ) of the graphite particle. An emissivity of 0.8 was assumed for the cases discussed in this report. This is considered to be a realistic value for the graphite body under the general conditions of re-entry. A change of emissivity will affect the surface temperature and the mass loss rate. Emissivities of ϵ = 0.5 and ϵ = 0 (no radiation from surface) are being substituted in a number of re-entry cases to determine what effects will occur. In addition, comparison of these results with those of other investigators is required.

b. Re-entry studies on 1/64" diameter particles.

Further work of a longer range nature will include:

a. Analytical studies on incorporation of free-molecule flow theory into the re-entry parameters for a range of particle sizes. This study is necessary to predict more accurately actual re-entry behavior. The present study has been based on continuum re-entry.

b. Study of the effect of varying drag coefficient during re-entry.

c. Possible incorporation of other oxidation theories into a digital program. Theories by Zlotnick, Waber, and Dennison have been studied on a preliminary basis during Phase I and techniques can be applied to render them suitable for computer calculation.

d. Modification of existing applicable theory on pure graphite to account for behavior of fueled graphite.

4.2 Experimental Program

Future work of an experimental nature is planned for the next phase of the NERVA program. Investigations are designed to include:

a. Further runs on unfueled graphite using improved insulated graphite holders to reduce heat loss from specimens. This will probably increase experimental mass loss rates.

b. Tests on fueled graphite materials in the same specimen shapes and sizes as the unfueled graphite. Depleted uranium, simulating the enriched uranium loading, will be used to keep rad[illegible]tivity to the lowest level possible.

~~CONFIDENTIAL~~
~~RESTRICTED DATA~~
~~Atomic Energy Act - 1954~~

c. Tests to simulate other altitudes and velocities.

d. Study of shadowgraphs and color films of specimens before, during and after exposure to determine the effects of contour changes in the specimen shape which may cause difficulty in the interpretation of unit mass loss rates.

e. Tests at shorter run times, provided equilibrium temperature can be established faster in the specimens than in the initial cases reported here. This will help to eliminate difficulties associated with change of specimen shape and large changes in radius.

5.0 SUMMARY AND CONCLUSIONS

Analytical and experimental programs have been carried out on unfueled graphite materials with the object of determining mass loss rates due to oxidation during re-entry. From the results obtained, an attempt was made to predict the maximum size of graphite particles which would be reduced to a 25 micron diameter before reaching an altitude of 100,000 feet. This particle size would then be assigned as the necessary maximum particle size for any type of destruct mechanism which is designed to eliminate the radiation hazard from re-entering nuclear reactor parts.

The work on unfueled material was performed as a prelude to a study on fueled material, because a number of existing theories on the combustion of pure graphite could be studied analytically while there was no developed theory on the burn-up of fueled graphite. The first task was to determine whether existing theory could be verified by experimental work on simulated re-entry using unfueled material.

The analytical program involved the application of S.M. Scala's theory on oxidation of graphite during re-entry to an IBM 7090 computer program. Scala's theory was chosen because it appeared to be the most logical and because it could be reduced to a digital machine program without excessive difficulty. The input parameters and output data were formulated into a flow-type block diagram which consisted of a set of differential equations to be solved using an iterative method. In this manner, a step-by-step computation could be made at descrete time intervals during re-entry to give information on trajectory, aerodynamic heating rates, oxidation and sublimation of the graphite particles. Spheres of 1" to 1/64" initial diameter were chosen to re-enter at altitudes of 300 and 65 nautical miles and at initial temperatures of 4000°R and 300°R. Re-entry angles varied from 1° to 90°. A single re-entry velocity of 25,000 ft/sec assumed.

Results of the analytical program showed that pure graphite particles of 1/32" diameter will be consumed by oxidation above 100,000 feet, for any re-entry angle, if oxidation is assumed to continue below 1000°R. No mass loss occurs due to sublimation, since surface temperatures do not become high enough. Shallow re-entry angles are the most favorable for burn-up. The initial particle temperature at either altitude studied has no effect on total mass loss of any particle size considered.

The first series of tests was carried out on pure graphite specimens in an arc plasma wind tunnel. Three simulated points on a typical re-entry trajectory were chosen for exposing the specimens, corresponding to altitudes of 350,000 feet, 250,000 feet and 190,000 feet, with velocities of 25,500 feet/sec, 24,000 feet/sec and 17,500 feet/sec, respectively. The specimens were hemispheres of 1/2", 1/4" and 1/8" diameter, mounted in graphite holders, and were exposed in the plasma stream for various times to give measurable mass losses. The stream consisted of a mixture of oxygen and nitrogen to simulate the air composition at given altitudes. One series of runs on 1/2" specimens was made in pure argon to determine effects on the specimen without the occurrence of oxidation. Surface temperatures were measured with optical and radiation pyrometers. The object of the experimental program was to determine mass loss rates as accurately as possible once the specimens had achieved an equilibrium surface temperature.

Average mass loss rates were calculated for each type of specimen under the different conditions of exposure and these values were used for comparison with the results predicted by analysis. The analytical and experimental data which were compared at the same points on the re-entry trajectory agreed within one order of magnitude in all cases, with most results differing by much smaller amounts. This agreement is considered to be quite good. The experimental data in all cases gave higher burn-up rates than the theory.

The initial work performed during this 6-month period does not permit final conclusions to be drawn on the size of graphite particles which will be destroyed during re-entry. Further experimental work is necessary on unfueled material and extensive effort is required on the measurement of fueled graphite burn-up rates. It is planned to extend the analytical work to include the free molecule flow regime during re-entry, as well as investigation of other theories on the mechanism and kinetics of graphite oxidation. A modified theory must be developed to account for the forthcoming experimental data on fueled graphite. With these points in mind, the work program for the next phase of the NERVA contract will include the following efforts:

a. Analytical studies on oxidation theories of Zlotnick, Waber and Dennison, with possible incorporation into a digital computer program.

b. Analytical studies of free-molecule theory incorporated into the re-entry parameters to predict more accurately aerodynamic heating.

c. Variation of re-entry parameters such as drag and lift, due to change of shape of re-entering body.

d. Correlation or modification of existing theory to predict oxidation characteristics of fueled graphite, based on experimental results.

e. Initiation of experimental arc plasma wind tunnel experiments on fueled graphite specimens and determination of mass loss rates.

f. Continuation of experiments on oxidation of unfueled graphite under improved test conditions for more accurate comparison with theory.

g. Final summation of re-entry behavior of fueled and unfueled graphite derived from all available analytical and experimental data.

REFERENCES

(1) Westinghouse Electric Corporation - "Nuclear Rocket Study" (Vol. VI) - Final Report to Air Force Flight Test Center, Edwards Air Force Base, California (1961).

(2) Martin Company - "Nuclear Rocket Safety Study" - MND-2517 (Final Report (August 9, 1961).

(3) S. M. Scala - "A Study of Hypersonic Ablation" - General Electric Missile and Space Vehicle Dept. - T.I.S. Document No. R595D438 (September, 1959).

(4) J.A. Moore and M. Zlotnick - "Combustion of Carbon in an Air Stream" - ARS Journal (October, 1961)

(5) J.T. Waber - "Kinetics of Oxidation in a Gas Stream" - Metals for Supersonic Aircraft and Missiles (Book), ASM Publication (1958).

(6) M.R. Dennison - "The Turbulent Boundary Layer on Chemically Active Ablating Surfaces" - Journal of the Aero/Space Sciences, V.28 (1961) pp. 471-479.

(7) Air Research and Development Command - "Handbook of Geophysics for Air Force Designers" - (1957)

(8) Kemp and Riddell - "Re-entry Heat Transfer to Satellite Vehicles" - Jet Propulsion, V. 27 (February, 1957).

(9) L. Lees - "Laminar Heat Transfer over Blunt Nosed Bodies at Hypersonic Flight Speeds" - Jet Propulsion (April, 1958).

(10) P.D. Cohn - "The Experimental and Analytical Programs for Re-entry Burn-up of SNAP Reactors," ARS Space Power Systems Conference, Santa Monica, California (1960).

(11) R. Oehrli, - "Applied Structural Heating and Cooling", The Martin Company ER-7977-3K-M, (January, 1959.)

(12) L. Lees, - "Recovery Dynamics - Heat Transfer at Hypersonic Speeds in a Planetary Atmosphere", Lecture 64, Lectures in Space Technology, University of California Engineering Extension, (February, 1958).

(13) B. Kivel, - "Radiation from Hot Air and Stagnation Heating", AVCO Research Laboratory, Research Report 79.

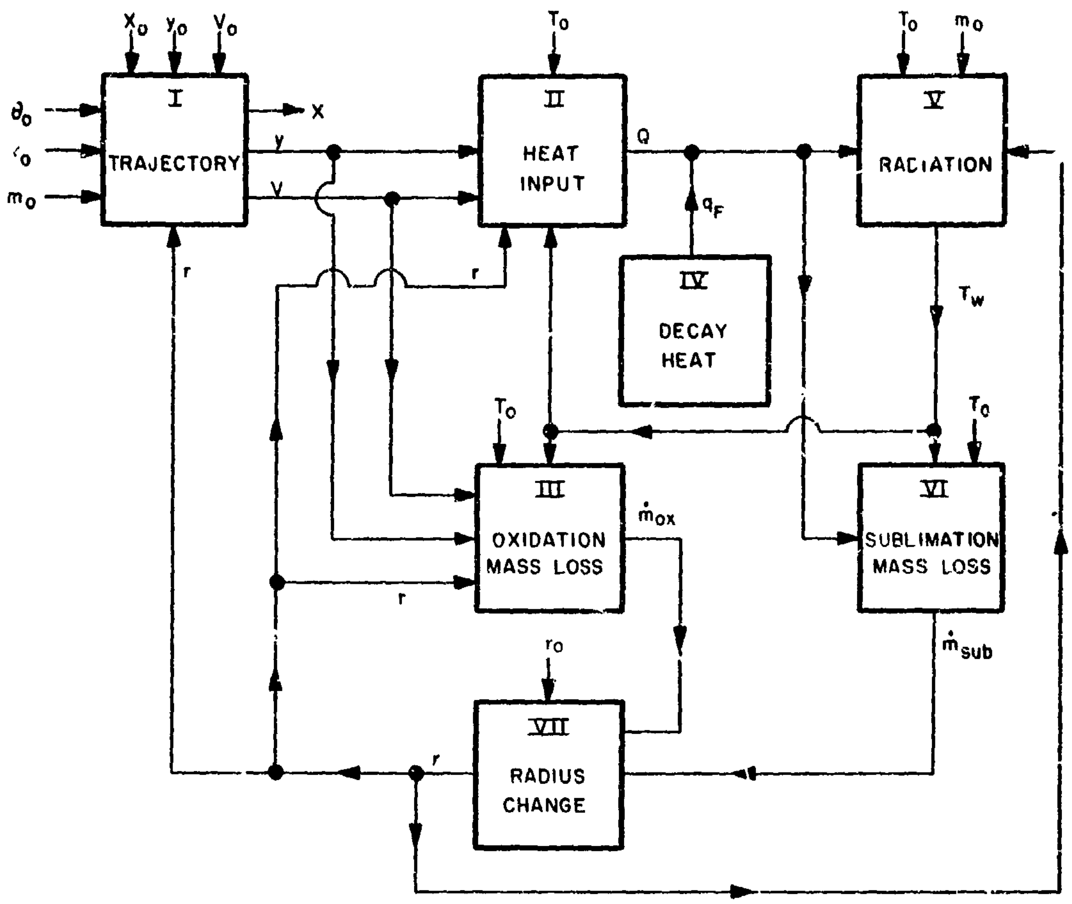

SYMBOLS		UNITS
V_o	INITIAL RE-ENTRY VELOCITY	FT /SEC
θ_o	INITIAL RE-ENTRY ANGLE	DEGREES
m_o	INITIAL PARTICLE MASS	LBS
r_o	INITIAL PARTICLE RADIUS	FT.
X_o	INITIAL ORBITAL LOCATION ($X_o = o$)	
y_o	INITIAL ALTITUDE	FT
y	ALTITUDE	FT
V	VELOCITY	FT /SEC.
T_o	INITIAL SURFACE TEMPERATURE	°R
T_w	PARTICLE SURFACE TEMPERATURE	°R
Q	CONVECTIVE HEAT INPUT (STAGNATION POINT)	$BTU/FT^2 SEC.$
q_F	FISSION PRODUCT DECAY HEAT INPUT (VOLUME)	$BTU/FT^3 SEC$
$\dot{m}_{ox}$	OXIDATION MASS LOSS RATE	$LBS/FT^2 SEC.$
$\dot{m}_{sub}$	SUBLIMATION MASS LOSS RATE	$LBS/FT^2 SEC.$
r	NEW RADIUS	FT.

Figure 2.1 570A638

Graphite Particle Re-Entry Analytical Model

		1/64"	1/32"	1/24"	1/16"	1/8"	1/4"	1/2"	1"
θ	1°			X		X			
	5°	X	X	X	X	X	X	X	X
	10°			X		X			
	30°	X	X	X	X	X	X	X	X
	90°		X	X	X	X	X	X	X
V_E	25, 000 ft/sec	X	X	X	X	X	X	X	X
y	1.8×10^6 ft	X	X	X	X	X	X	X	X
	4×10^5 ft			X		X			
T_w	$4000^{\circ}R$	X	X	X	X	X	X	X	X
	$300^{\circ}R$		X	X		X	X		X

Figure 2.2

Analytical Cases for Graphite Particle Re-Entry

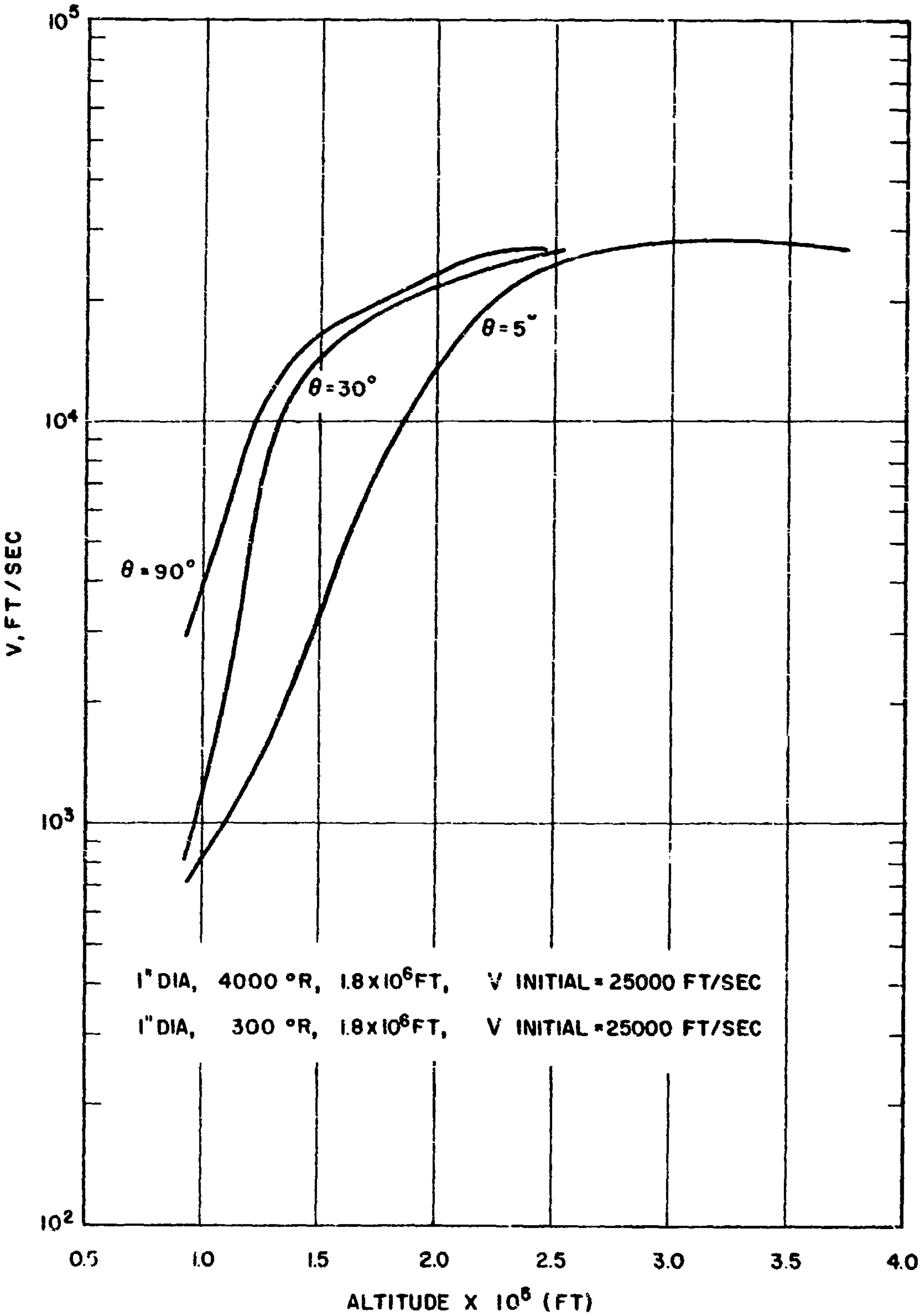

Figure 2.3 547181

Particle Velocity as a Function of Altitude

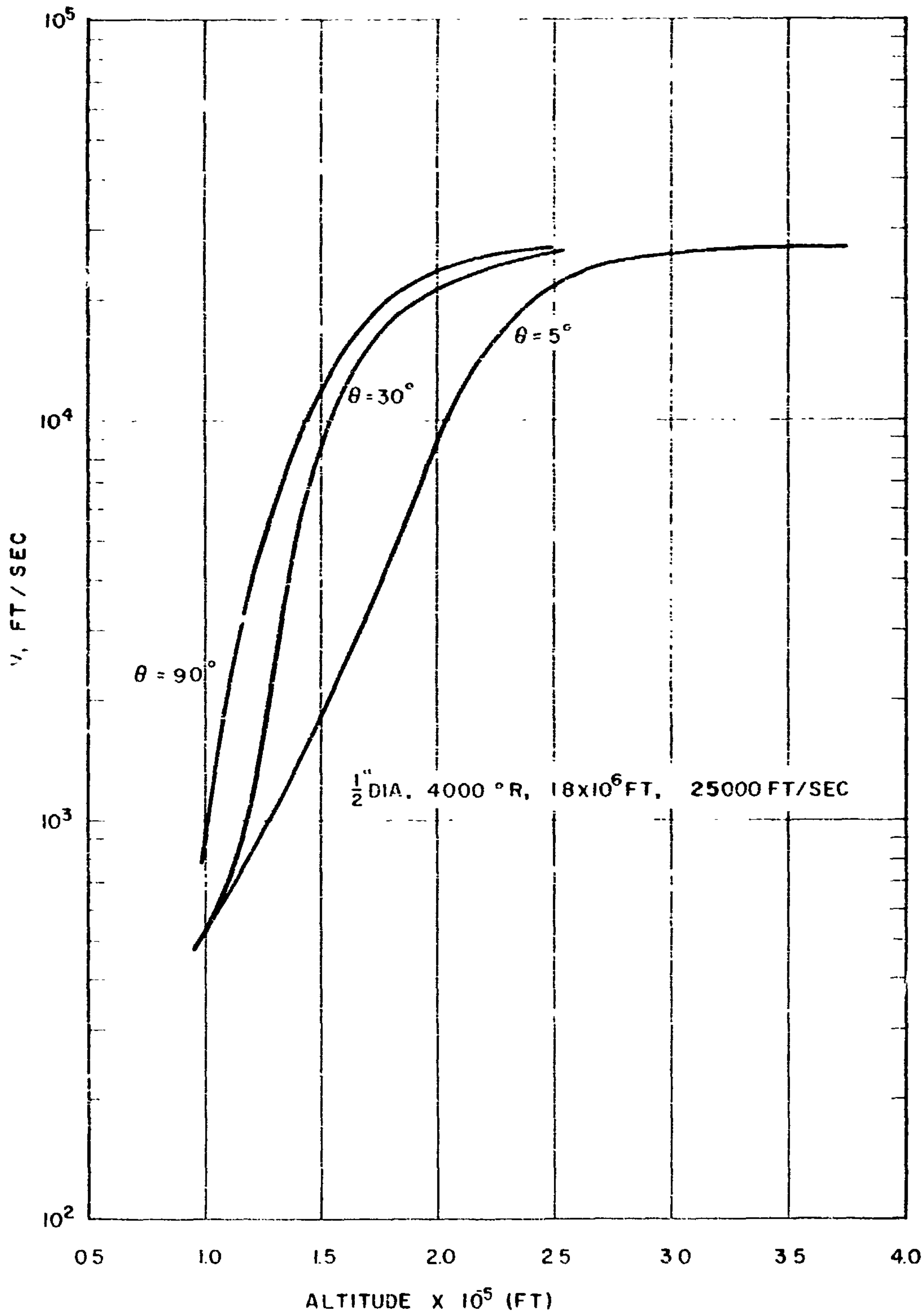

Figure 2.4

547182

Particle Velocity as a Function of Altitude

~~CONFIDENTIAL~~
~~RESTRICTED DATA~~
~~Atomic Energy Act 1954~~

Astronuclear

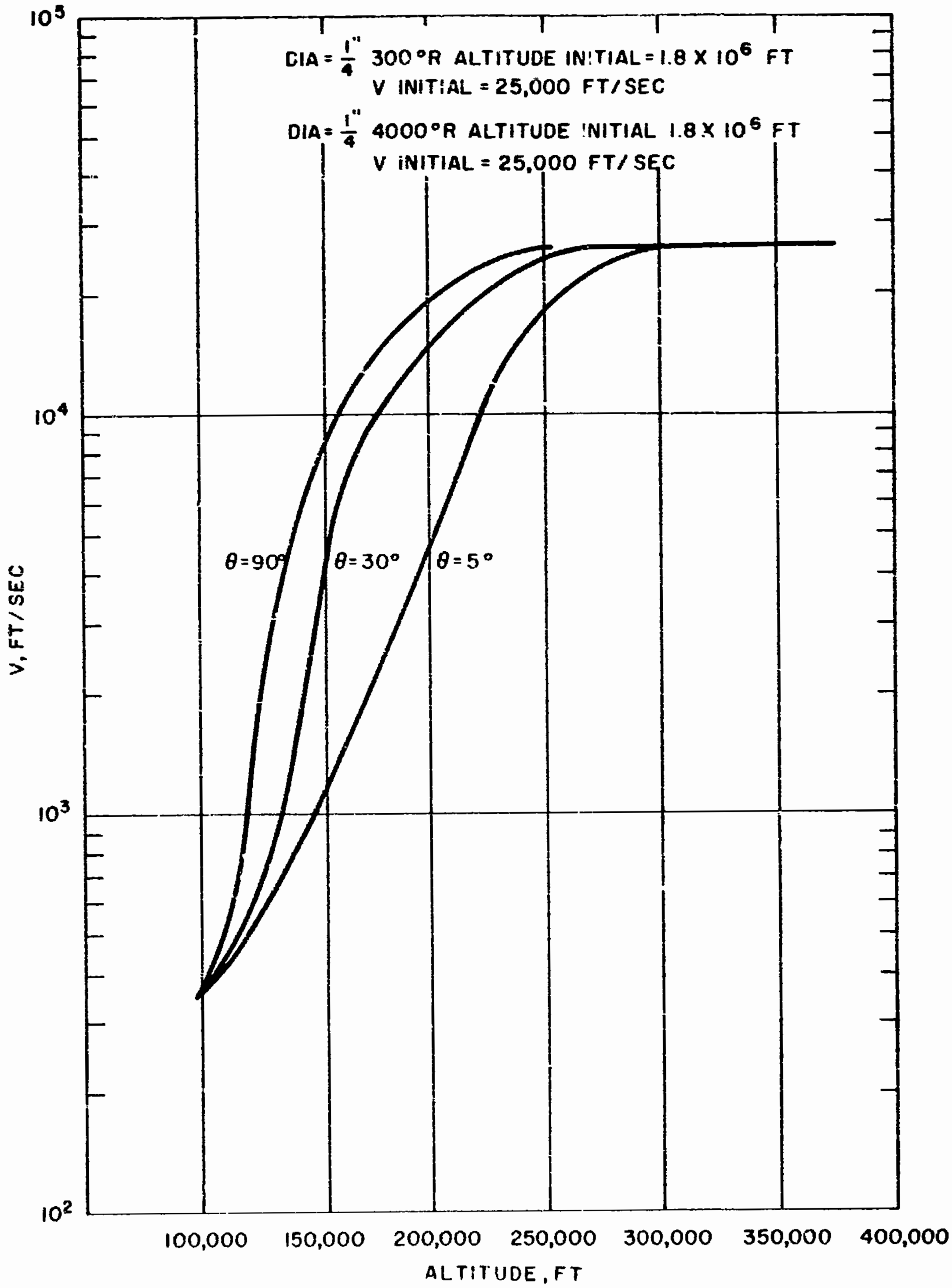

Figure 2 5

547183

Particle Velocity as a Function of Altitude

~~CONFIDENTIAL~~
~~RESTRICTED DATA~~
~~Atomic Energy Act 1954~~

Astronuclear

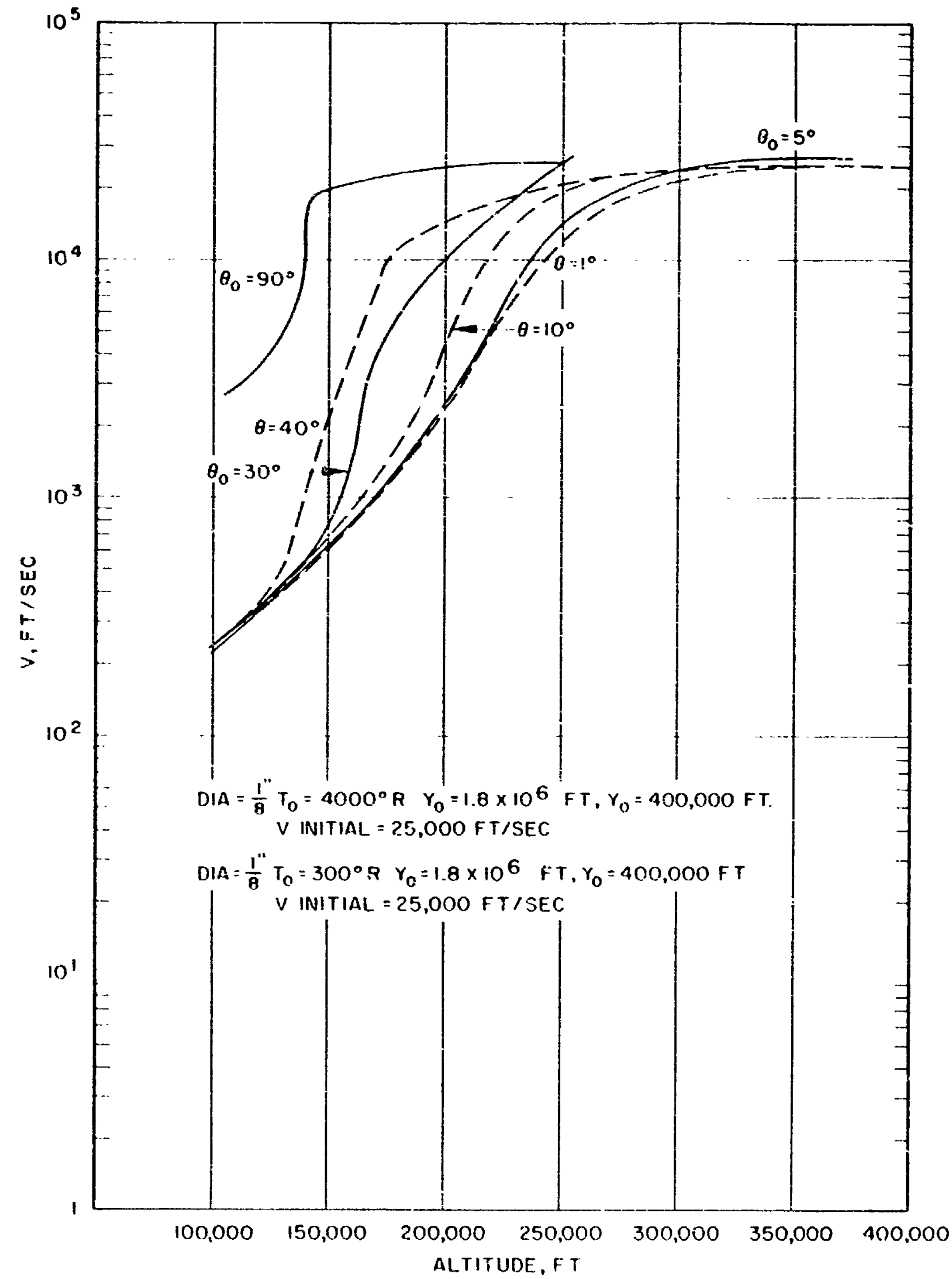

Figure 2.6

Particle Velocity as a Function of Altitude

547184

Astronuclear

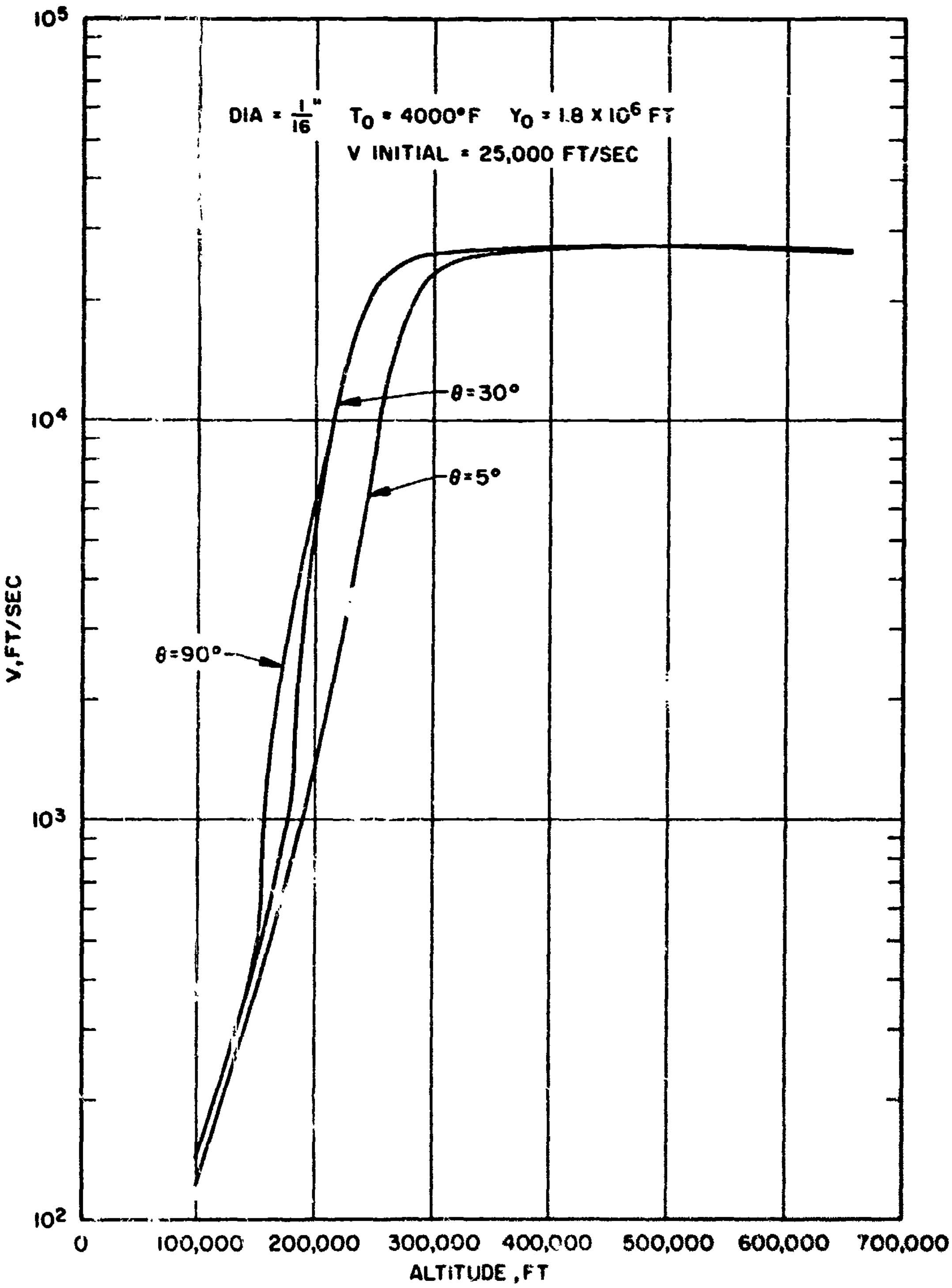

Figure 27

547185

Particle Velocity as a Function of Altitude

~~CONFIDENTIAL~~
~~RESTRICTED DATA~~
~~Atomic Energy Act - 1954~~

Astronuclear

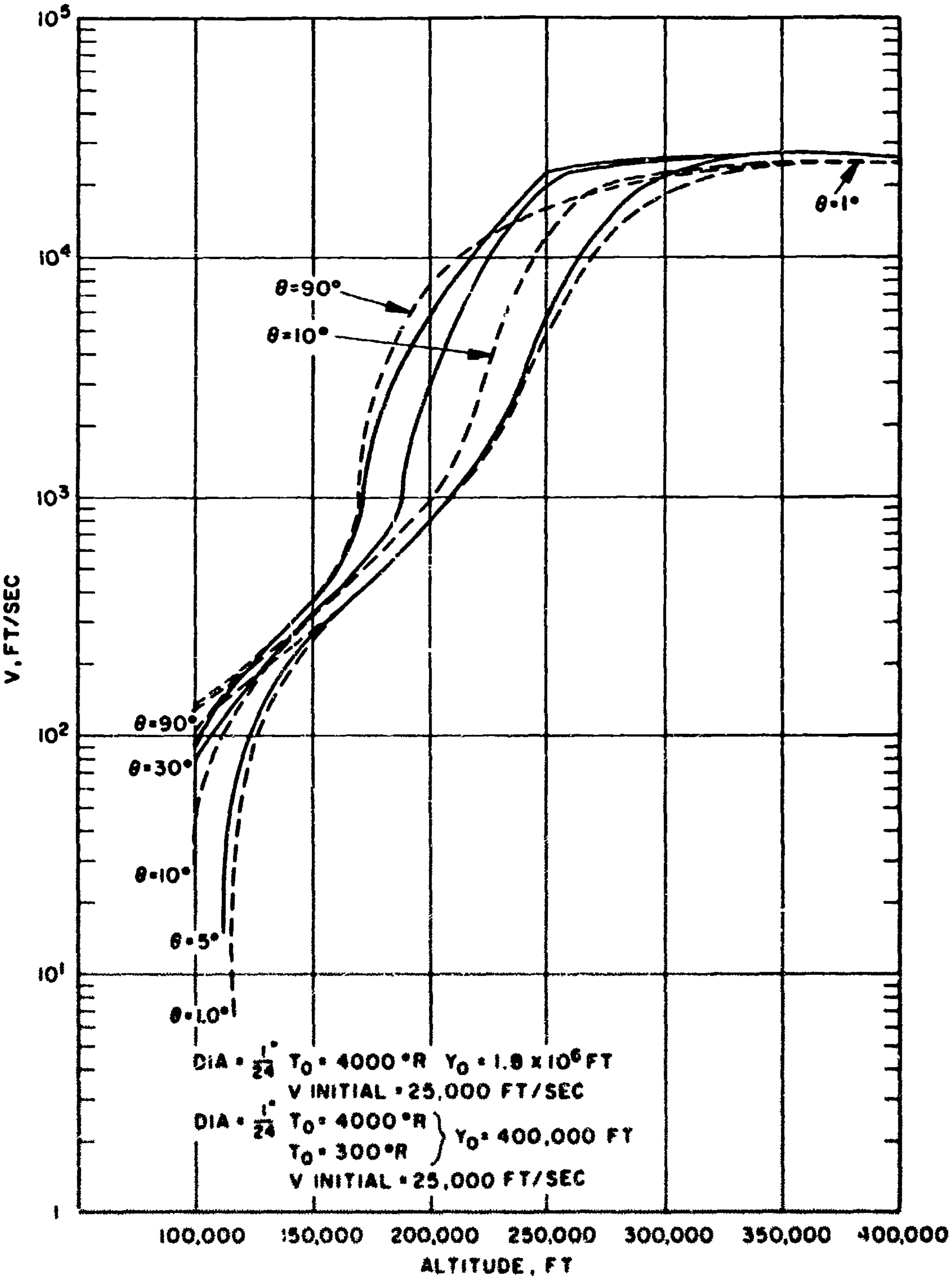

~~CONFIDENTIAL~~
~~RESTRICTED DATA~~
~~Atomic Energy Act - 1954~~

Figure 2.9

547196

Particle Velocity as a Function of Altitude

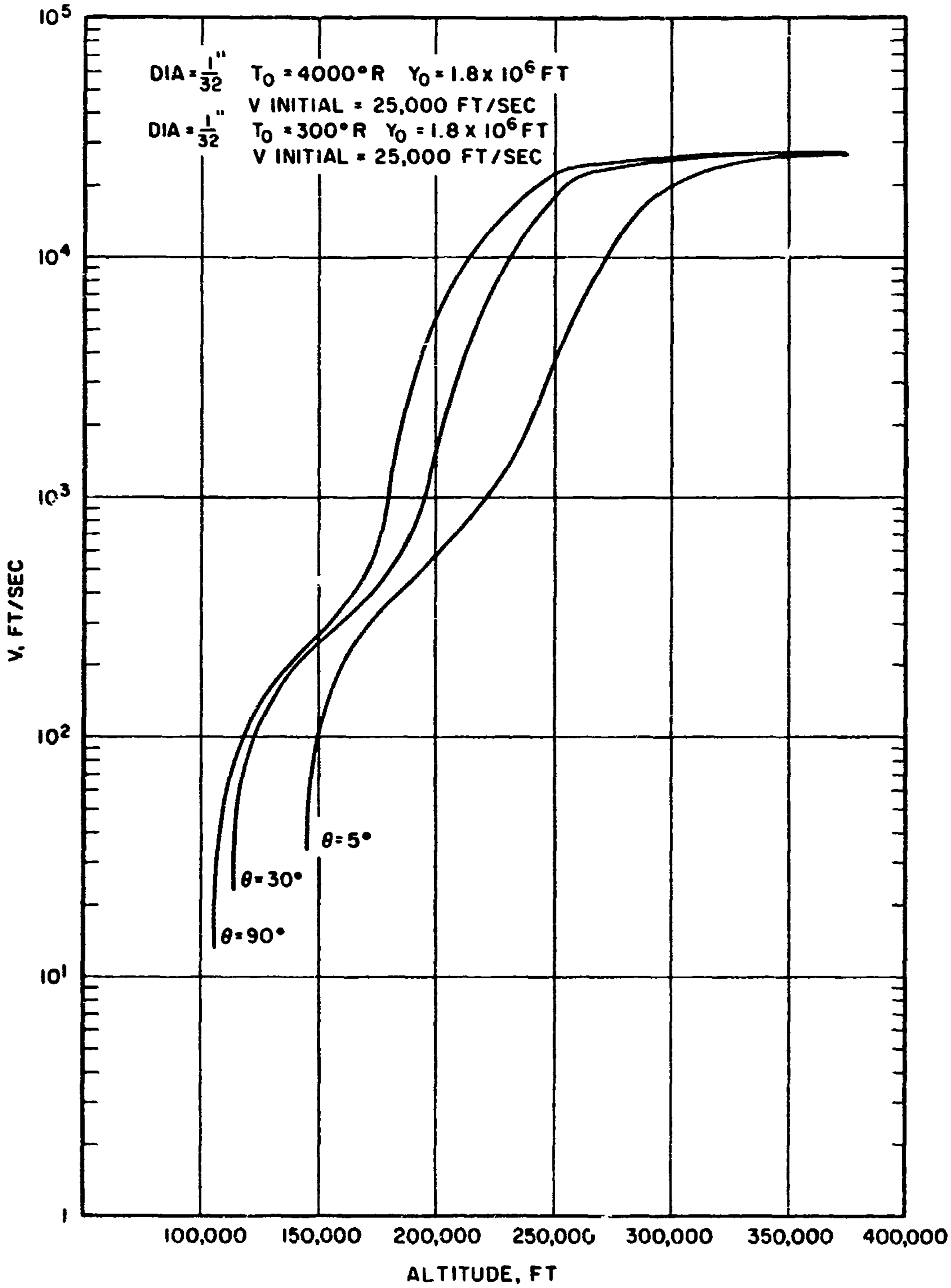

Figure 2.9 547187

Particle Velocity as a Function of Altitude

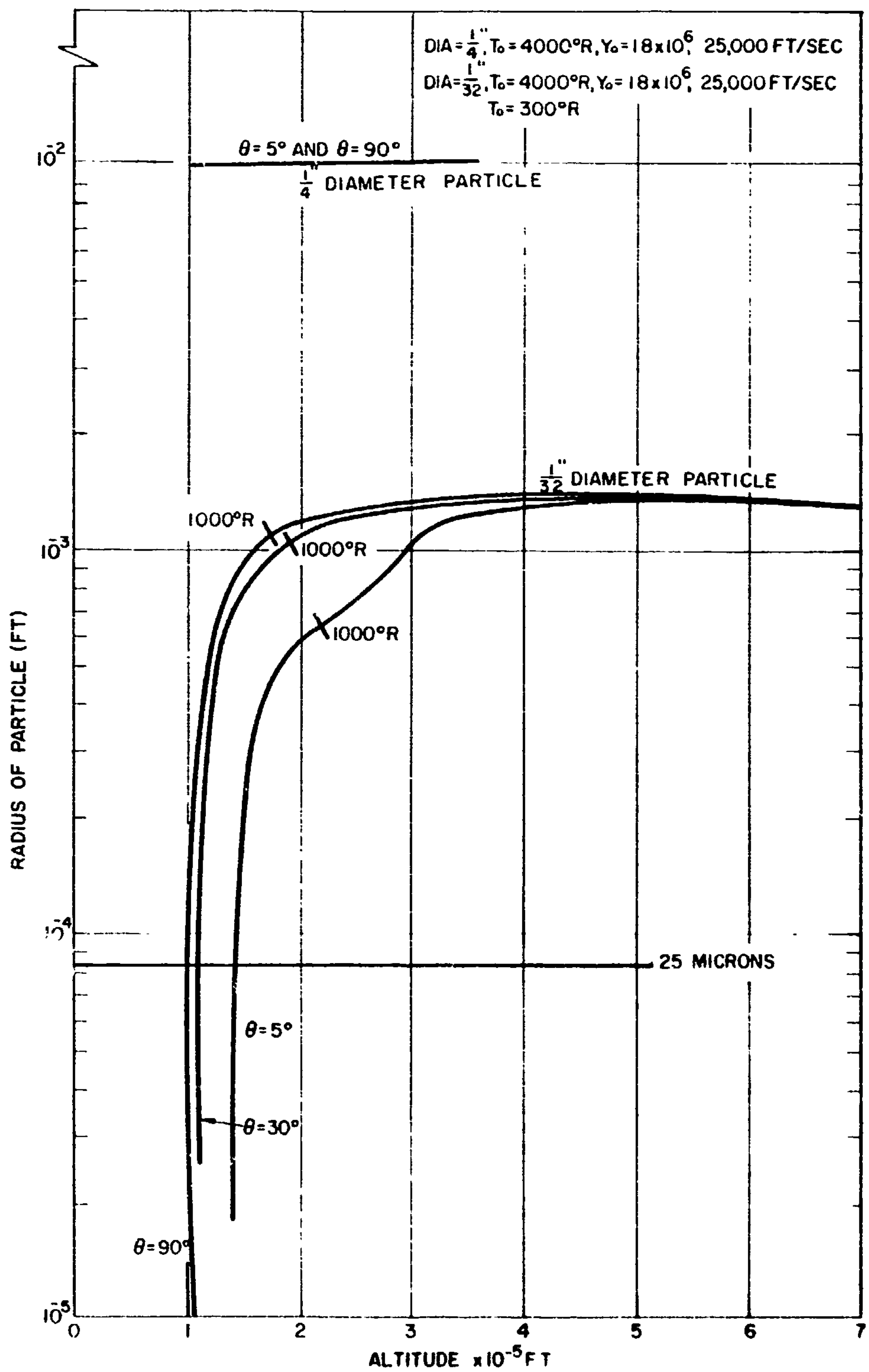

Figure 2 10

547193

Particle Radius as a Function of Altitude

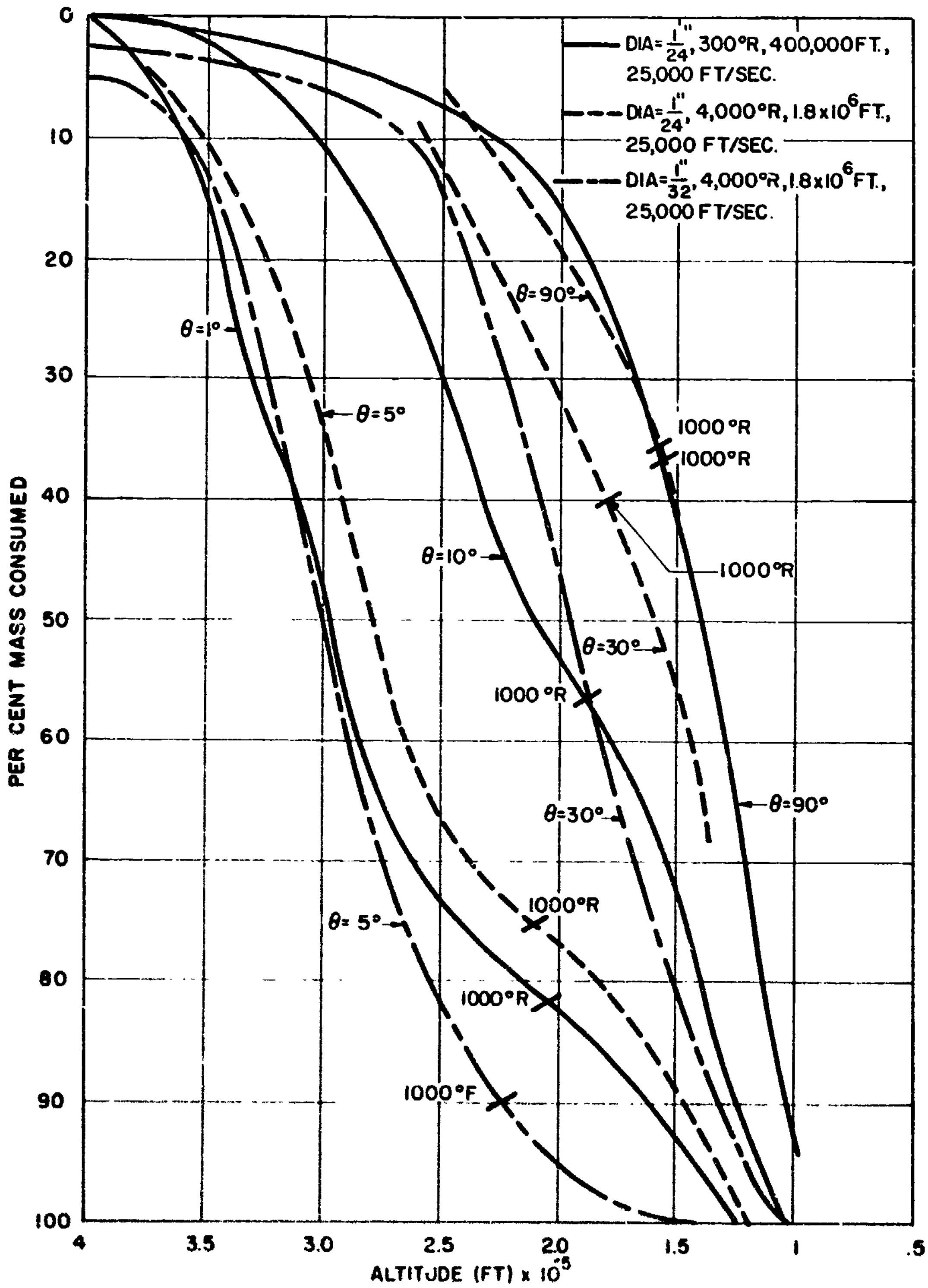

Figure 2.11

Percent Mass Consumed as a Function of Altitude

547192

~~CONFIDENTIAL~~
~~RESTRICTED DATA~~
~~Atomic Energy Act - 1954~~

Astronuclear

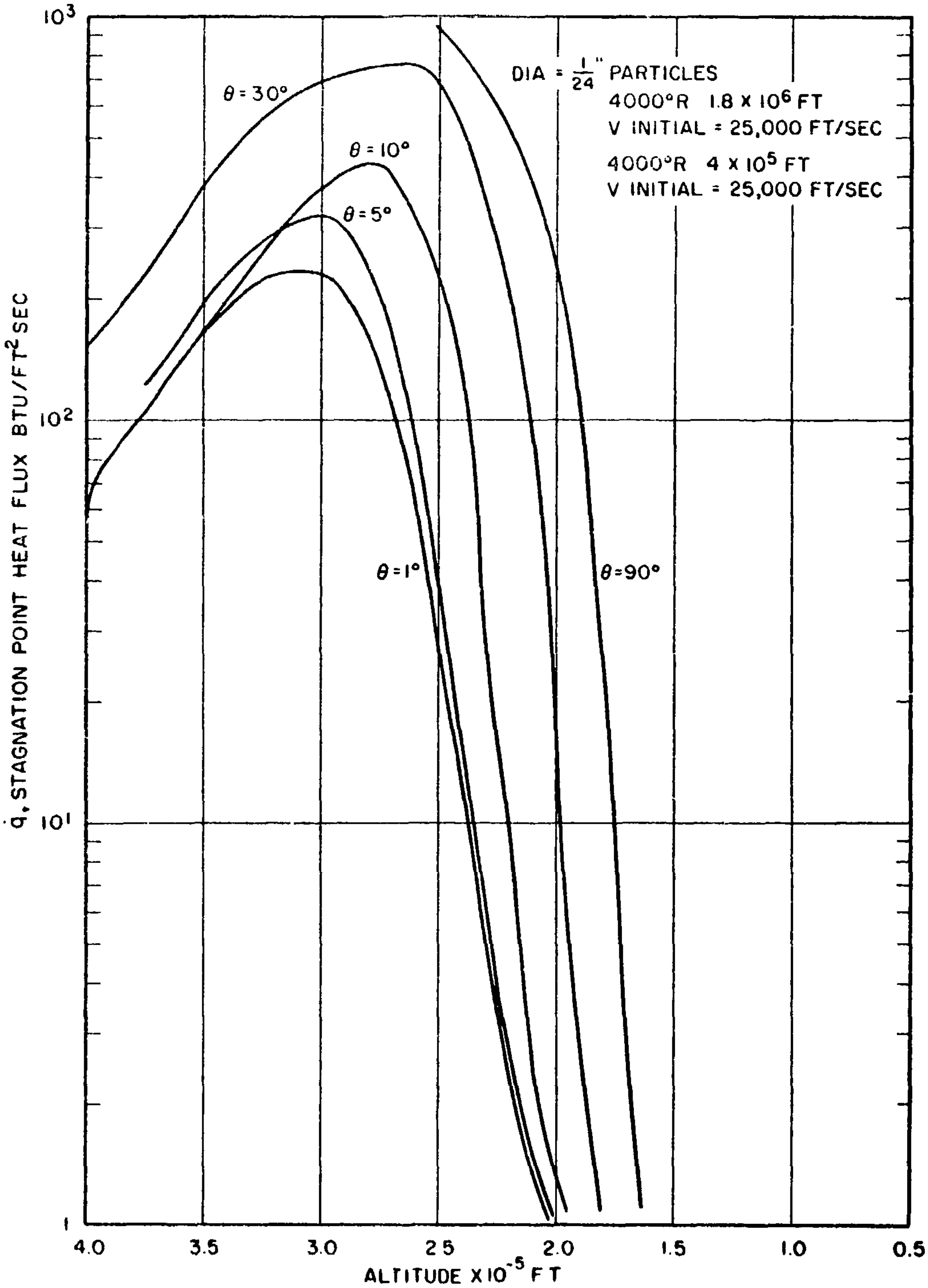

~~CONFIDENTIAL~~
~~RESTRICTED DATA~~
~~Atomic Energy Act - 1954~~

Figure 2 12

547138

Stagnation Point Heat Flux as a Function of Altitude

Astronuclear

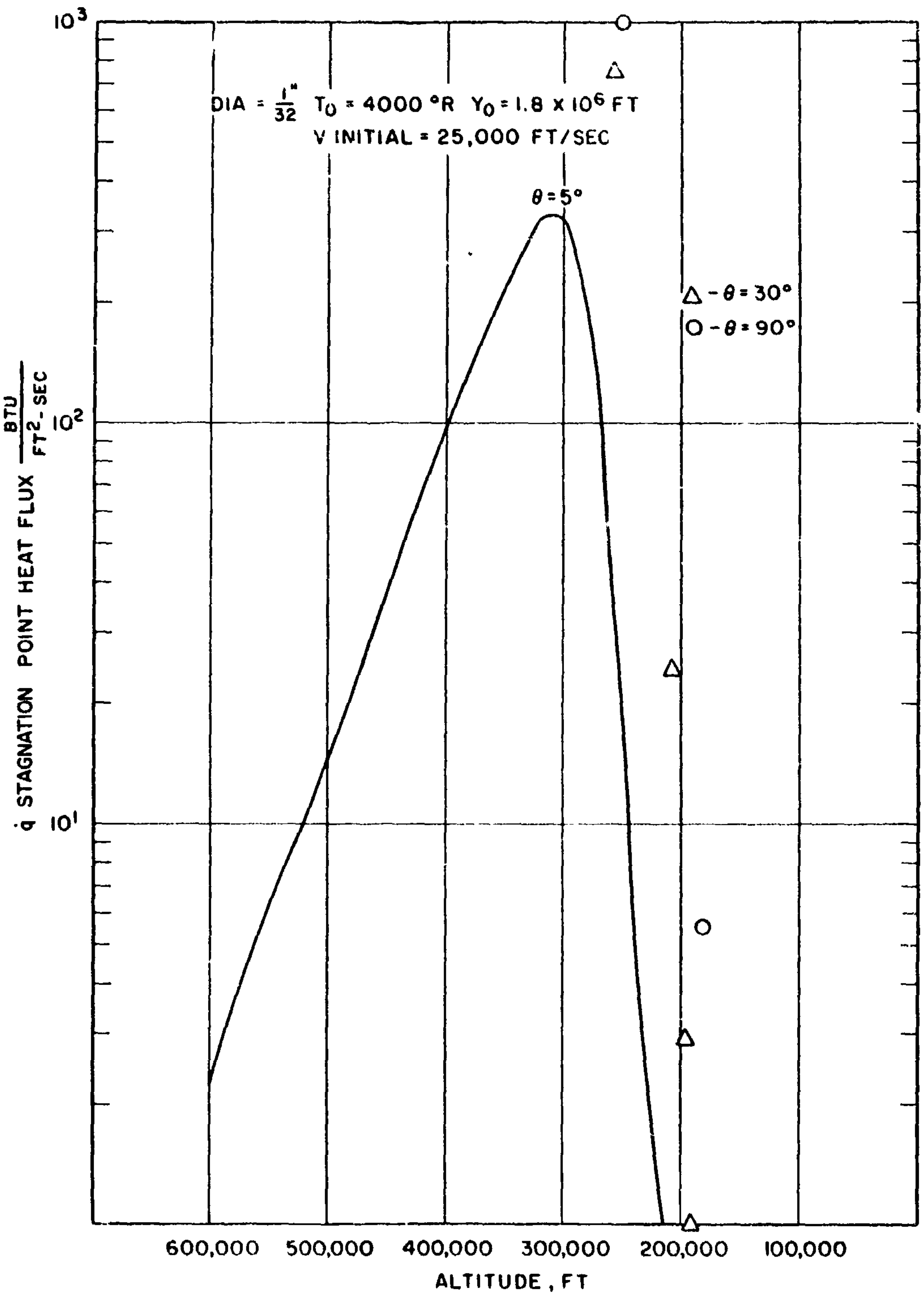

Figure 2.13 547190

Stagnation Point Heat Flux as a Function of Altitude

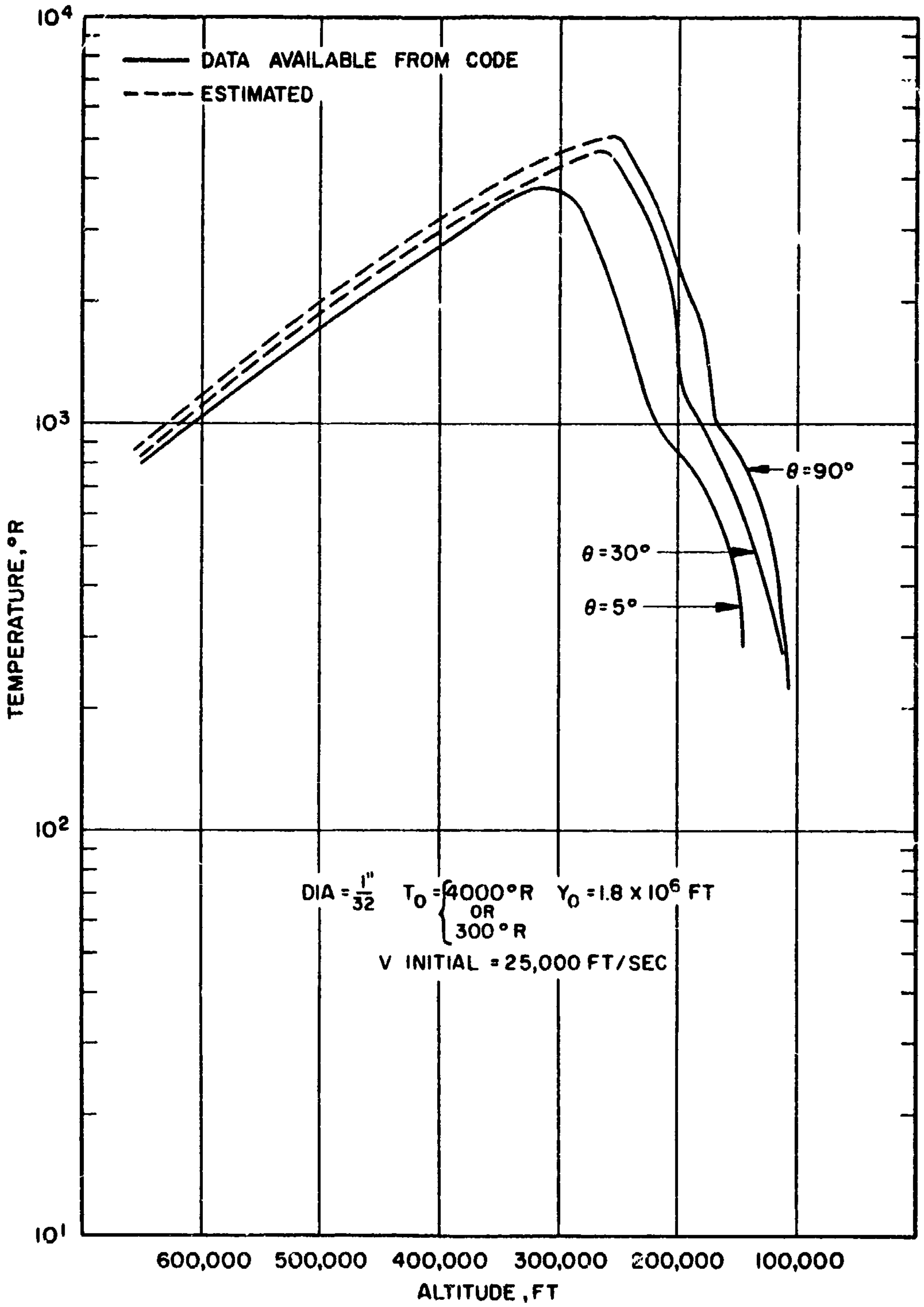

Figure 2.14 547191

Particle Surface Temperature as a Function of Altitude

Astronuclear

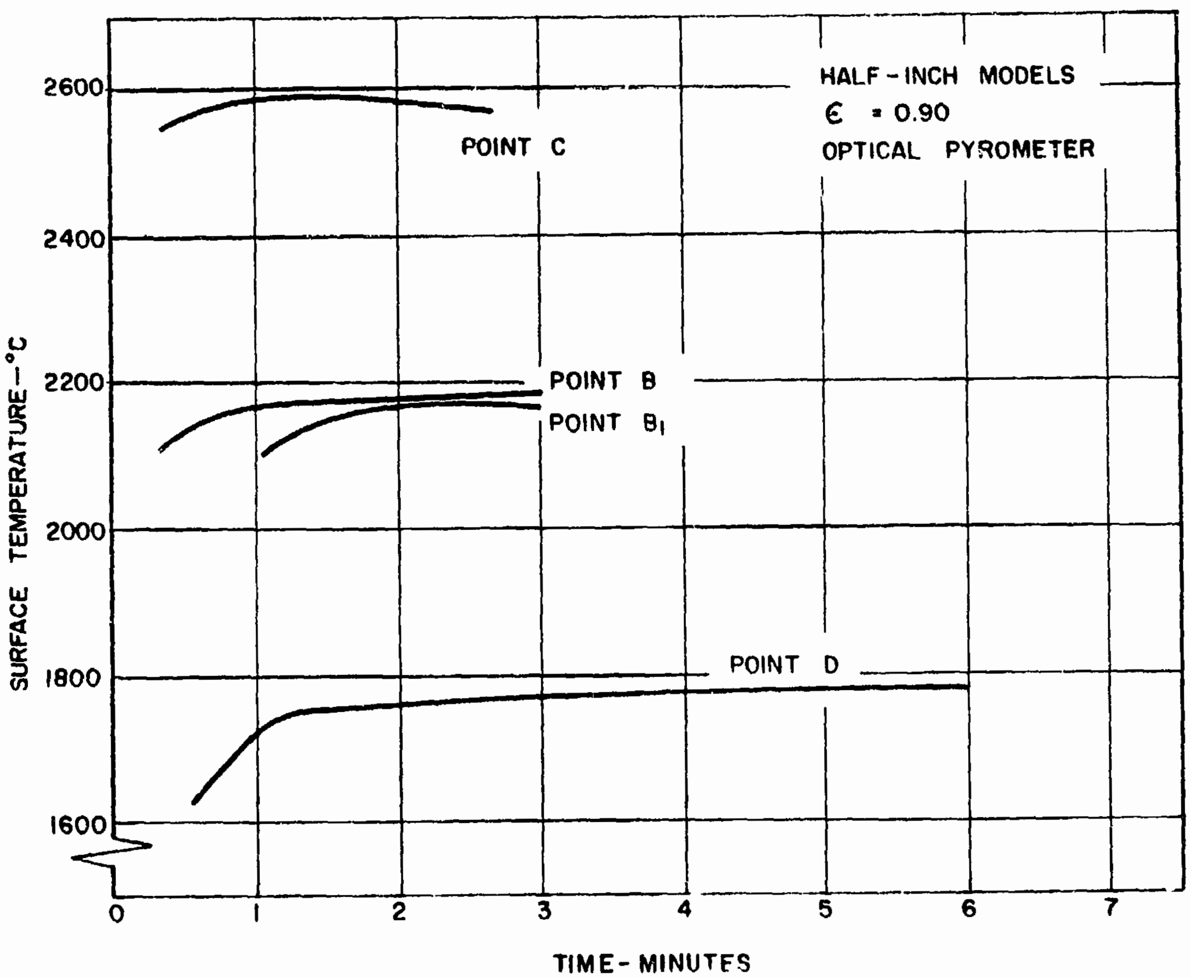

Figure 3.1 547165

Representative Surface Temperatures for Half-inch Models

~~CONFIDENTIAL~~
~~RESTRICTED DATA~~
~~Atomic Energy Act 1954~~

Astronuclear

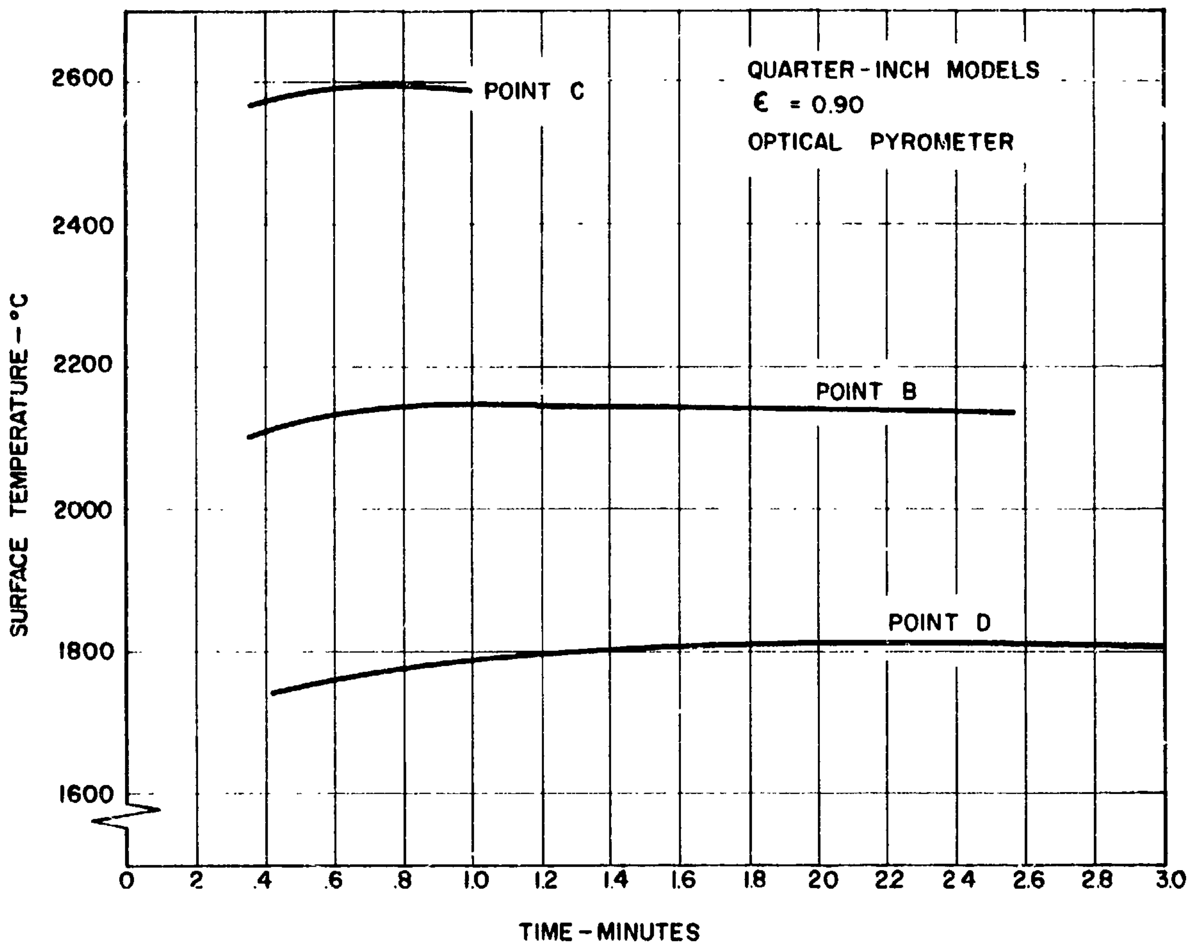

Figure 3.2 547166

Representative Surface Temperatures for Quarter-inch Models

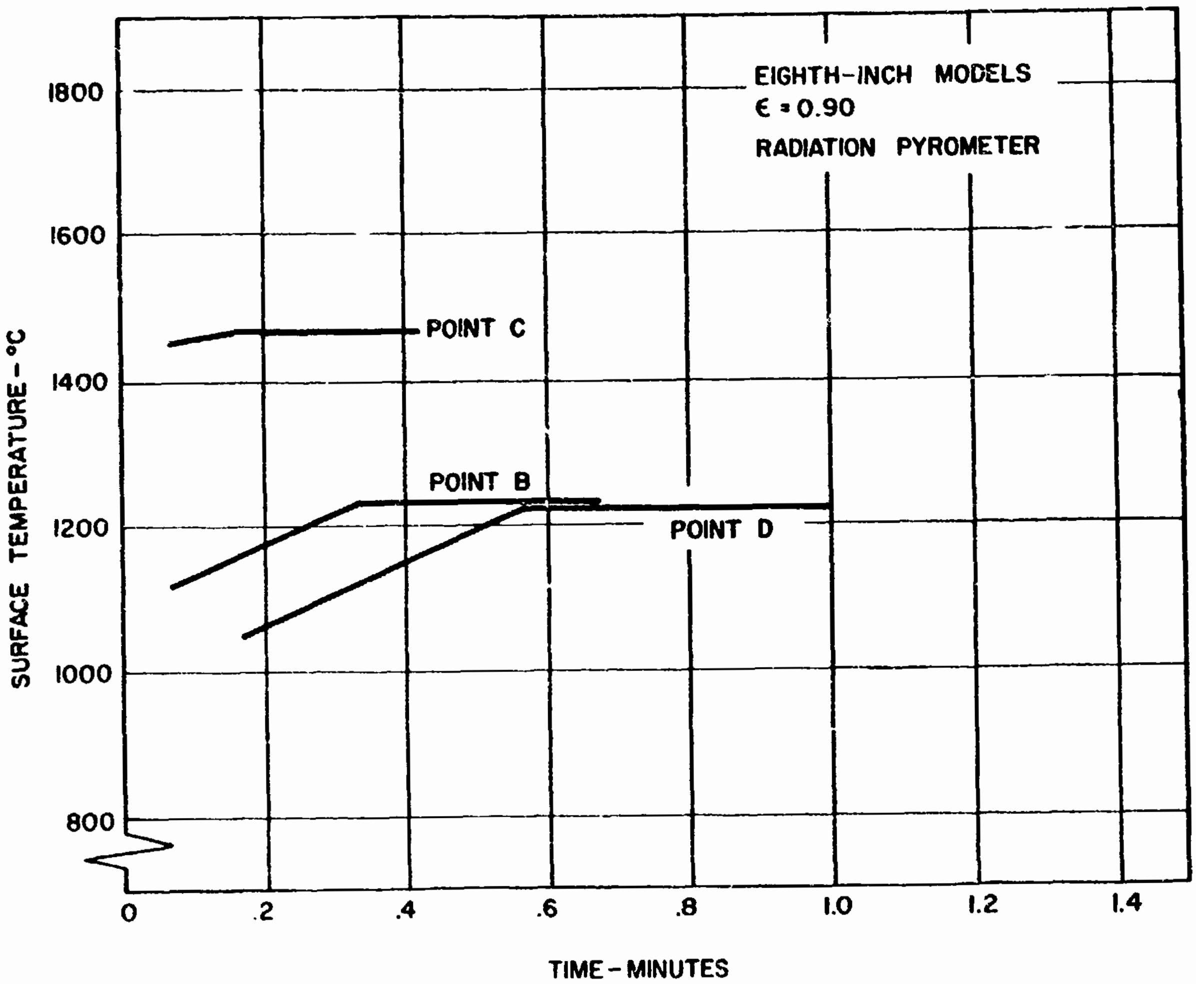

Figure 3.3 547167

Representative Surface Temperatures for Eighth-inch Models

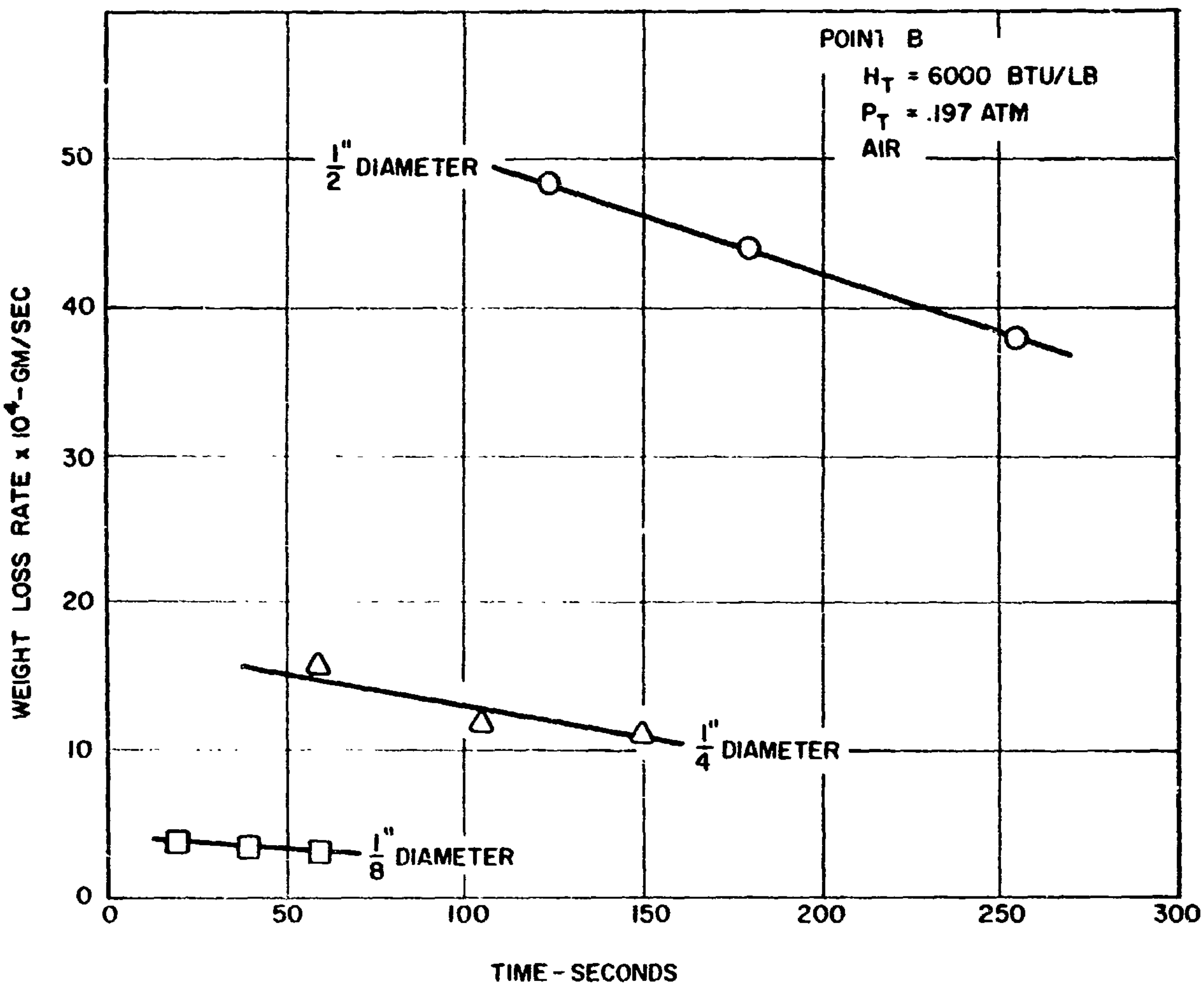

Figure 3 4

Weight Loss Rate – Point B

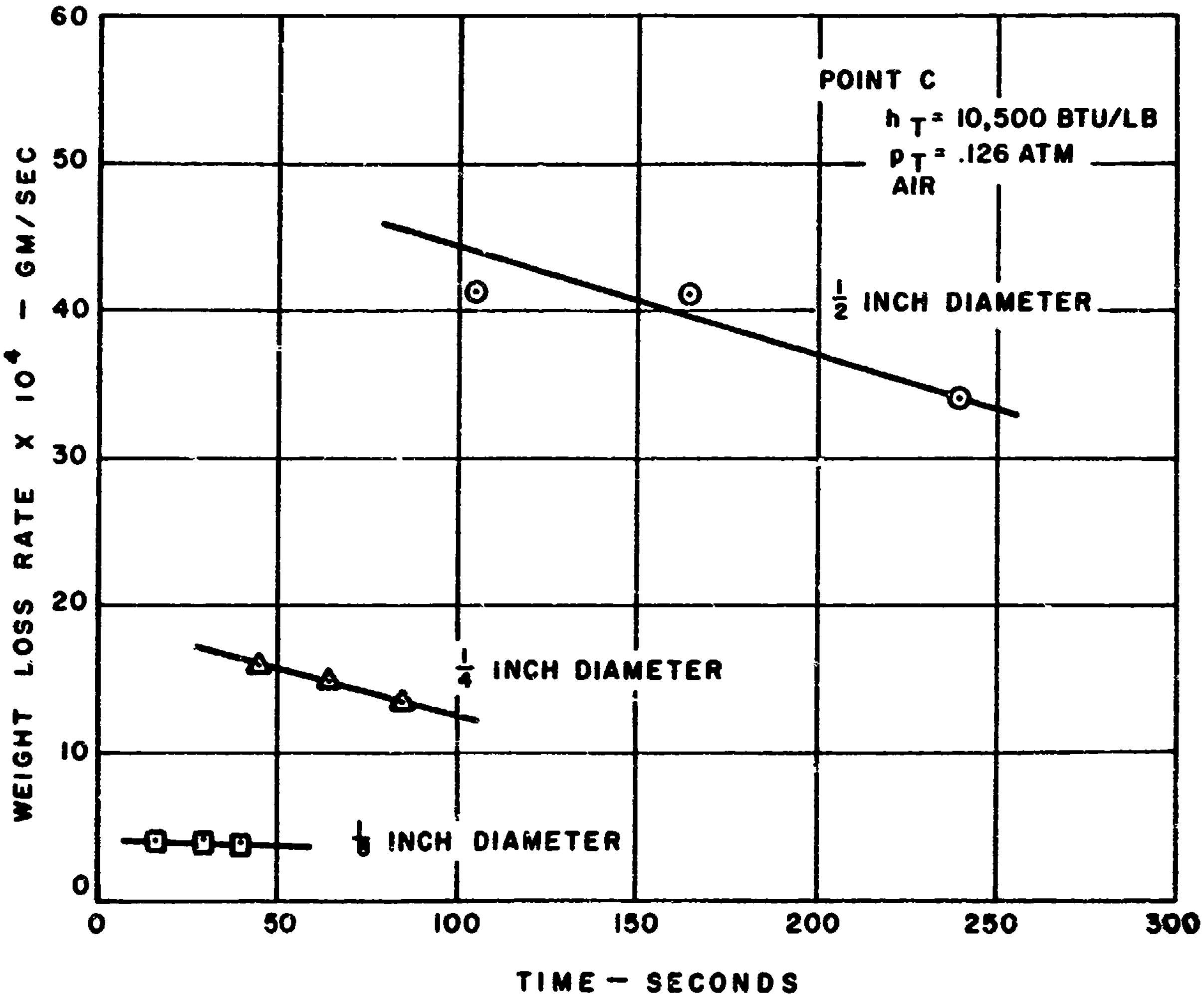

Figure 3 5

547169

Weight Loss Rate - Point C

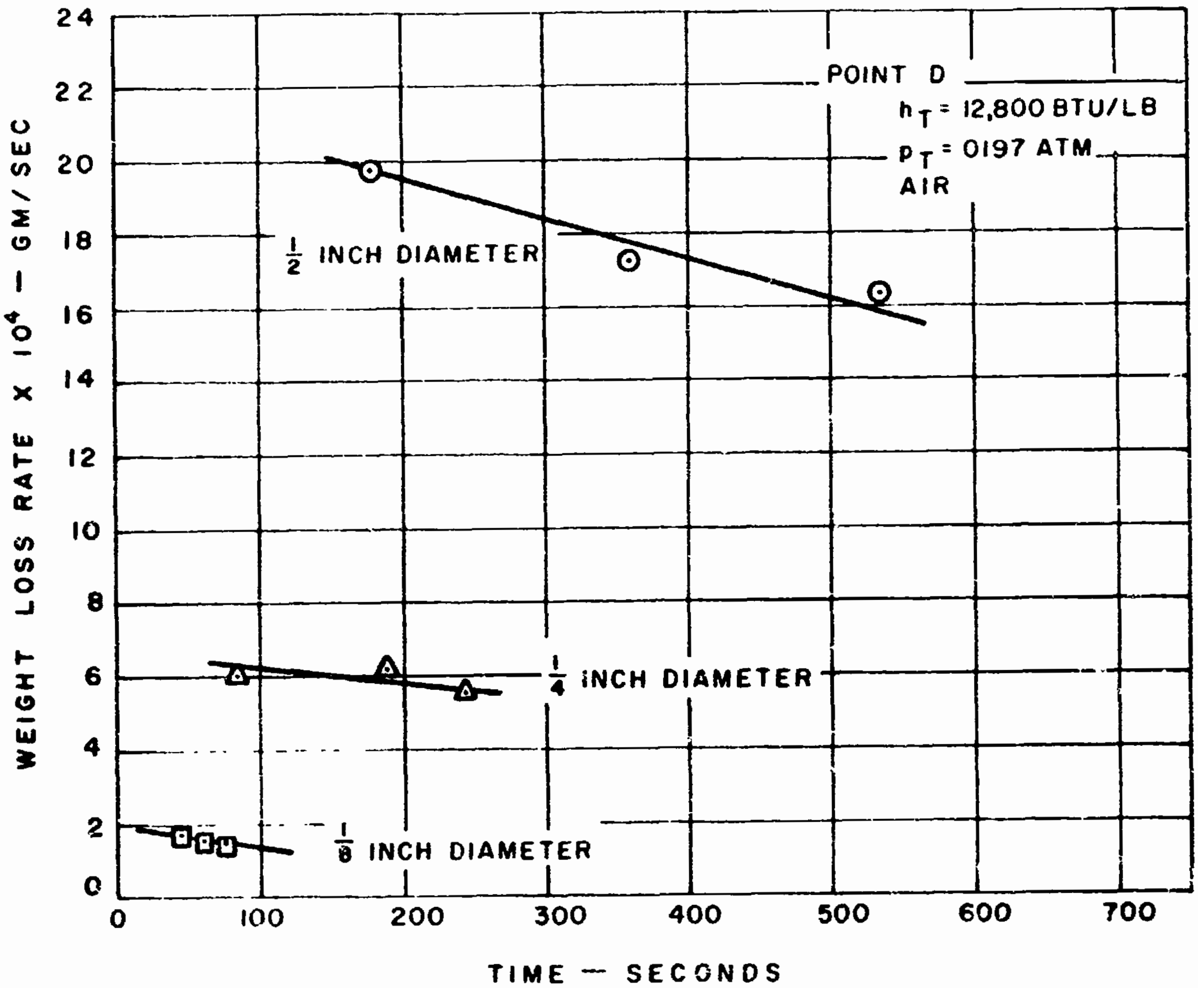

Figure 3 6

Weight Loss Rate - Point D

547170

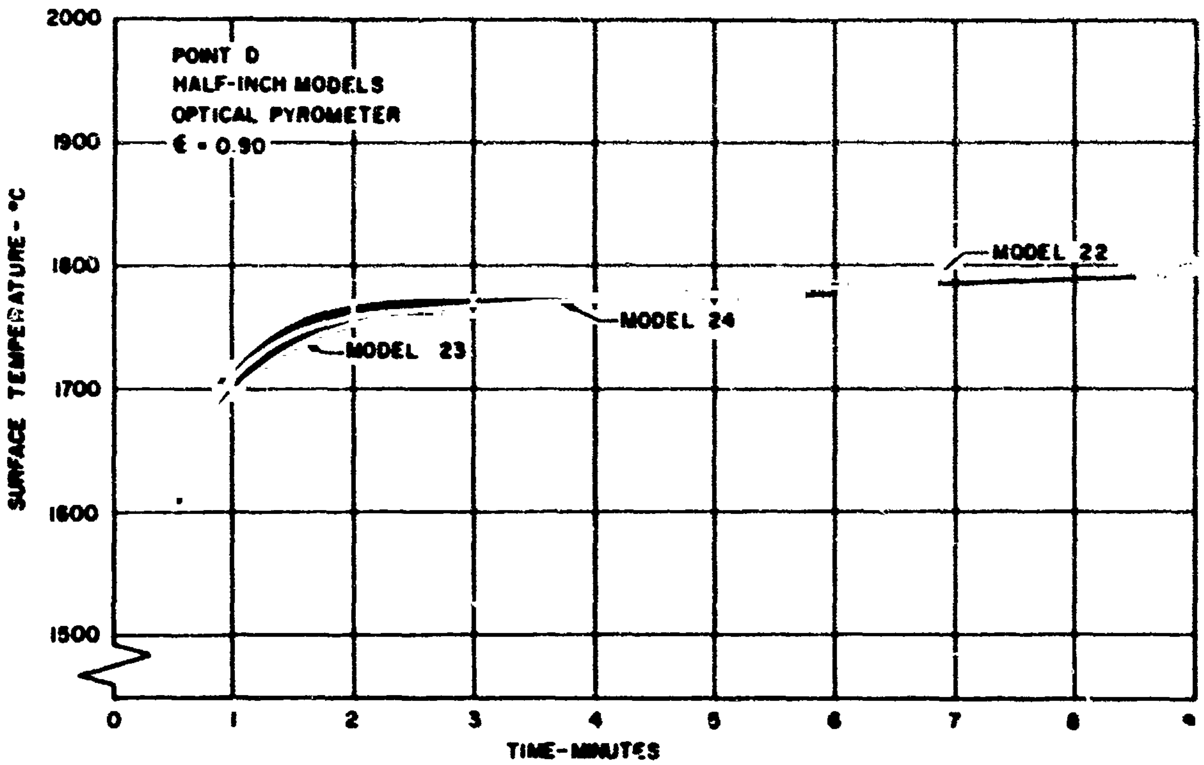

Figure 3.7 547171

Specimen Surface Temperature as a Function of Exposure Time

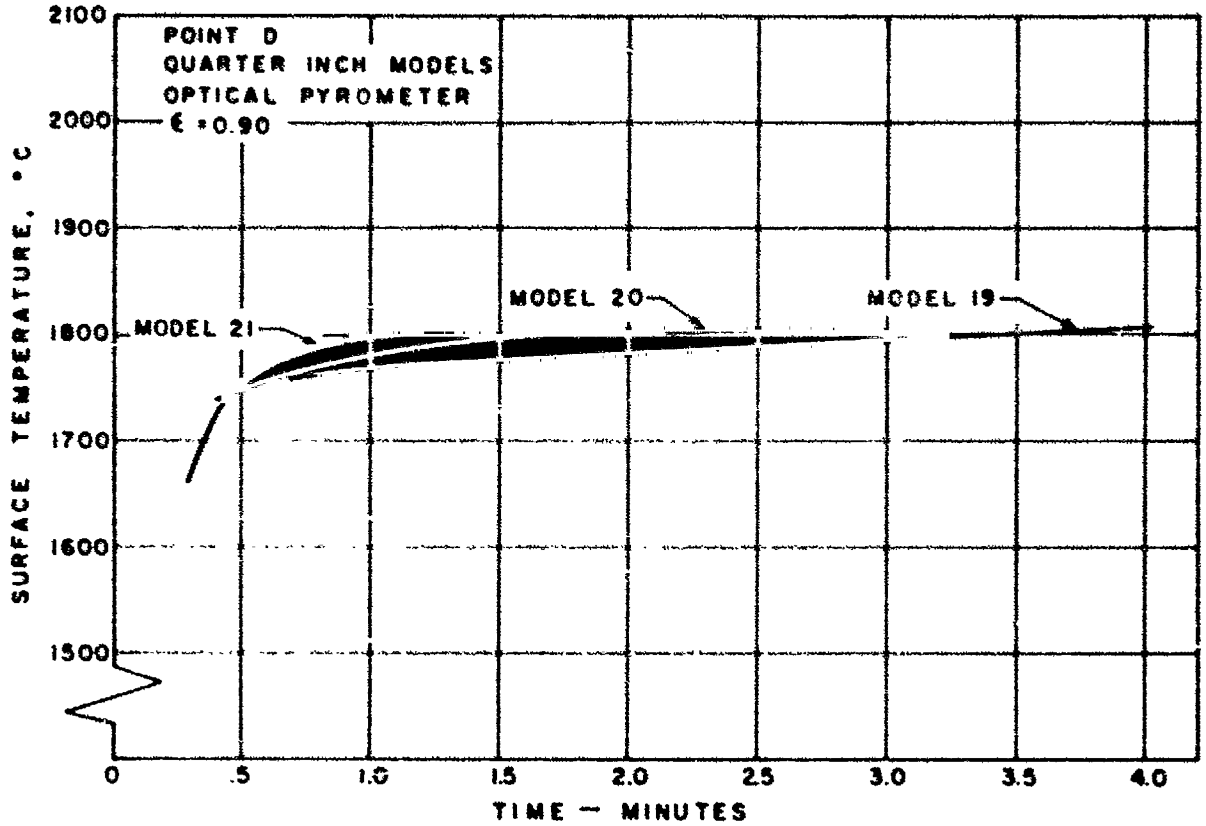

Figure 3 3 547172

Specimen Surface Temperature as a Function of Exposure Time

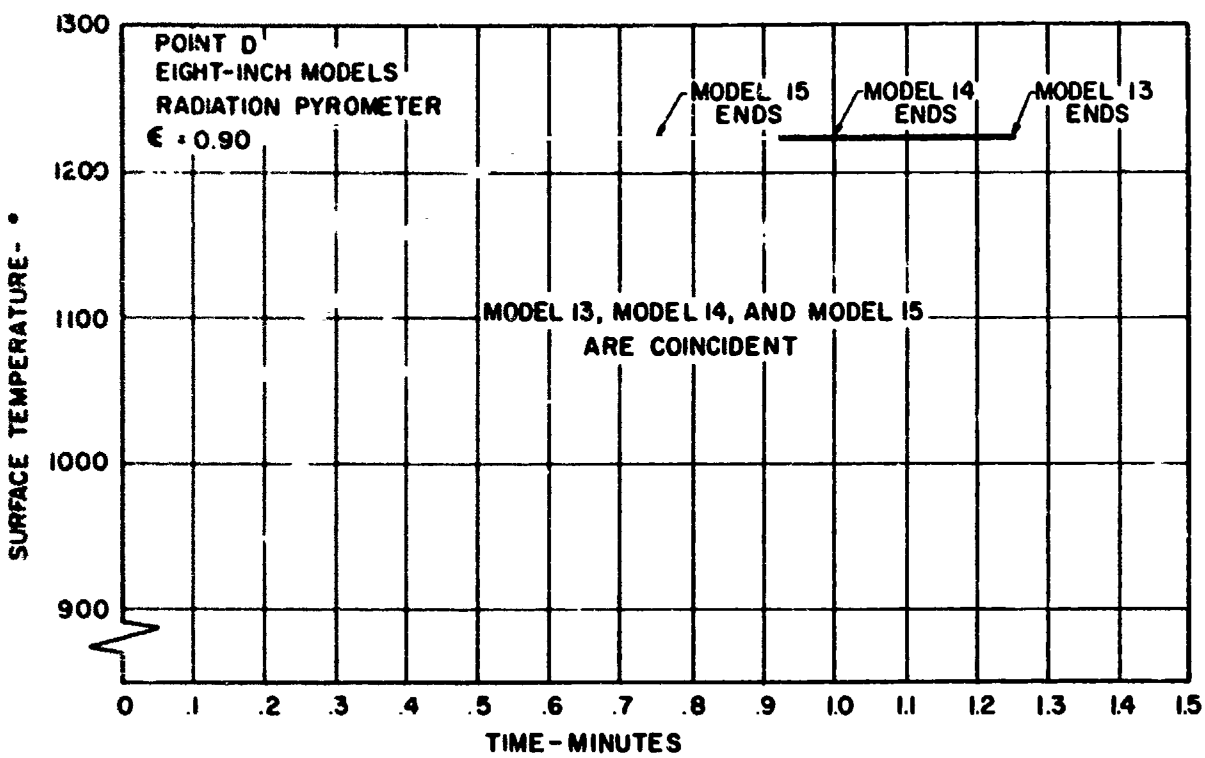

Figure 3.9 547173

Specimen Surface Temperature as a Function of Exposure Time

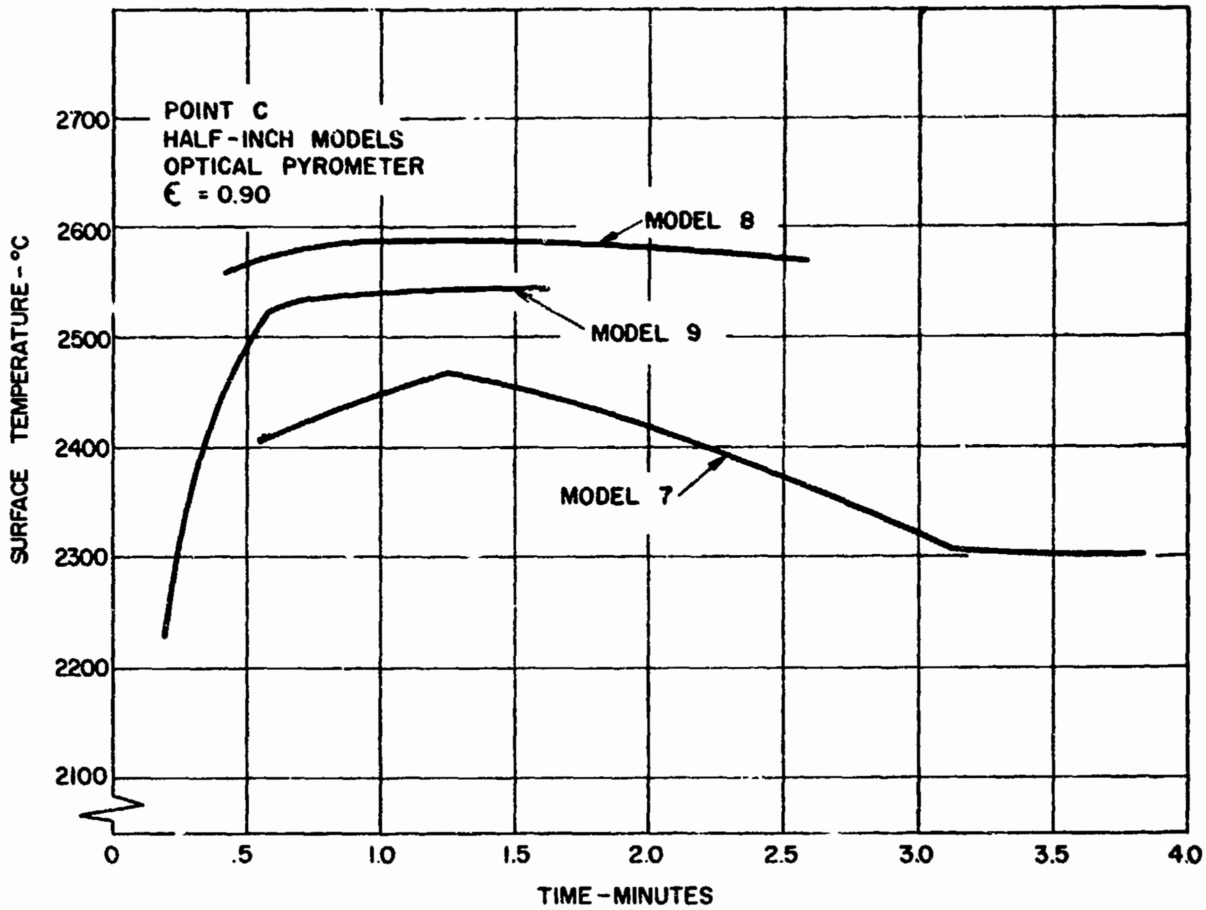

Figure 3.10 547174

Specimen Surface Temperature as a Function of Exposure Time

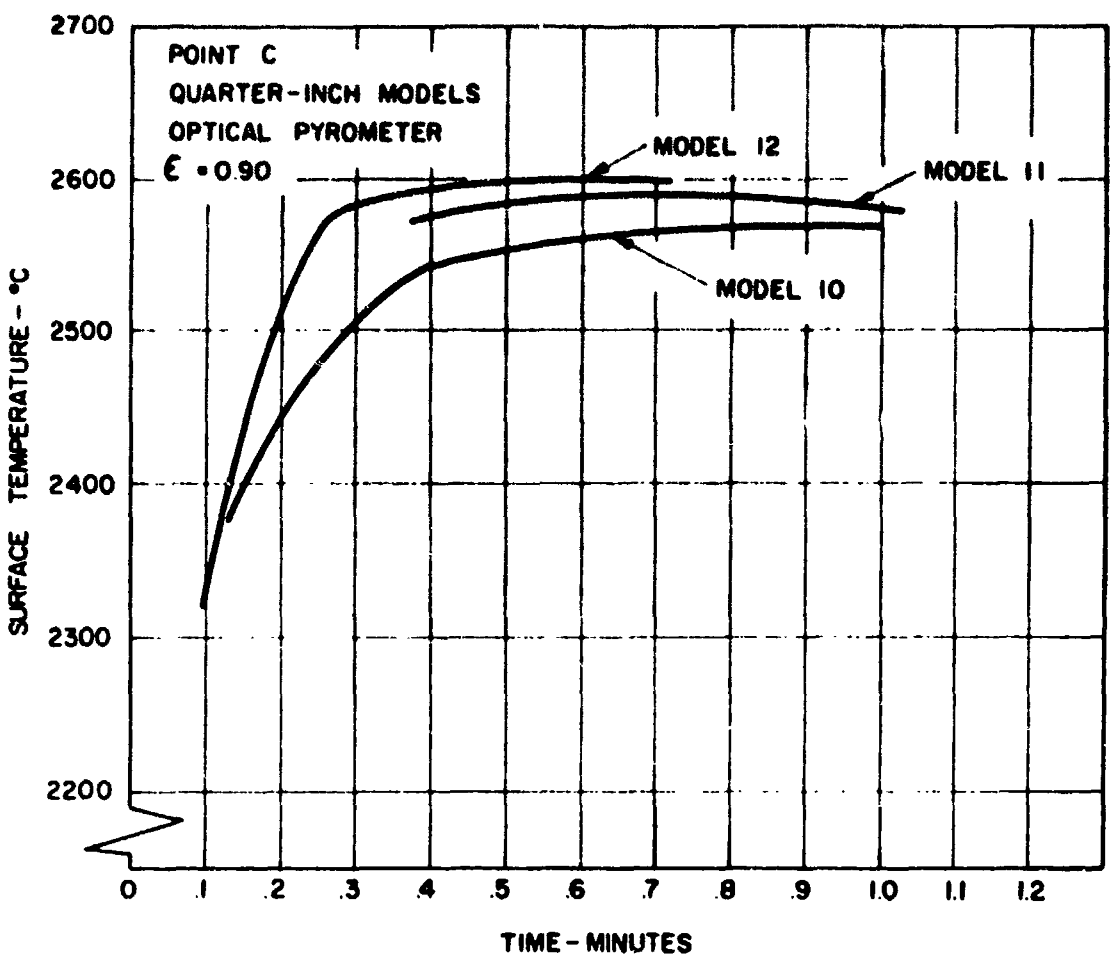

Figure 3.11 547175

Specimen Surface Temperature as a Function of Exposure Time

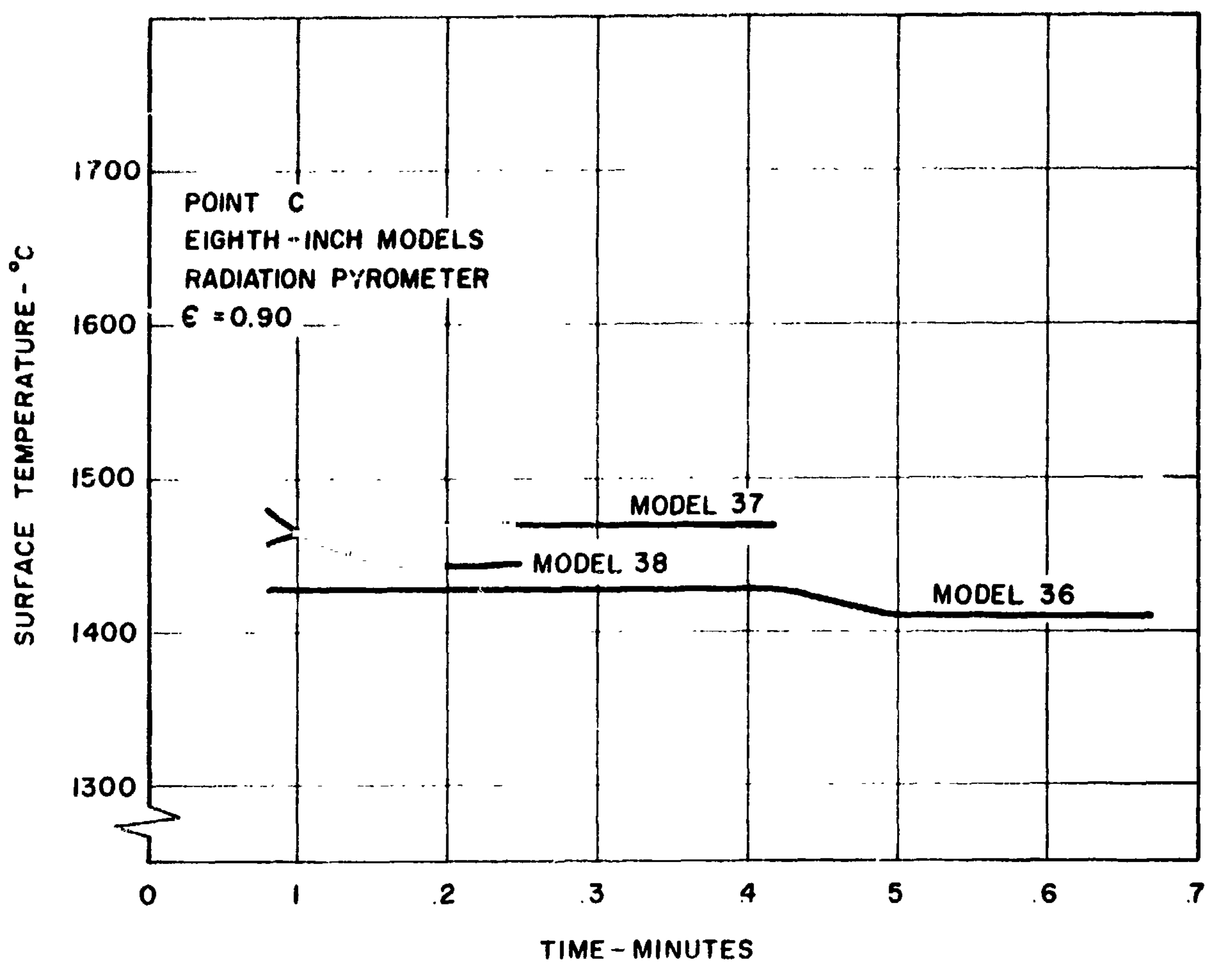

Figure 3.12

Specimen Surface Temperature as a Function of Exposure Time

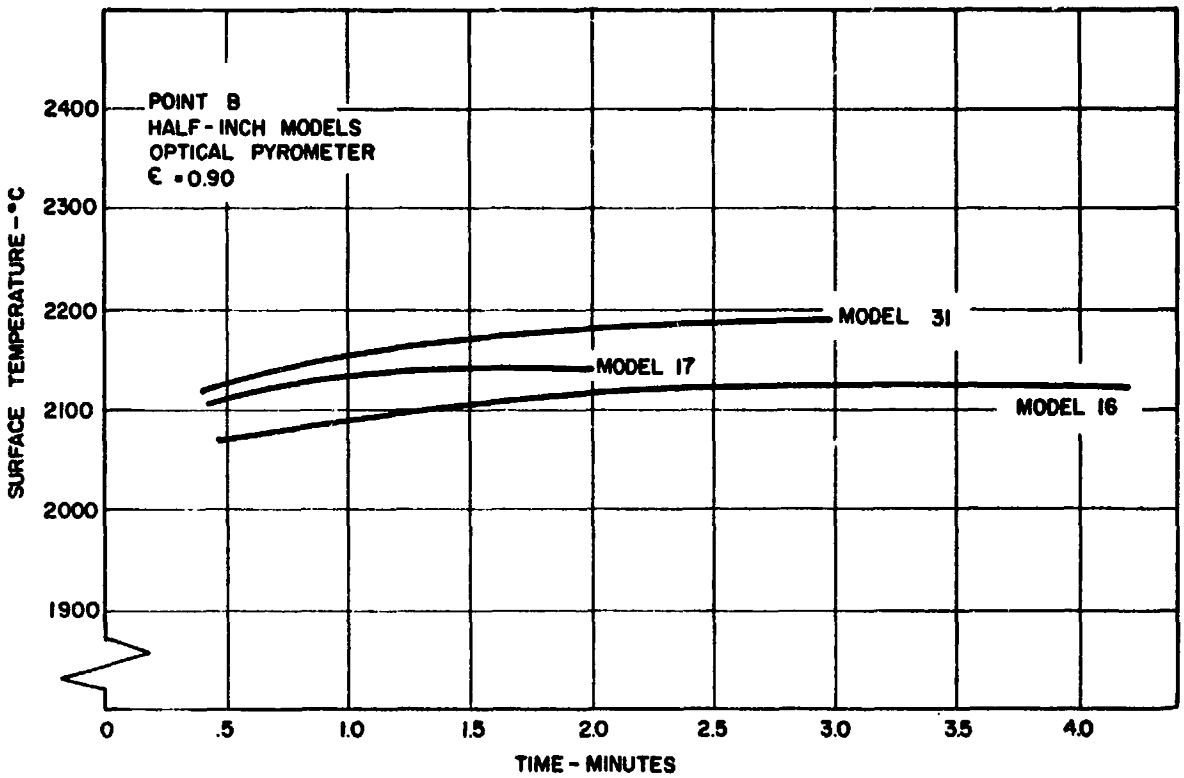

Figure 3.13 547177

Specimen Surface Temperature as a Function of Exposure Time

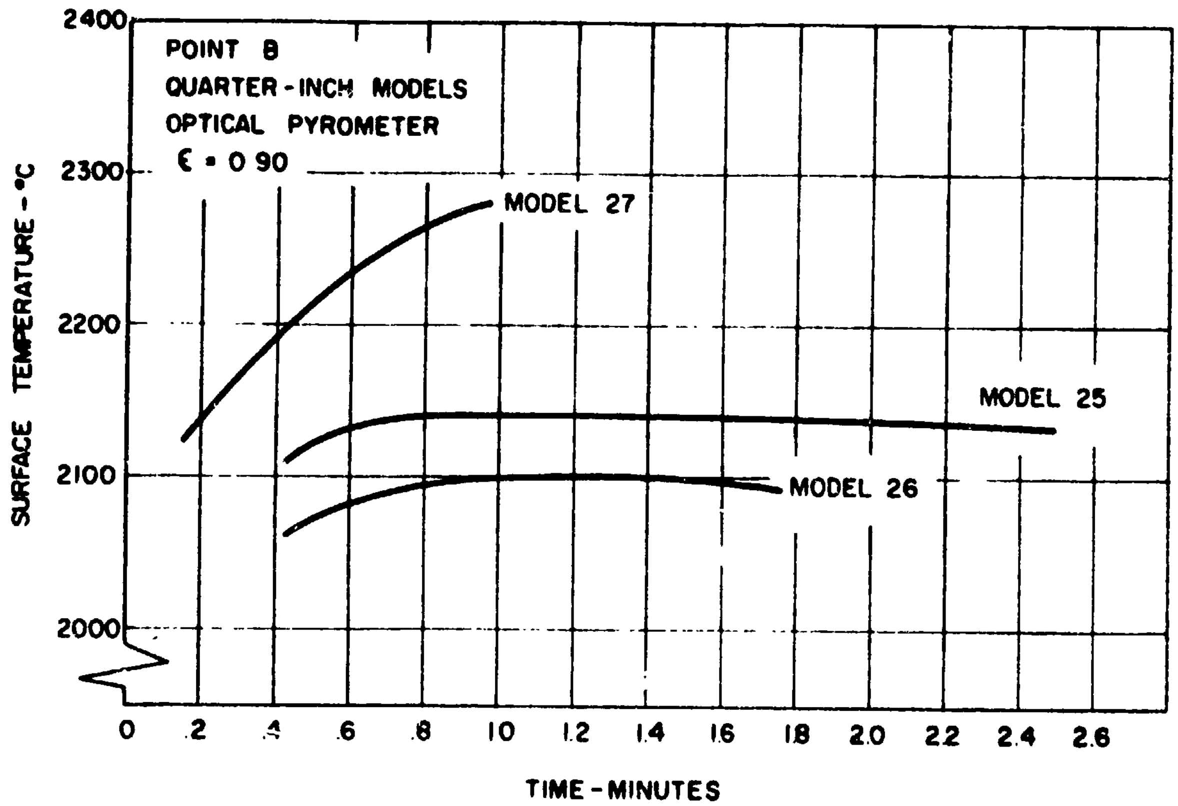

Figure 3.14 547178

Specimen Surface Temperature as a Function of Exposure Time

~~CONFIDENTIAL~~
~~RESTRICTED DATA~~
~~1954~~

Astronuclear

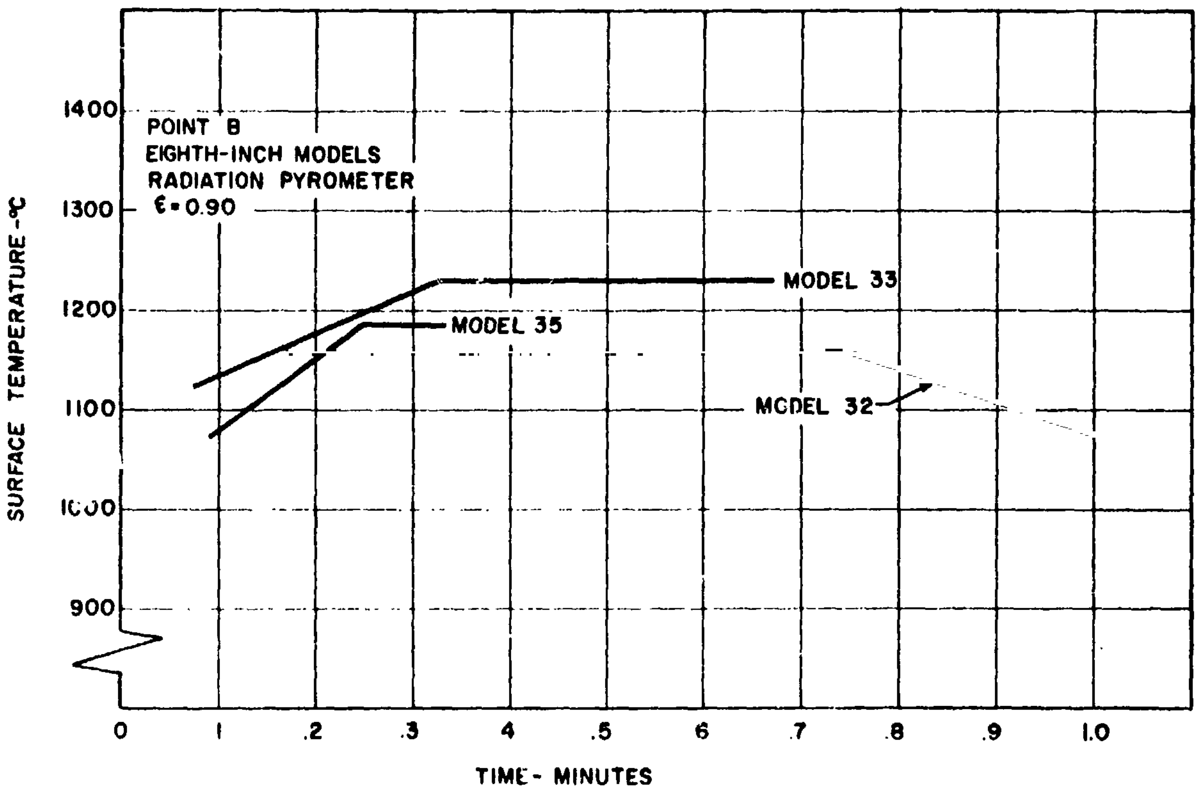

~~CONFIDENTIAL~~
~~RESTRICTED DATA~~
[redacted]

Figure 3.15

547179

Specimen Surface Temperature as a Function of Exposure Time

Astronuclear

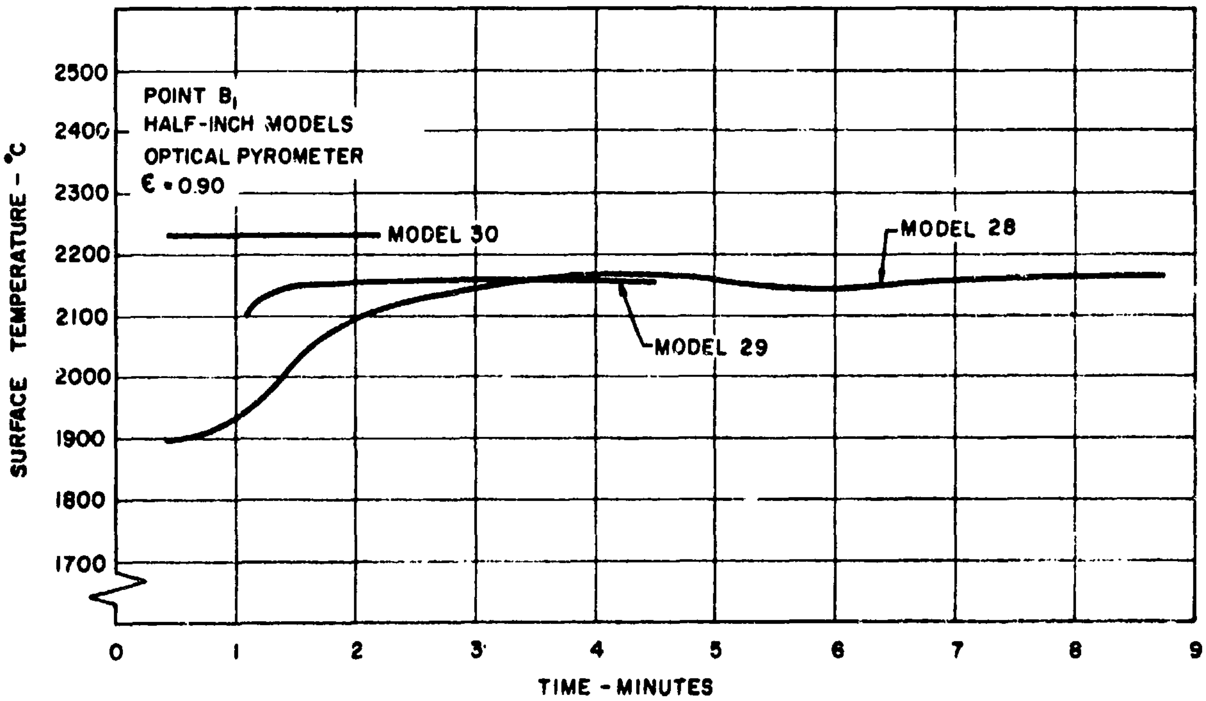

Figure 3.16 547180

Specimen Surface Temperature as a Function of Exposure Time

~~CONFIDENTIAL~~
~~RESTRICTED DATA~~
~~Atomic Energy Act - 1954~~

Astronuclear
WANL-TNR-040

WESTINGHOUSE ELECTRIC CORPORATION
ASTRONUCLEAR LABORATORY
P. O. Box 10864
Pittsburgh 36, Pa.
March, 1962

SURVEY OF FISSION PRODUCT RELEASE FROM NERVA FUEL MATERIAL

(Title Unclassified)

NERVA NUCLEAR SUBSYSTEM

~~CONFIDENTIAL~~
~~RESTRICTED DATA~~
~~Atomic Energy Act - 1954~~

TABLE OF CONTENTS

	Page
1.0 Introduction	1
2.0 Theoretical Examination of Problem	2
3.0 Review of Literature	4
3.1 LASL Data	5
3.2 Data from Other Sources	19
3.3 Fission Product Release from Related Materials	24
4.0 Discussion of Fission Product Release Data	27
5.0 Recommendations for Fission Product Release Experiments	31
6.0 Acknowledgements	33
7.0 Bibliography	35

LIST OF TABLES

1	Summary of Conditions for Fueled Graphite Fission Product Retention Studies at LASL - Conditions for LASL Experiments	6
2	Retention of Fission Products in Admixture and Solution Impregnated Fuel Samples Heated for 10 and 65 Minutes at 1925 - 1950°C	16 - 17
3	Retention of Fission Products in a Coated and Uncoated KIWI-A Prime Fuel Element Heated at 2150°C for 5 Minutes Plus 1 Minute Warmup	18
4	Diffusion of Some Fission Product Elements Under Varying Conditions of Accessibility to Specimen Surface	25
5	Comparison of Fission Product Release for Fueled Graphite (Admixture Type) and a UC-ZrC Solid Solution at 2400°C	26

LIST OF FIGURES

Figure	Title	Page
1	Theoretical Model of Fission Product Release From Fueled Graphite. For all of the Diffusion Paths Indicated The Possibility of Rate Limiting Surface (Such as Evaporation or Oxidation) or Interface Reactions Must Be Considered.	3
2	Fission Product Retention After Heating 30 Seconds At the Indicated Temperatures (Reference 1958-1)	8
3	Fission Product Retention After Heating at a Temperature of 2400°C for the Indicated Times (Reference 1958-1)	9
4	Fission Product Retention After Heating at 1925°C For the Indicated Times (Reference 1961-1)	10
5	Fission Product Retention After Heating at 2400°C For The Indicated Times (Reference 1961-)	11
6	Fission Product Retention in Fueled Graphite Heated at 2400°C for the Given Times. (References 1958 - 1 and 1961-1)	12
7	The Effect of a Pyrolytic Carbon Coating on Fission Product Retention in a Solution - Impregnated Fuel Specimen (Reference 1961-1) The Fuel was Heated For 120 Minutes at Temperature.	13
8	Fission Product Retention for KIWI B-4 Fuel for 0.5 and 5 Minute Heating Times (Reference 1961-2) (All Exterior Surfaces Coated With Pyrolytic Carbon Except Where Noted).	14
9	Fission Product Retention for KIWI B-4 Fuel (Reference 1961-2) (All Exterior Surfaces Coated With Pyrolytic Carbon Except Where Noted).	15
10	Fission Product Retention at 1900°C for Solution Impregnated Fuel (Reference 1953-1)	21
11	Diffusion Coefficients for Fission Products in Graphite (Reference 1959-3)	22

(List of Figures Cont'd)

Figure	Title	Page
12	A Comparison of the "in Pore" and "in Grain" Diffusion Constants for Caesium, Strontium, and Barium in Graphite (Reference 1961-7)	23
13	Xe^{133} Retention in UC_2 Particles at 1700°C (Reference 1961-3)	28
14	Ba^{140} Retention in UC_2 (30 w/o UC_2) Graphite Compacts (Reference 1961-3)	29
15	Schematic Diagram of Proposed Irradiation Capsule for NERVA Fuel Material	34

ACKNOWLEDGMENTS

The authors are grateful to L. D. P. King, G. A. Cowan and E. Bryant for their assistance in providing some of the recent LASL data.

SURVEY OF FISSION PRODUCT RELEASE FROM NERVA FUEL MATERIAL

1.0 INTRODUCTION

One of the major sources of concern in regard to the eventual use of nuclear rockets is related to the fission product activity of the reactor core after operation of the reactor. The problem of determining the fission product inventory for any given set of operating conditions requires knowledge of the fission product release under a wide variety of conditions. In particular, the requirements for data on fission product release from NERVA fuel material arise in the following ways:

1) Fission product release during ground and flight testing of KIWI reactors.
2) Use of fission product release data to determine the operating behavior of fuel in KIWI reactors; this includes total burnup and power, power and temperature distribution, and operation of individual fuel elements.
3) Fission product release from an intact core during a decay heat cycle.
4) Fission product release during a nuclear transient which results in fragmentation of the fuel.
5) Fission product release from fuel fragments during re-entry heating.
6) Fission product release from an intact core by water leaching or fuel-water chemical reactions.

The information required must provide both a basic understanding of the mechanism of fission product release as well as engineering data which may be of a more immediate concern. The basic understanding of fission product release is required because there are many factors which can greatly affect the release rates. These include such things as method of fuel fabrication, fuel composition, type of cladding, hydrolysis reactions, thermal cycling and atmosphere effects (vacuum, helium, hydrogen, and air).

The primary purpose of the present paper is to consider the problem of fission product release from an intact core during a decay heat cycle. This work is part of the over-all safety and hazards analysis of the NERVA program. In particular, the present paper describes the results of a literature review of fission product release from fueled graphite and considers the problem of planning an experimental program which would provide the kind of fission product release data required in several phases of the NERVA program.

2.0 THEORETICAL EXAMINATION OF PROBLEM

The NERVA fueled graphite is a dispersion-type fuel in which a fuel bearing phase, UC_2, is dispersed in a porous graphite matrix. Figure 1 shows a schematic representation of a clad UC_2 - graphite dispersion fuel. The model shown in Figure 1 will be used to analyze the various mechanisms of fission product release from fueled graphite. The basic mechanisms of fission product release involve fission fragment escape by recoil and solid state diffusion. Solid state diffusion can be further subdivided by considering diffusion within graphite grains or within the cladding as contrasted with diffusion within the pores between individual graphite grains. As shown in Figure 1, the typical paths for release of fission products involve various combinations of recoil and diffusion mechanisms. In the case of fueled graphite where the UC_2 particles are relatively small (the order of 5 microns or less) the major faction of the fission product atoms recoil from the fuel particles (estimated at about 80%) and come to rest within the graphite lattice or in the pores. For this reason, processes 1 and 2 in Figure 1

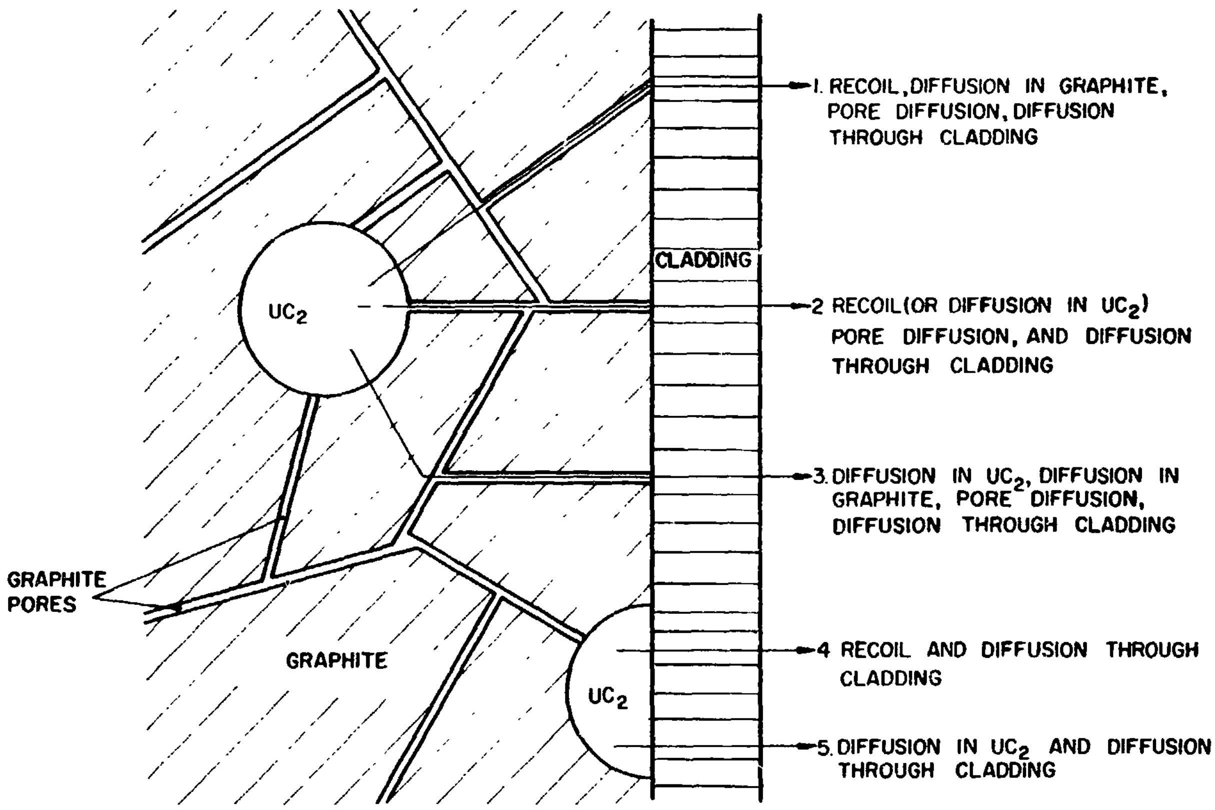

Figure 1 570A633

Theoretical Model of Fission Product Release From Fueled Graphite. For all of the Diffusion Paths Indicated the Possibility of Rate Limiting Surface (Such as Evaporation or Oxidation) or Interface Reactions Must be Considered.

are probably the most likely paths for fission product release in fueled graphite. One further point to consider relative to the diffusion paths in Figure 1 is the possibility of rate limiting surface or interface reactions which may control fission product release.

Some additional factors which must be considered in the analysis of fission product release from fueled graphite include open and closed porosity, cracks within the fuel-bearing or matrix phases, vaporization and corrosion of the fuel, and chemical interactions between fission products and the matrix and cladding phases. These considerations indicate that it is exceedingly difficult to obtain quantitative correlations between experimental variables and the basic mechanisms of fission product release. However, in experiments with carefully controlled variables, it should be possible to identify which of the many factors considered are contributing significantly to the release of fission products.

3.0 REVIEW OF LITERATURE

As indicated in Figure 1, the problem of fission product release from fueled graphite can be considered in terms of the various individual processes which make up the total release. In this case, we would then be interested in the diffusion of fission products in UC_2, graphite, in the pores between graphite crystals, and in cladding materials such as NbC or pyrolytic carbon. Unfortunately there is little or no information available on these specific subjects. Most of the available information on fission product release from fueled graphite was obtained on material of widely varying quality, density, composition, and fabrication techniques. For these reasons, it is not surprising that the fission product release data vary over a large range. In most cases, the reasons for the variations in behavior cannot be identified.

The bibliography acquired in the review of the literature covers three principal areas of study. They are as follows:

1) Results of fission product release studies by Los Alamos Scientific Laboratory (LASL) on several forms of KIWI fuel material.

2) Studies of fission product release from fueled graphite carried out in laboratories where the principal interest was in use of the fuel in a high temperature, gas-cooled (central-station) power reactor.

3) Fission product release on related materials such as UC, UC_2, and UO_2.

The following review of the literature will proceed in the same order as the list of topics given above. The primary emphasis will be on the results obtained at LASL since these studies were carried out on material which was identical to or closely related to the KIWI B-4 material.

3.1 <u>LASL Data</u>

Table 1 summarizes some of the significant factors which describe the type of fueled graphite used in each of the LASL experiments. These factors include the sample dimensions, the fuel loading, and type of specimen tested; i.e., admixture or solution impregnated. Admixture refers to a fuel made from a mixture of fuel and matrix particles (this is the type of material which has been used in the KIWI reactors) whereas solution impregnated refers to graphite which has been impregnated with a uranium containing solution such as uranyl nitrate. The LASL radiochemical data is given in terms of the Mo^{99} concentration which is assumed to be completely retained within the fuel material independent of temperature history.

TABLE 1

SUMMARY OF CONDITIONS FOR FUELED GRAPHITE FISSION PRODUCT RETENTION STUDIES AT LASL

CONDITIONS FOR LASL EXPERIMENTS

Variables	1958-1*	1960-1	1960-2	1961-1	1961-2
Sample dimensions	D = 0.240 inch L = 1.00 inch	KIWI-A PRIME D = 0.75 inch L = 9 inches 4 holes; 0.180-inch diameter	D = 0.230 inch L = 0.375 inch	D = 0.230 inch L = 0.375 inch	KIWI-B-4 element - 19 hole hex (3/4 inch across flats) 0.10-inch diameter holes L = 12 inches
Sample composition	150 mg U/cc	Not given in reference	100 mg U/cc	97 mg U/cc	Lined** = 200 mg U/cc Unlined = 450 mg U/cc
Type of specimen tested	Admixture	Admixture	Admixture and Solution Impregnated	Admixture and Solution Impregnated	Admixture
Heating atmosphere	Helium	Flowing He	Helium	Flowing He	Flowing He (p = 500 psi, Flow = 10 lbs/hr)

* Numbers refer to references given in bibliography.
** The lining referred to is NbC. All the specimens, described in this reference, were coated with pyrolytic carbon.

Several examples of the types of fission product release data available from LASL are shown in Figures 2 through 5. On comparing the results shown in these graphs, it is important to note the conditions given in Table 1 which define the fuel type, dimensions and sample loading. For example, Figure 6 shows a comparison of data presented in Reference 1958-1* and 1961-1 for material of somewhat different loading. The differences in the two sets of results may be due to the variation in fuel loading or may indicate the inherent scatter of the data which may be expected in this type of experimentation.

Table 2 gives two examples of the effect of fuel type on fission product retention. For the case of the samples heated for 10 minutes at 1925°C, retention is always greater for the admixture sample as compared to the solution impregnated sample. However, after 65 minutes at 1950°C, Sr, Ag, Cs, Nd, and Eu are retained to a greater extent in the solution impregnated fuel. These results indicate little, if any, difference in fission product retention of admixture and solution impregnated fuel material.

Since the current designs of the KIWI B-4 element require a NbC cladding on the inside surfaces of the fuel element holes and a pyrolytic carbon coating on the external surfaces of the element, considerable attention has been given to the effects of coatings on fission product release. Examples of these results are shown in Table 3 and Figures 7, 8, and 9. The results shown in Table 3, obtained on KIWI A-Prime fuel elements heated for 5 minutes at 2150°C, reveal that the highly retained fission products such as Y^{91} and Cs^{144} were not noticeably affected by the coating. The highly diffusable species such as Cd^{155} and Ag^{111} on the other hand were much more strongly retained in the coated element. Figure 7 shows this same behavior. In addition, Figure 7 shows the effect of the pyrolytic

* Refers to references given in bibliography.

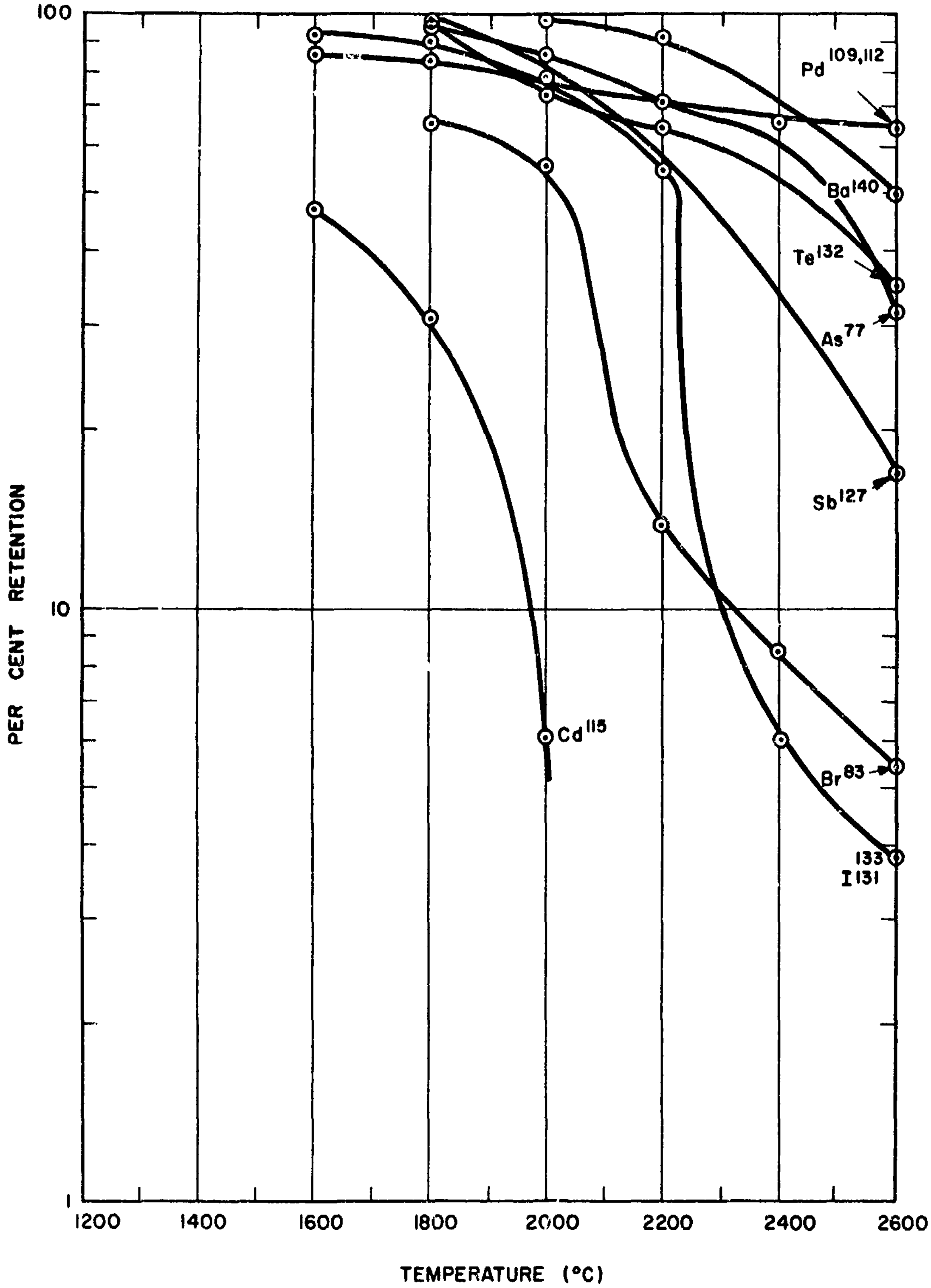

Figure 2 547009
Fission Product Retention After Heating 30 Seconds At the Indicated Temperatures (Reference 1958-1)

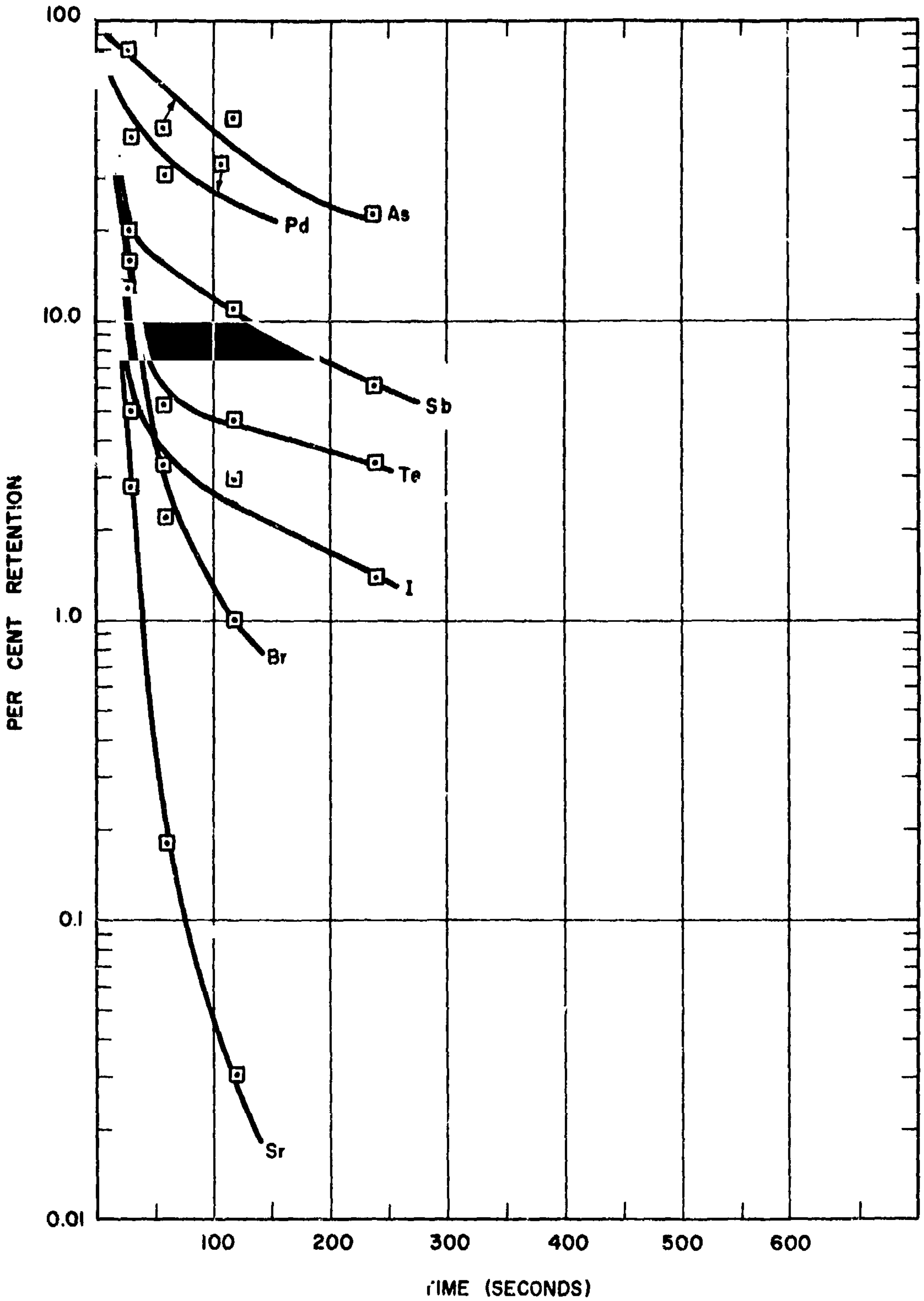

Figure 3 547008
Fission Product Retention After Heating at a Temperature of 2400°C for the Indicated Times (Reference 1958-1)

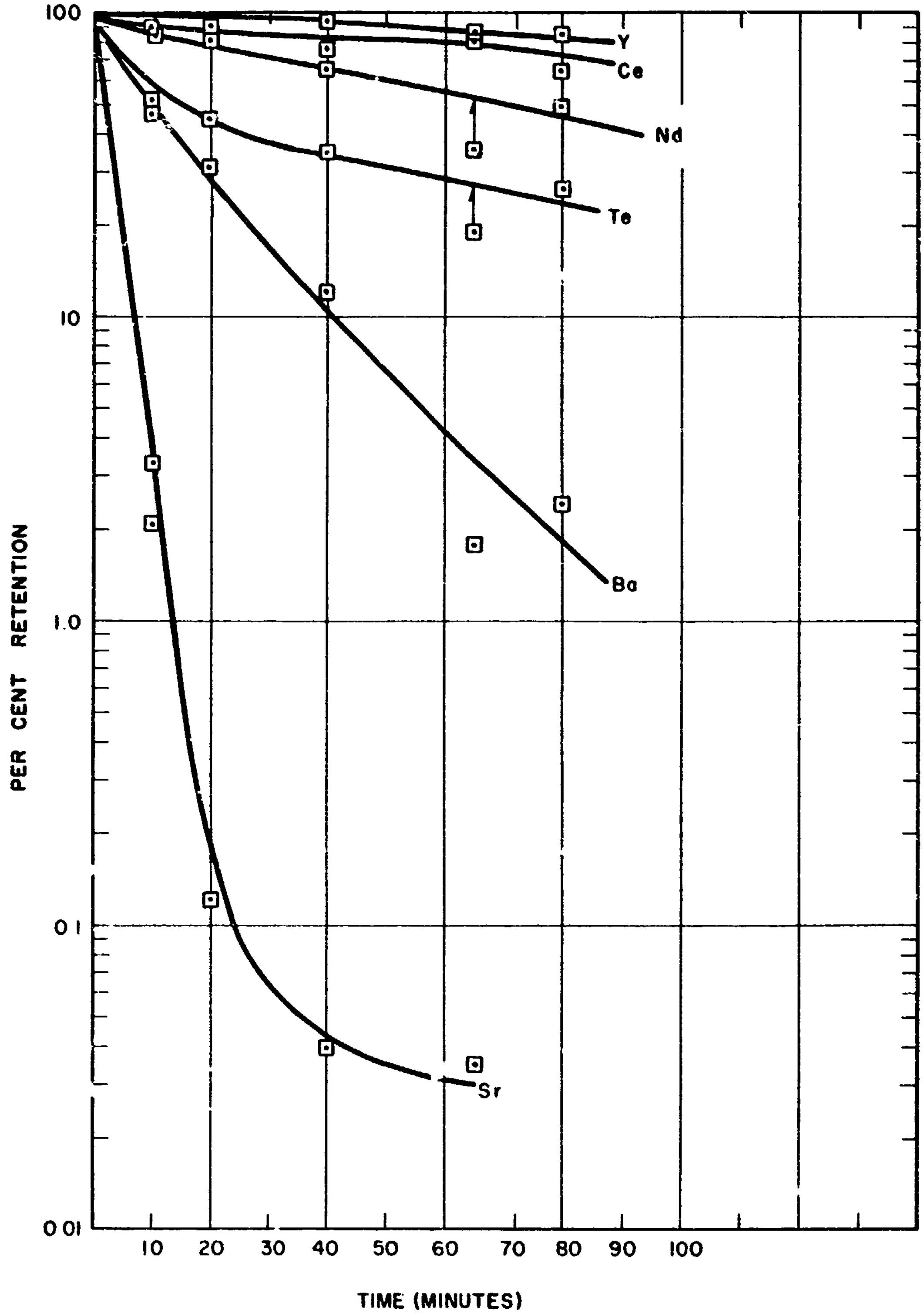

Figure 4

547007

Fission Product Retention After Heating at 1925°C For the Indicated Times (Reference 1961-1)

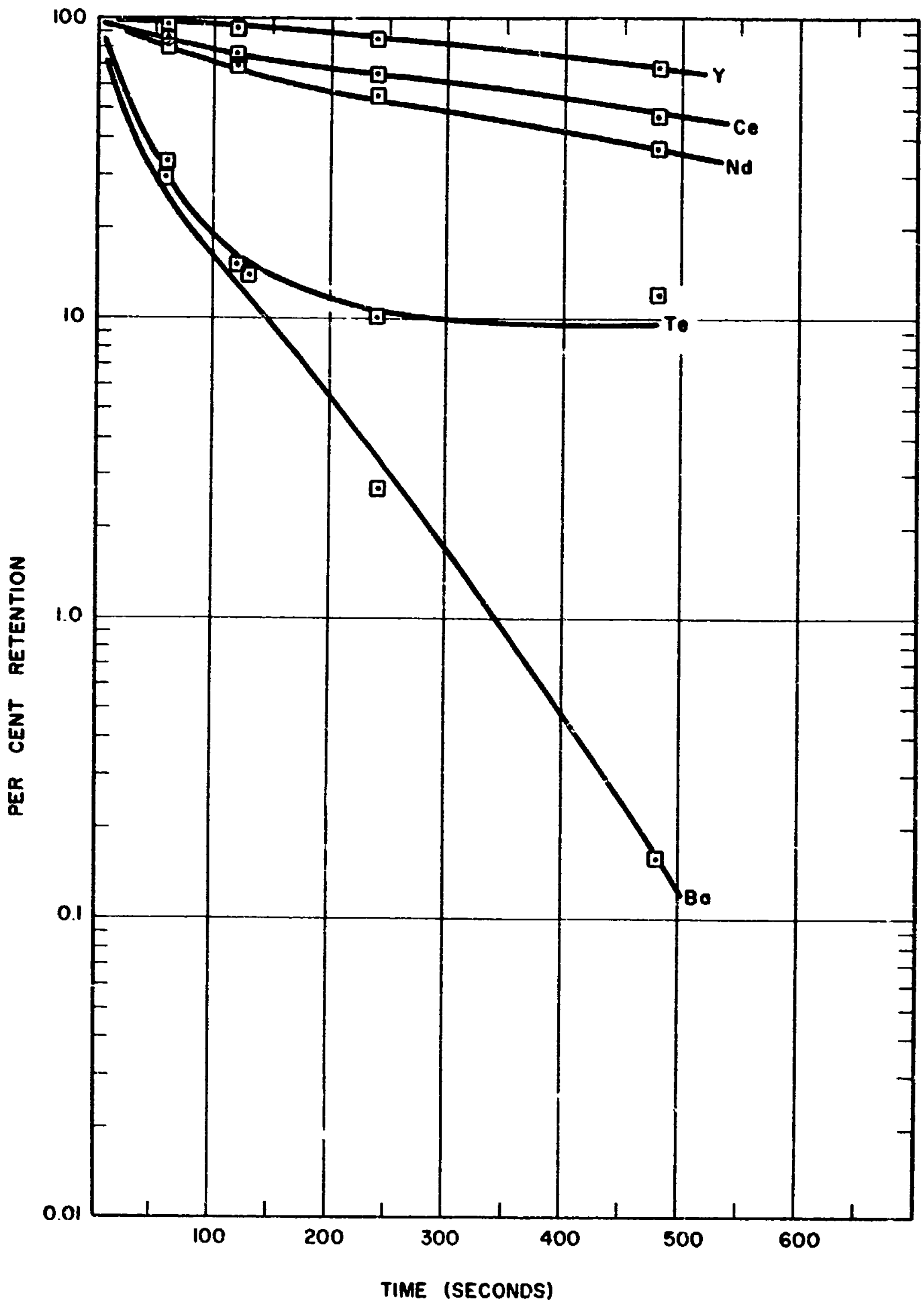

Figure 5

547006

Fission Product Retention After Heating at 2400°C For the Indicated Times (Reference 1961-)

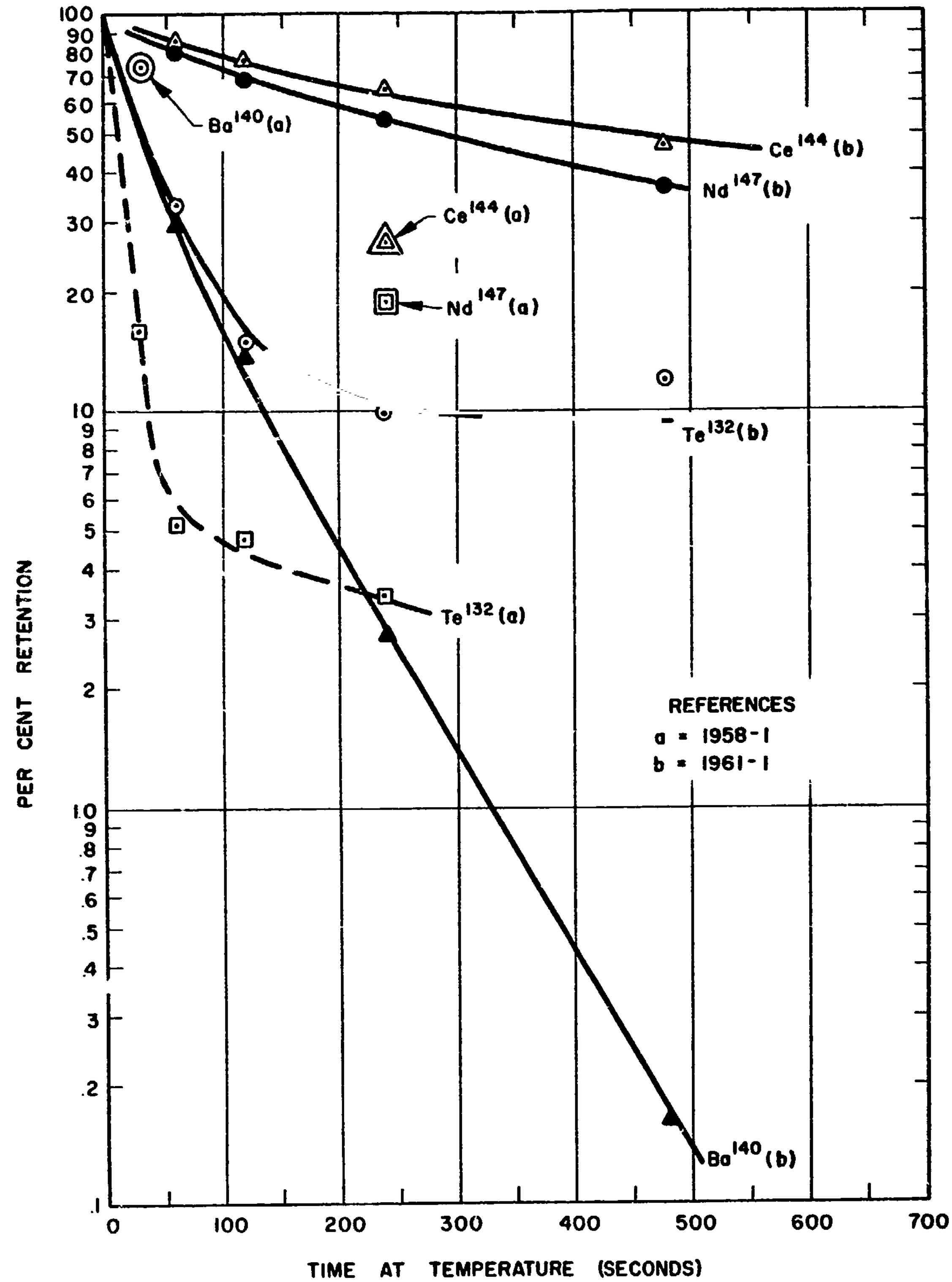

Figure 6 547004
Fission Product Retention in Fueled Graphite Heated at 2400°C for the Given Times. (References 1958-1 and 1961-1)

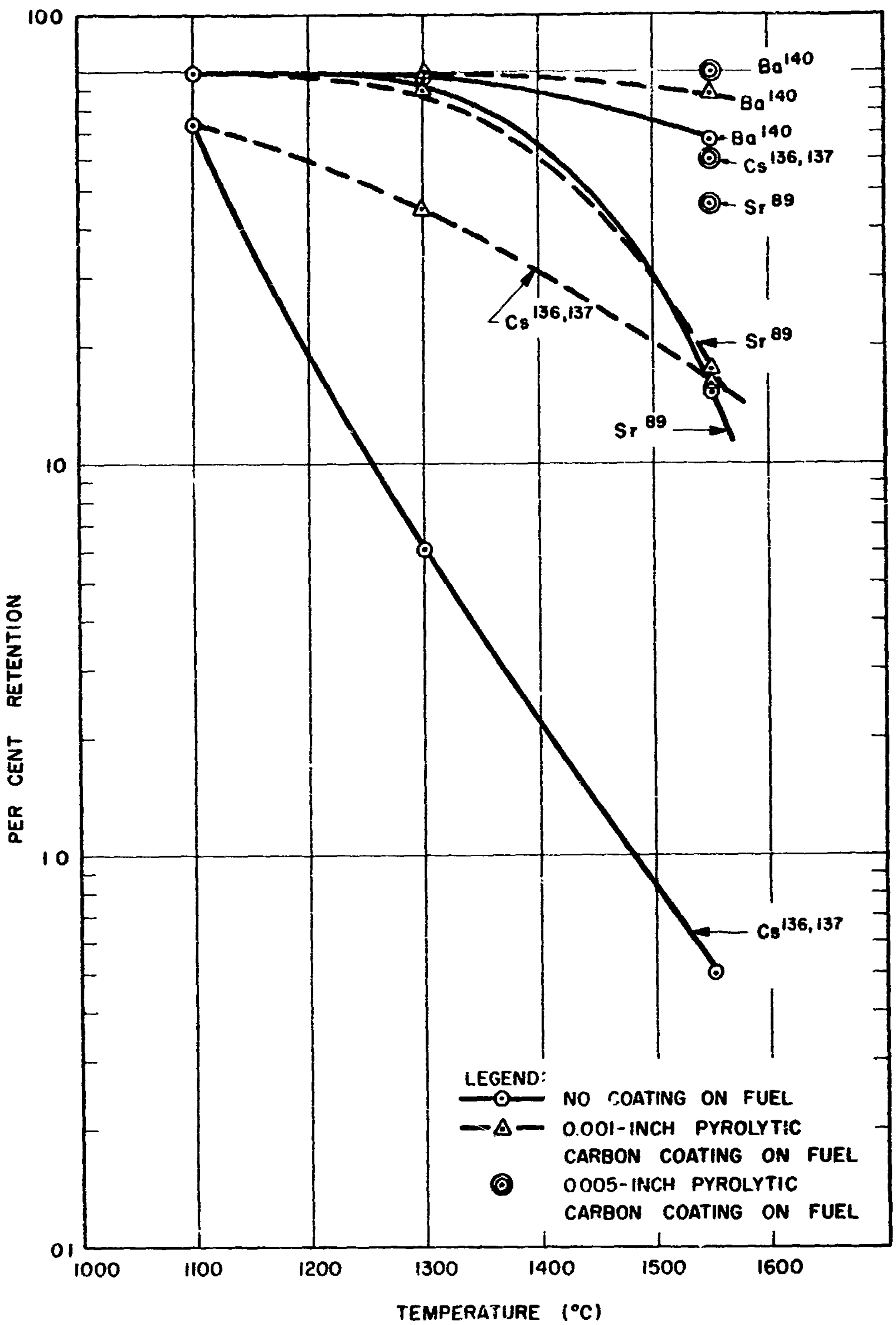

Figure 7 547002

The Effect of a Pyrolytic Carbon Coating on Fission Product Retention in a Solution - Impregnated Fuel Specimen (Reference 1961-1) The Fuel Was Heated for 120 Minutes at Temperature.

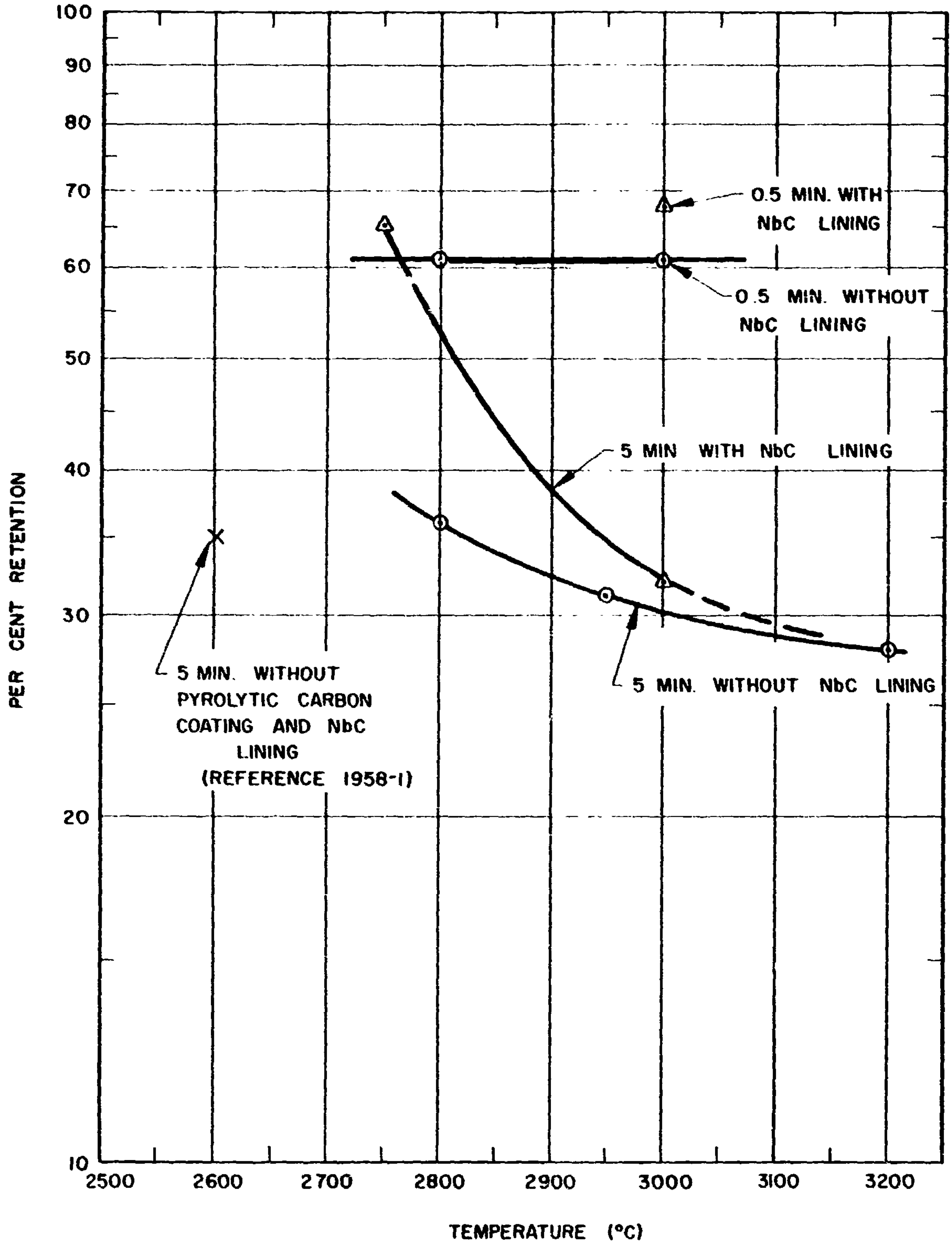

Figure 8 547000
Fission Product Retention for KIWI B-4 Fuel for 0.5 and 5 Minute Heating Times (Reference 1961-2) (All Exterior Surfaces Coated with Pyrolytic Carbon Except Where Noted).

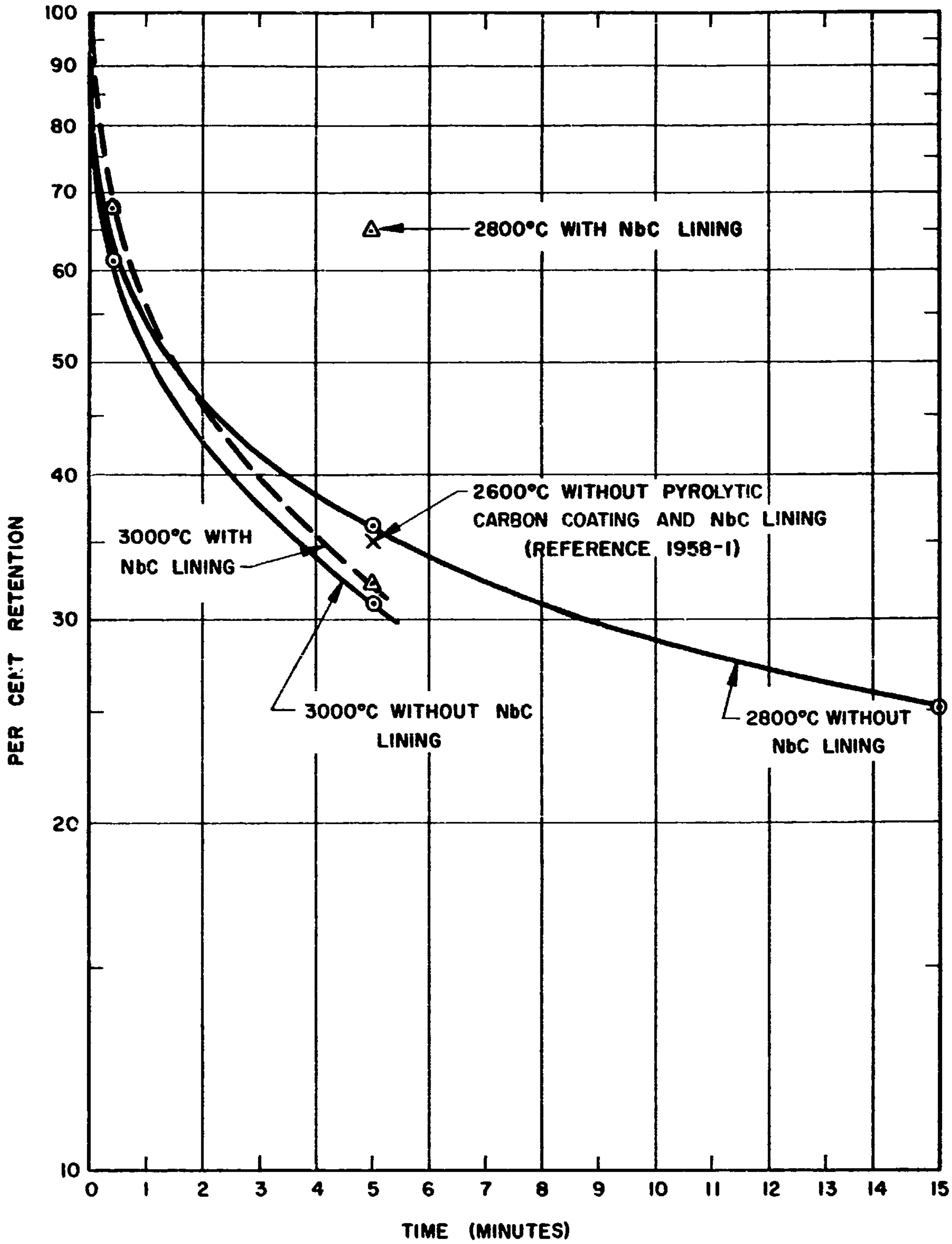

Figure 9 547001

Fission Product Retention for KIWI B-4 Fuel (Reference 1961-2) (All Exterior Surfaces Coated With Pyrolytic Carbon Except Where Noted).

[redacted]

TABLE 2

RETENTION OF FISSION PRODUCTS IN ADMIXTURE AND SOLUTION IMPREGNATED FUEL SAMPLES HEATED FOR 10 AND 65 MINUTES AT 1925 - 1950°C

A. 10 Minutes at 1925° ± 15°C (1960 - 2)

GROSS RETENTION OF FISSION PRODUCTS

Matrix Type	Sr^{89}	Cd^{115}	Sn^{125}	Te^{132}
Soln. Imp.	0.0034	0.0021	~0.024	0.17
Soln. Imp.	0.0032	0.0023	-----	0.18
Admix.	0.026	0.0034	~0.19	0.55
Admix.	0.030	0.0038	-----	0.57

Matrix Type	$Cs^{136,137}$	Ba^{140}	Ce^{144}	Eu^{156}
Soln. Imp.	~0.01	0.31	0.97	0.0034
Soln. Imp.	~0.01	0.23	0.96	0.0057
Admix.	0.096	0.56	0.99	0.052
Admix.	~0.086	0.54	1.00	0.060

Table 2 Con't

B. 65 Minutes at 1950°C (1961-1)

	% RETAINED	
Fission Product	Solution Impregnated	Admixture
Sr^{89}	0.06	0.04
Y^{91}	88.4	94.8
Ag^{111}	0.15	0.04
Cd^{115}	0.01	0.08
Sn^{125}	0.06	0.79
Sb^{127}	0.25	2.2
Te^{132}	9.0	21.0
$Cs^{136,137}$	0.3	0.1
Ba^{140}	0.2	2.0
Ce^{144}	69.8	91.9
Nd^{147}	34.7	27.9
Eu^{156}	0.88	0.12

Astronuclear

TABLE 3

RETENTION OF FISSION PRODUCTS IN COATED AND UNCOATED KIWI-A PRIME FUEL ELEMENTS HEATED AT 2150°C FOR 5 MINUTES PLUS 1 MINUTE WARMUP

(1960 - 1)

Fission Product	% Retained* Uncoated	% Retained* Coated**
Sr^{87}	12.6	32.5
Y^{91}	92.4	93.3
Ag^{111}	0.03	14.0
Cd^{115}	0.03	5.5
Sn^{125}	52.0	95.0
Sb^{127}	50.2	70.0
Te^{132}	62.4	69.0
Cs^{136}	31.8	84.0
Cs^{137}	32.2	85.0
Ba^{140}	64.1	64.1
Ce^{144}	92.7	90.6
Sm^{153}	56.0	54.1
Eu^{156}	22.0	40.1

* Based on 100% Retention of Mo^{99}

** NbC Coating on Hole Surfaces

CONFIDENTIAL
RESTRICTED DATA
Atomic Energy Act - 1954

coating thickness on fission product retention. For all the elements examined, the thicker coating appeared to give a significant increase in fission product retention.

Figures 8 and 9 show the gross retention of gamma-emitting fission products in uncoated and coated KIWI B-4 samples. The data indicates that the effect of the NbC lining on fission product retention decreases as the temperature increases. In particular, the results shown in Figures 8 and 9 give an indication of the fission product release which might be expected during a decay heat cycle. The results indicate that approximately 70 per cent of the gamma-emitting fission products would be released during a 5-minute decay heat cycle at 3200°C.

The data given in Figures 8 and 9 are not directly comparable to that given previously since there are a variety of elements contributing to the measured activity. The initial rapid decrease in activity is probably due to the loss of the more volatile high yield fission products species (1961-2). The transition elements Zr, Nb, Mo, and Tc, and the triad elements, Ru, Rh, and Pd are presumably responsible for the decreasing loss rate as the retention goes below 30 per cent. One may expect that the rate of loss will continue to decrease with time and that increased temperature will be necessary to produce further significant reduction in activity in a reasonable period of time. It may be noted that the purpose of the decay heat cycle would be to give rise to considerable greater fission product release (95% or greater) than is obtainable with the heating times and temperatures used in the present study.

3.2 Data From Other Sources

In general, the fission product release data obtained by groups considering the use of fueled graphite in central station gas-cooled reactors were obtained at temperatures considerably below that of interest to the nuclear rocket program. For this reason, much of the data given by the references do not contain data pertinent to the present discussion. However, there are some specific and general pieces of information which will be presented.

Figure 10 shows the fission product retention in solution impregnated fuel material containing approximately 200 milligrams of uranium per cubic centimeter. A comparison of Figures 4 and 10 shows that the fission product retention for both solution impregnated and admixture fuel are in relatively good agreement. This result is consistent with the data presented in Table 2.

One of the most useful ways of analyzing fission product release data is to determine a diffusion coefficient for a given element in fueled graphite. The results of several determinations of diffusion coefficients are shown in Figures 11 and 12. The calculated values of the diffusion coefficients given in Figure 11 as reported by Oak Ridge (1959-3) are based on the experimental data obtained in the early fission product release studies at North American Aviation Laboratory (1951-1, 1952-1, 1953-1, 2, and 3) and LASL (1958-1).* Figure 12 shows some relatively recent work from Great Britain (1961-7) which gives a comparison of the diffusion rates for fission products within the graphite grains and along the pores of the graphite. The pore diffusion process could not be described by either molecular or viscus flow. The results indicate that the rate controlling process in pore diffusion is an activated surface migration on the pore walls of the graphite.

* At this time there is some question as to the validity of the equations used in the calculation of the diffusion coefficients. This point will be checked in further analysis of the data.

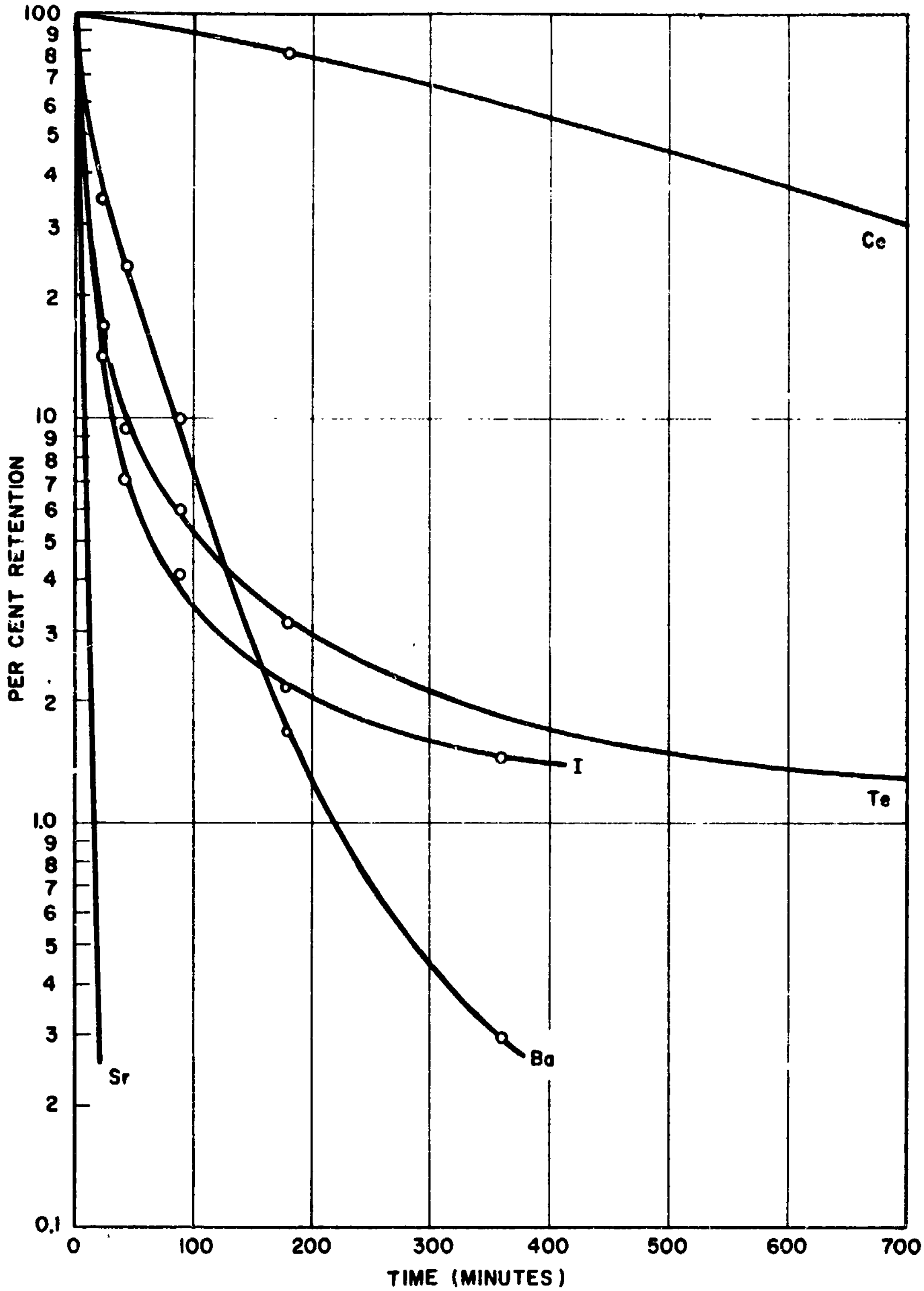

Figure 10 547055

Fission Product Retention at 1900°C for Solution Impregnated Fuel (Reference 1953-1)

~~CONFIDENTIAL~~
~~RESTRICTED DATA~~
~~Atomic Energy Act - 1954~~

Astronuclear

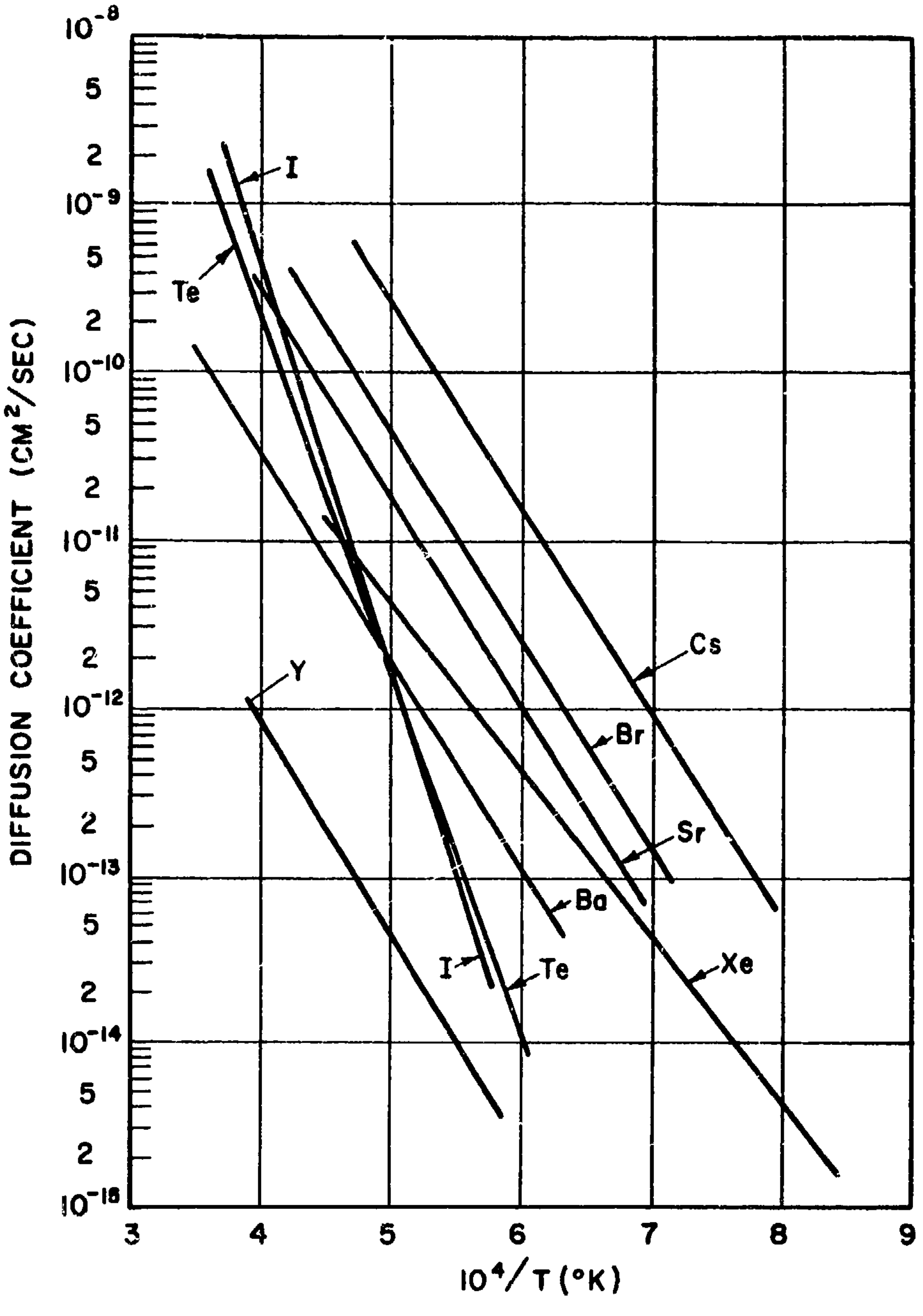

~~CONFIDENTIAL~~
~~RESTRICTED DATA~~
~~Atomic Energy Act - 1954~~

Figure 11

547056

Diffusion Coefficients for Fission Products in Graphite (Reference 1959-3)

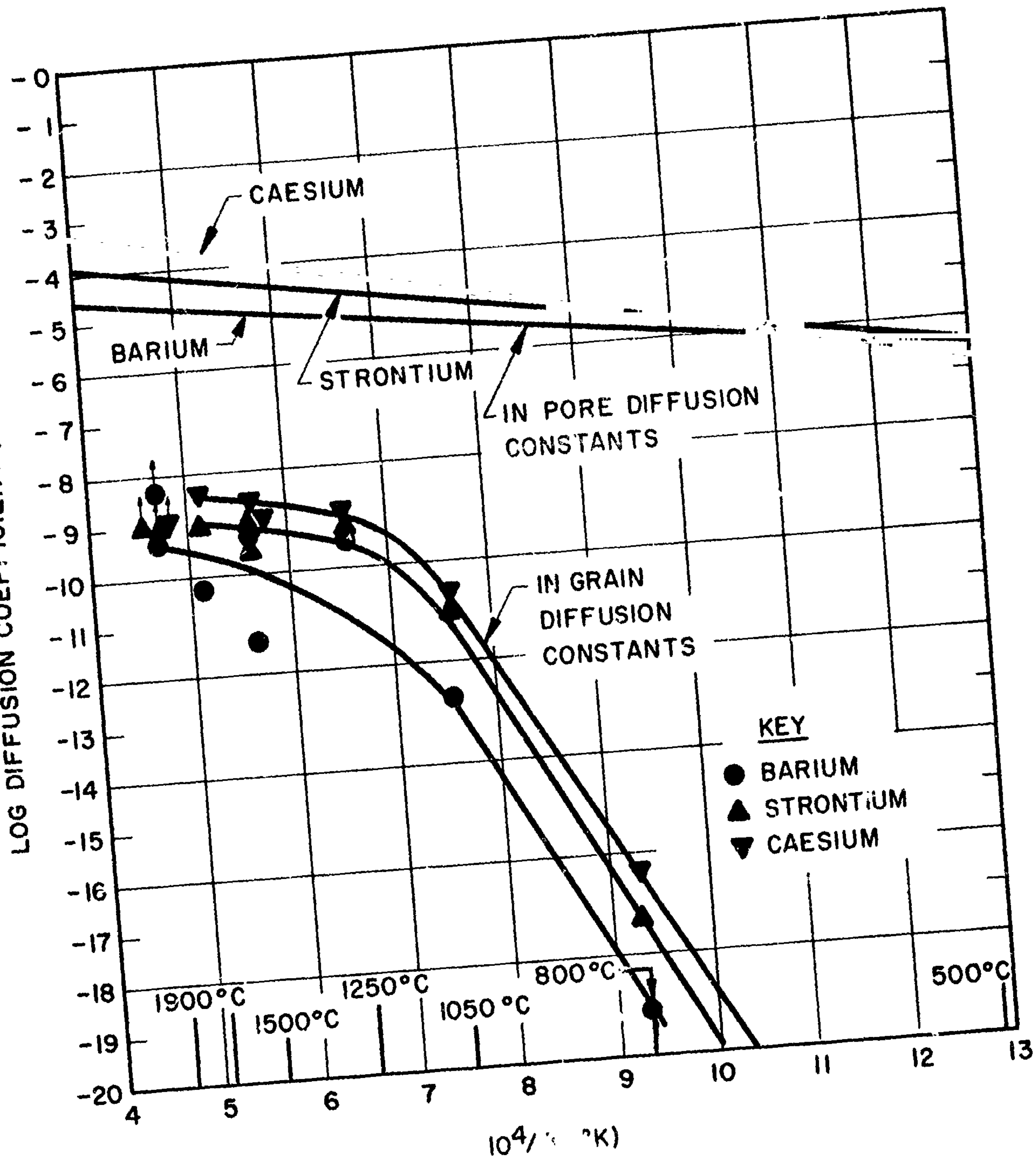

57

Figure 12
A Comparison of the "in Pore" and "in Grain" Diffusion Constants for Caesium, Strontium, and Barium in Graphite (Reference 1961-7)

The British studies (1961-7) also illustrate an interesting effect of oxygen on the rate of fission product release. It was found that the amounts of Sr and Ba released from the samples in the fission product release experiments were not as great as would be expected from the diffusion constants obtained from analysis of the concentration profiles within the samples. This result was attributed to the fact that the Sr and Ba oxides are thermodynamically stable at the experimental temperatures and react with graphite to give only a low partial pressure of the metal vapors. Thus, the actual fission product release rate was controlled by the decomposition of the fission product oxide.

In all the studies reported on fission product release, there was only one mention made of a sample size effect on fission product release (1953-1). The release rates for Ba (and possibly Pr) were significantly affected by geometry as indicated by the data given in Table 4. The explanation for the size dependence of fission product release is not known. It is anticipated that it is related to some aspect of pore diffusion rather than diffusion within graphite crystals.

3.3 Fission Product Release from Related Materials

The most complete studies of fission product release from nuclear fuel material have been carried out on UO_2. The results of these studies have been reviewed recently by Lustman (1961-9). The work on UO_2 indicates the complexity of the problem of fission product release and points out the magnitude of effort required to obtain an understanding of the problem. One further point, it was suggested by Long (1960-5) that approximate value for the diffusion rates of fission products in solid uranium oxide may be obtained by using the known values for diffusion in UO_2.

Fission product release studies have been carried out on a solid solution of UC in ZrC (1959-1). Results of experiments carried out at 2400°C are shown in Table 5.

TABLE 4

DIFFUSION OF SOME FISSION PRODUCT ELEMENTS UNDER VARYING CONDITIONS

ACCESSIBILITY TO SPECIMEN SURFACE* (1953-1)

Description of Diffusing System	Percentage of Element Remaining in Sample after 3 Hours at 1700°C		
	Iodine	Barium	Strontium
Top disc in stack of three	36	24	0.32
Middle disc in stack	35	44	0.44
Bottom disc in stack resting on unfueled graphite	40	30	0.75
Two discs balanced on edge	39	0.8	0.25

* Samples were impregnated graphite discs 0.62 - inch diameter and 0.1 - inch thick. Fission product release studies were made on the sample in various positions as indicated in the table.

TABLE 5

COMPARISON OF FISSION PRODUCT RELEASE FOR FUELED GRAPHITE (ADMIXTURE TYPE) AND A UC-ZrC SOLID SOLUTION AT 2400°C

Isotope	Per Cent Retention of Fission Product: Admixture Fueled Graphite* (4 min. at 2400°C)	UC-ZrC** (3 hrs. at 2400°C)
Sr^{89}	-----	6
Y^{81}	-----	51
Ru^{103}	70	100
Rh^{105}	92	52
Ag^{111}	-----	1
Cd^{115}	-----	15
Sn^{125}	0.1	7
Sb^{127}	6.2	8.4
I^{131}	1.4	19
Te^{132}	3.4	8
$Cs^{136,137}$	0.26	65
Ba^{140}	-----	9
Ce^{144}	27	41
Nd^{147}	19	30
Eu^{156}	74	33

* (1960 - 2)

** Fuel Contains 20 Mole Per cent Uc (1959 -1).

along with results obtained on fueled graphite. It should be noted that the results obtained on the UC-ZrC (20 mole per cent UC) solid solution were obtained after 3 hours whereas the fission product release data for the admixture fuel were obtained after 4 minutes. It can be seen that fission product release from the solid solution is several orders of magnitude less than that from fueled graphite. The estimated diffusion rates of fission products from the UC-ZrC solid solution range from 10^{-4} to 10^{-6} centimeters square per second at 2400°C.

Several interesting results concerning the diffusion of fission products from coated particles dispersed in graphite had been obtained from studies related to the high temperature gas cooled reactor program (1960-3, 4, 6 and 1961-3, 5, 6) One of the fuels considered for this program consists of either UC_2 or ThC_2-UC_2 particles coated with pyrolytic carbon dispersed in graphite. Results of release of Xe and Ba from the particles alone are shown in Figures 13 and 14. Figure 13 illustrates the xenon retention in coated and uncoated UC_2 particles. The results clearly indicate the significant effect of a 70 micron coating of pyrolytic carbon on fission product retention. The results shown in Figure 14 were obtained on a UC_2-graphite compact where the UC_2 concentration was approximately 30 per cent. The effect of the 35 micron pyrolytic carbon coating on fission product retention is clearly indicated.

4.0 DISCUSSION OF FISSION PRODUCT RELEASE DATA

The survey of the literature on fission product release from fueled graphite clearly indicates the deficiencies of the experimental data with respect to the particular needs of the NERVA program. The value of the available data may be described as follows:

1) There is sufficient data available to permit rough estimates of the magnitude of fission product release for relatively short time operation

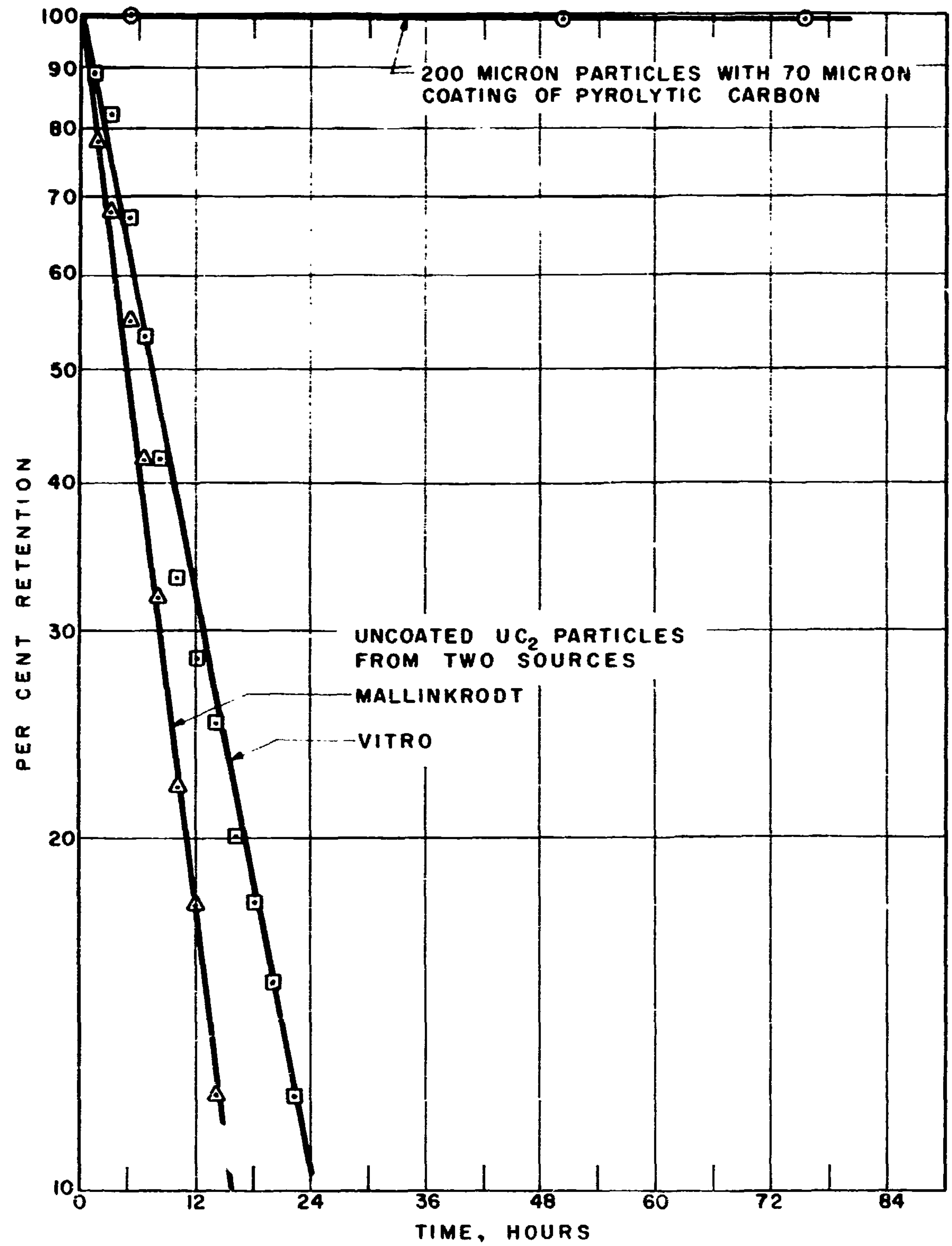

Figure 13

547058

Xe^{133} Retention in UC_2 Particles at 1700°C (Reference 1961-3)

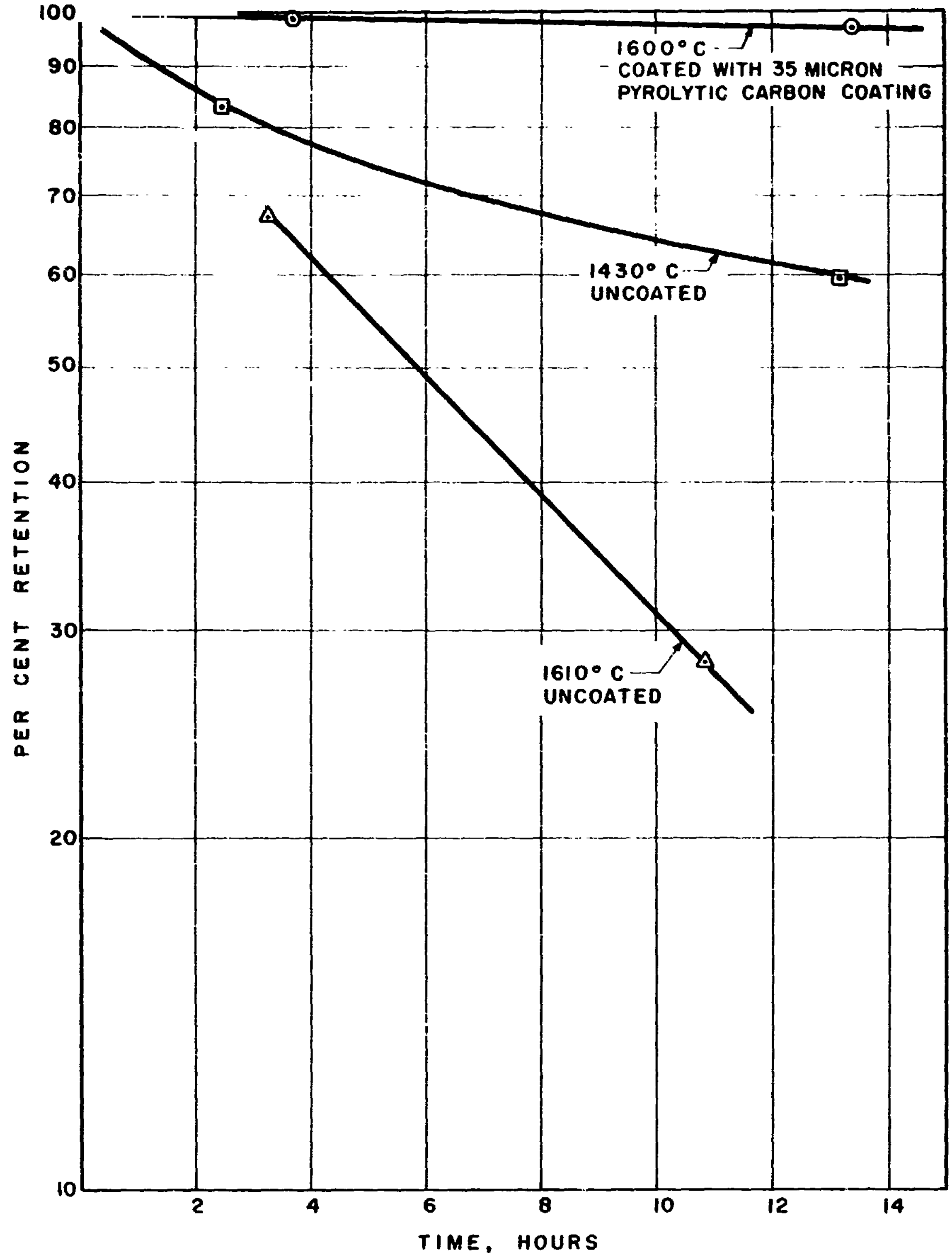

Figure 14

547059

Ba^{140} Retention in UC_2 (30 w/o UO_2) Graphite Compacts (Reference 1961-3) of the nuclear rocket and post-operation heating of core material.

2) The available results can be put in an analytical form to permit use in analysis of fission product release under such conditions as re-entry heating and decay heat cycle.

The studies to date, however, have not treated fission product release as a function of such factors as fabrication variables, composition, coating variables, temperature history and atmosphere effects. The work conducted to date forms an excellent point of departure for future experiments, which are required to meet the ultimate needs of the NERVA program.

Consideration of the specific data needed for the safety and hazards analysis of the nuclear rocket leads to the selection of the following goals for future fission product release experiments.

1) Study of fission product release during various decay heat cycles as a function of:

   a. Prior operating temperature and burnup of the fuel material
   b. Number of operating cycles of the fuel material prior to the decay heat cycle
   c. Time and temperature of the decay heat cycle
   d. Atmosphere present during decay heat cycle (vacuum, hydrogen, helium and possibly oxygen)

2) Study of fission product release during re-entry heating. This would involve:

   a. Setting up an analytical model for fission product release
   b. Combined analysis of re-entry heating and fission product

release

c. Fission product release experiments on fragmented fuel material

d. Possible ablation studies on irradiated fuel material to determine fission product release.

5.0 RECOMMENDATIONS FOR FISSION PRODUCT RELEASE EXPERIMENTS

An experimental program will be described which can provide the kind of fission product release data eventually required for the safety and hazards analysis of the NERVA program. These experiments involve irradiation of encapsulated sections of NERVA fuel material at the temperatures and burnups desired. Experiments can be carried out on short lengths of fuel material, such as KIWI B-4 samples of various geometric sections, which would be suitable for yielding quantitative information on fission product release. Samples would be irradiated for times and temperatures corresponding to NERVA conditions. The irradiated fuel material would then be subjected to the following series of experiments:

1) Post-irradiation examination of the fuel and determination of fission product release.

2) Post-irradiation heating experiments to determine fission product release during various heating cycles.

3) Re-irradiation of the irradiated material at NERVA conditions by re-inserting the fuel into a reactor.

4) Re-irradiation of the irradiated fuel material at higher temperatures to approximate a decay heat cycle.

The experimental approach described above can be accomplished by irradiating fuel sections in a reactor hydraulic rabbit facility. The period of irradiation can be controlled from about 15 seconds up to several weeks. The temperature of the fuel during irradiation could vary from approximately operating temperature to the sublimation temperature (3350°C) or higher. The flux in several of the currently operating test reactors is such that a 5-minute NERVA irradiation can be accomplished in a period of somewhat less than 10 minutes. The difference in irradiation time is not considered to be significant. These experiments would permit:

1) A close mock-up of a decay heat cycle.
2) Irradiation of fuel material at NERVA operating temperatures.
3) Studies of the physical behavior of fuel material during irradiation at very high temperatures ($>$ 3000°C). These experiments would permit an examination of the structural lifetime or disintegration (by vaporization or other means) of fueled graphite. This study would provide useful information to other NERVA studies such as the definition of a maximum credible incident and fuel behavior during a nuclear transient destruct.
4) Variation of the atmosphere within the capsule.
5) Wide variation in specimen geometry. Experiments can be carried out on sections of KIWI B-4 material or on fragments of fuel material such as might be formed by a nuclear transient or explosive destruct system.

~~CONFIDENTIAL~~
~~RESTRICTED DATA~~
~~Atomic Energy Act - 1954~~

6) A large number of studies to be made in a short period of time at relatively low cost.

A schematic diagram of an irradiation capsule which would permit variation of the fuel temperature up to the sublimation temperature or higher is shown in Figure 15. The fuel material would be surrounded by either graphite or NbC. An alternate fuel configuration is shown in Figure 15 which would also permit studies of the diffusion of fission products in graphite, pyrolytic carbon, or NbC. An irradiation capsule of similar design is currently being used for high temperature (up to 3500°C) irradiation experiments on carbide fuel material.

6.0 ACKNOWLEDGEMENTS

The authors are grateful to L. D. P. King, G. A. Cowan and E. Bryant for their assistance in providing some of the recent LASL data.

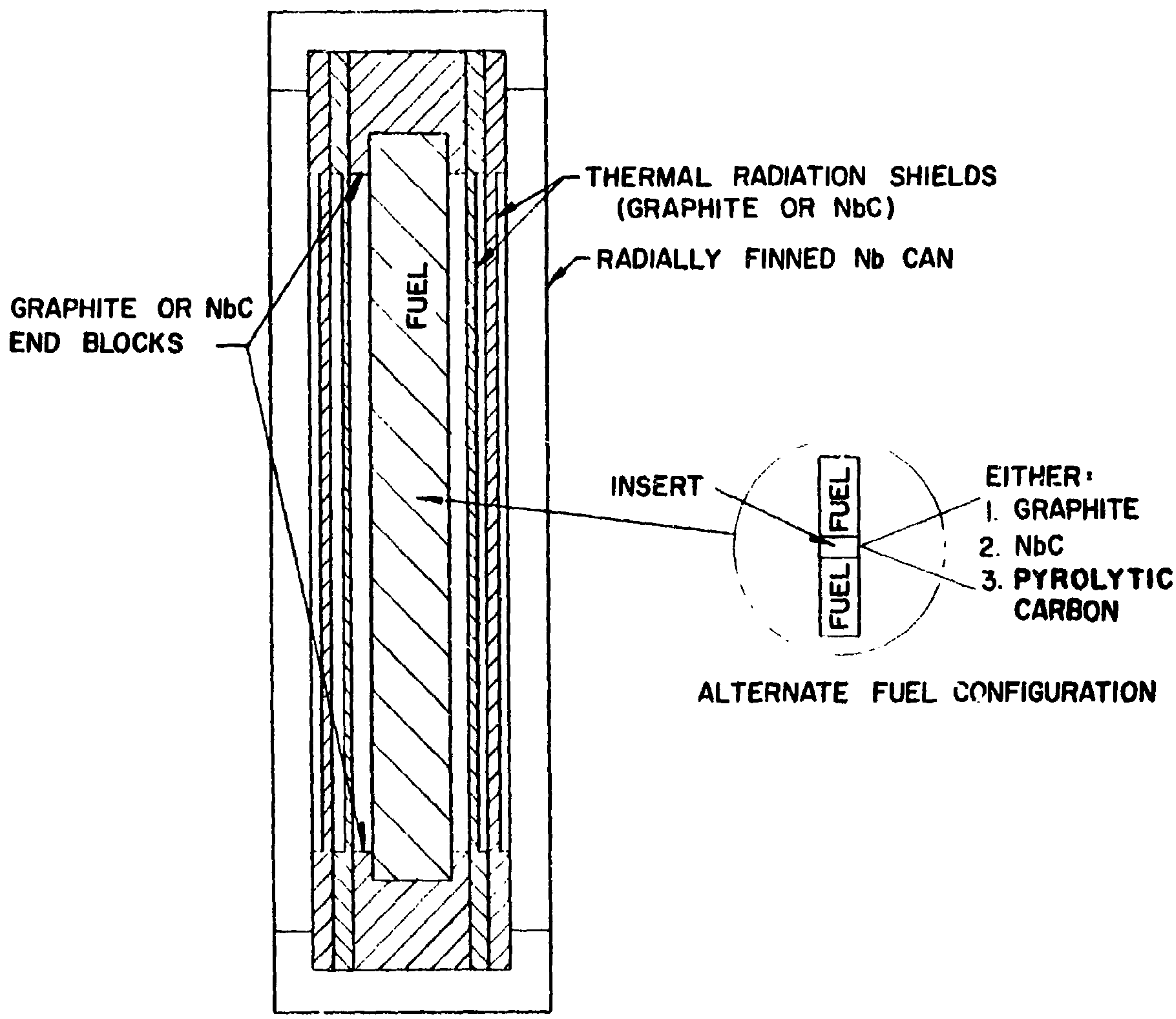

Figure 15 570A629

Schematic Diagram of Proposed Irradiation Capsule for NERVA Fuel Material

7.0 BIBLIOGRAPHY

FISSION PRODUCT RELEASE FROM FUELED GRAPHITE AND RELATED MATERIALS

1951

1. C. A. Smith and C. T. Young, "Diffusion of Fission Fragments from Uranium Impregnated Graphite," NAA-SR-72, (May 4, 1951).

1952

1. D. Cubicciotti, "The Diffusion of Xenon from Uranium Carbide Impregnated Graphite at High Temperatures," NAA-SR-194 (October 13, 1952).

1953

1. L. B. Doyle, "High Temperature Diffusion of Individual Fission Elements from Uranium Carbide Impregnated Graphite," NAA-SR-255 (September 11, 1953).
2. C. T. Young and C. A. Smith, "Preliminary Experiments on Fission Product Diffusion from Uranium Impregnated Graphite in the Range 1800 - 2200°C," NAA-SR-232 (June 17, 1953).
3. C. T. Young, "High Temperature Diffusion of Individual Fission Products from Small Uranium Impregnated Graphite Samples under Neutron Bombardment," NAA-SR-247 (September 1, 1953).

1958

1. G. A. Cowan and C. J. Orth, "Diffusion of Fission Products at High Temperatures from Refractory Matrices," 1958 Geneva Conference, P/613 LASL Data.
2. N. R. Large and G. N. Walton, "Migration of Non-Gaseous Fission Products through Graphite," AERE C/M 346, 1958.
3. L. R. Zumwalt, "Fission Product Traps for Use in High-Temperature Gas-Cooled Graphite Reactors," GAMD-304, 1958.

1959

1. "LASL Plasma Thermocouple Development Program," LAMS-2396, December 20, 1959.

2. T. A. Lane, et.al., "A Study of Problems Associated with Release of Fission Products from Ceramic Fuels in Gas-Cooled Reactors," ORNL-2851 (October 27, 1959).

3. W. B. Cottrell, et.al., "The HGCR-1, A Design Study of a Nuclear Power Station Employing a High-Temperature Gas-Cooled Reactor with Graphite-UO_2 Fuel Elements," ORNL-2653, 1959.

1960

1. J. E. Sattizahn and J. D. Knight, "Release of Fission Products from KIWI-A and KIWI-A Prime Reactors," LASL Office Memorandum to G. A. Cowan, J-11-1017, June 27, 1960 (Confidential).

2. J. E. Sattizahn, "Diffusion of Fission Products," LASL Office Memorandum to G. Best, February 5, 1960.

3. "Fuel Element Development Program for the Pebble Bed Reactor," Quarterly Progress Report, February 1 to April 30, 1960, NYO-9058. (Sections 3 and 4, Fission Product Retention by Pyrolytic Carbon Coatings).

4. "Fuel Element Development Program for the Pebble Bed Reactor," Quarterly Progress Report, May 1, 1960 to July 31, 1960, NYO-9061. (Sections 3 and 4 on Fission Product Retention by Coatings).

5. Long, G., "Diffusion of Fission Products in UO_2 and UC," The First Conference on Nuclear Reactor Chemistry (October 12, 1960).

6. "Progress on Ceramic Coated Fuel Particles at Batelle," BMI-1468 (September 12, 1960).

1961

1. Wolfsberg, J. E. Sattizahn, and E. Bryant, LASL Office Memorandum to G. Cowan, June 29, 1961.

2. Monthly Status Report for LASL NERVA Activity for Period Ending October 20, 1961, (Confidential).

3. "40-MW(E) Prototype High-Temperature Gas Cooled Reactor - Research and Development Program," Quarterly Progress Report for Period Ending March 31, 1961, GA-2204.

4. A. R. Saunders, "A Study of Fission Product Transport Mechanisms in High-Temperature Gas-Cooled Reactor Fuel Elements, ORNL-3145, (July 13, 1961).

5. "Fission Gas Pressure at Operating Temperatures of HGTR Fuels," ORNL 3102, Gas-Cooled Reactor Project Quarterly Progress Report for Period Ending March 31, 1961.

6. "Fuels Evaluation; Fission Gas-Retention Properties of UC_2 Particles Coated with Pyrolytic Carbon, ORNL 3160, Metallurgy Division Annual Progress Report for Period Ending May 31, 1961.

7. J. Bromiey and N. R. Large, "The Migration of Fission Products in Aritificial Graphite," AERE-R-3832, 1961.

8. R. B. Korsmeyer, "Fission Product Transport Through Graphite Matrices, CF-61-3-75 (ORNL), 1961.

9. B. Lustman, "Irradiation Effects in UO_2" Chapter in UO_2: Properties and Nuclear Applications, Edited by J. Belle, Navel Reactors Handbook, USAEC, Washington, D. C., 1961.